UKRI Science and Technology Facilities Council

Central Laser Facility Annual Report

2020–2021

Central Laser Facility
Science & Technology Facilities Council
Rutherford Appleton Laboratory
Harwell Campus
Didcot, Oxfordshire OX11 0QX
T: +44 (0)1235 445647
E: clfannrep@stfc.ac.uk
W: www.clf.stfc.ac.uk

The production team for this Annual Report was as follows:

Editor: Raoul Trines

Production: Tracey Burge and Raoul Trines

Section Editors: Hamad Ahmed, David Carroll, Ian Clark, Dave Clarke, Rob Clarke, Marco Galimberti, James Green, Chris Hooker, Gabriel Karras, Robert Lees, Ian Musgrave, Pedro Oliveira, Rajeev Pattathil, Jonathan Phillips, Alex Robinson, Dan Symes, Martin Tolley, Christopher Tynan, Adam Wyatt

This report is available on the CLF website at www.clf.stfc.ac.uk

Design, layout and production: UKRI Creative Services (JRS)

Thanks to all of the above for their contribution towards producing this report and, of course, to all of the authors for their submissions.

Cover image: courtesy of Fisher Studios

Contents

Foreword

John Collier
Director, Central Laser Facility, STFC Rutherford Appleton Laboratory, Harwell Campus, Didcot, UK
Email address: **john.collier@stfc.ac.uk** Website: **www.clf.stfc.ac.uk**

In its 45-year history, the Central Laser Facility (CLF) has never experienced such a challenging time as during 2020/21, with the COVID-19 pandemic that swept the world. Despite most staff and users being prevented from coming to site, and operations being severely curtailed, we still managed to maintain an active community, and deliver scientific output and technical development of the highest order. Moreover, the Lasers for Science division introduced a Rapid Access mechanism to grant facility access for R&D related to the fight against COVID-19, enabling users in academia and industry to take early action in a time of need and demonstrating how the CLF is able to respond quickly to new challenges.

Based at the STFC Rutherford Appleton Laboratory in Oxfordshire, our laser facilities – **Vulcan, Gemini, Artemis, Ultra** and **Octopus** – are amongst the most advanced in the world. They enable research across a broad range of science areas, spanning physics, chemistry and biology, that is contributing to international efforts to solve major scientific, economic and societal challenges. Our suite of facilities is underpinned by considerable expertise and enabling capabilities, including computational **plasma physics**, **target micro-fabrication** and **engineering**, that help our users to push the boundaries of science and research.

In the near future, our new **Extreme Photonics Applications Centre (EPAC)** will open its doors to users. An exciting partnership between UKRI, MoD, academia and industry, we expect this new facility to deliver scientific breakthroughs and new solutions to challenging problems. In the last year, considerable progress has been made and the building itself has started to take shape. **EPIC**, the joint innovation centre with India, also continued to play a major role in developing ancillary technology solutions for our high power laser facilities and EPAC.

In addition to its user facilities, the CLF is home to the **Centre for Advanced Laser Technology and Applications (CALTA)**. A key success has been the development of a proprietary technology, DiPOLE, capable of delivering high energy pulses at high repetition rate for applications including advanced imaging, materials processing, non-destructive testing and fundamental science. This technology will be the laser pump source for EPAC. CALTA and the CLF's **Industry Partnerships and Innovation (IPI) group** also work with industrial partners to facilitate solutions to real-world problems by exploiting the CLF's extensive technological capability developed by our experts over many years

This annual report for the CLF offers an insight into some of the scientific and technical research that has been carried out by users of the CLF and its staff over the financial year 2020/21. I do hope that you enjoy reading this selection of abstracts, and feel inspired by the achievements of all those involved.

Professor John Collier FLSW
Director, Central Laser Facility

Highlights of 2020/21 include:

A collaboration between the CLF and the Chinese Academy of Sciences used **Vulcan** Target Area West to produce a terawatt of terahertz. High power and spectrally tunable driver light pulses are required for an ever-increasing number of strong-field applications, such as ultrafast coherent control over matter and light.

An international group of researchers used the CLF's **Gemini** Laser to implement AI in order to optimise a new type of particle accelerator. The study highlighted the possibility of exploiting machine learning techniques to produce a fully automated plasma accelerator, whilst synchronously uncovering never-before-seen insights into the fundamental physics of the machine.

An international collaboration involving the **Artemis** Laser Facility looked at an intriguing 2D material. 2D materials have the potential to result in devices that are smaller, run faster, and consume less power, as well as offering a wealth of other potentials such as foldable, flexible, transparent electronics, and perhaps even self-charging solar powered devices.

Octopus took delivery of a MINFLUX microscope that aims to bridge the resolution gap between light and electron microscopy, with the ultimate goal of structure determination in the cell. Its scanning Stimulated Emission Depletion (STED) super-resolution microscope was also upgraded, and has resulted in a number of high impact publications from the user community in areas including antimicrobial resistance and immunology.

Research began to develop the technology to study ultrafast details of reactions in chemistry, with **Ultra** at the hub. Work with UEA and the wider CLF aims to improve understanding of, and potentially control, photochemistry and photobiology to maximise efficiency yield, with many possible applications including the potential for improving the efficiency of man-made solar energy.

CALTA's DiPOLE laser was used in the first ever demonstration of laser shock peening (LSP) of Tungsten. A Proof of Concept award was announced to take the DiPOLE laser shock peening programme forward.

In **EPIC**, team members were recruited for targetry, engineering and detector work packages and the preliminary designs for some of the technical solutions got underway. The control system group became fully functional, working hand-in-hand with the CLF team, delivering several modules.

Our scientists continued to be creative and drive forward the **IPI Group's** innovation portfolio. An additional four proof-of-concept projects were introduced and the CLF filed two new patent families this year, giving a current total of 23 active patent families.

The **Plasma Physics Group** has continued to provide CLF users with theory and simulation support, including access to the PRISM suite and help with use of the CLF's SCARF resources.

The CLF's **Target Fabrication Group** successfully fielded its high rep-rate tape drive system in the Gemini target area. After two days of dedicated facility time to enable some de-bugging and modifications, it was used successfully on a commercial access run.

The design of a new building for **CLF Engineering** was commissioned. This building will allow us to bring all of the engineering lab spaces together into a central hub.

CLF technicians worked with colleagues across STFC to provide much needed ventilators for the NHS.

Overview of the Central Laser Facility (CLF)

Cristina Hernandez-Gomez
Central Laser Facility, STFC Rutherford Appleton Laboratory, Harwell Campus, Didcot, UK
Email address: **cristina.hernandez-gomez@stfc.ac.uk** Website: **www.clf.stfc.ac.uk**

Introduction

The CLF is a world leading centre for research using lasers in a wide range of scientific disciplines. This section provides an overview of the capabilities offered to our international academic and industrial community.

VULCAN

Vulcan is a versatile high power laser system that is composed of Nd:glass amplifier chains capable of delivering up to 2.6 kJ of laser energy in long pulses (nanosecond duration) and up to 1 PW peak power in a short pulse (500 fs duration) at 1053 nm. It currently has eight beam lines. Two of these beam lines can operate in either short pulse mode or long pulse mode, while the remaining six normally operate in a long pulse mode. The short-pulse and long-pulse systems operating jointly can be directed to two different target areas, enabling sophisticated interaction and probing experiments.

We have started to build the new short-pulse OPCPA beamline for the Vulcan TAP area, which will deliver a PW-level pulse (30 J in 30 fs) in addition to the existing PW (500 J, 500 fs) and long pulse (250 J) capabilities. The old Target Area East has now been refurbished as a new laser area (LA5) and will become the front-end for this beamline, housing the initial stages of amplification. The final stage of amplification will take place in laser area 4, which has been enlarged to accommodate this.

New ways of working were implemented during the COVID-19 pandemic to allow operations to continue with fewer people within the facility. These included the remote operation of diagnostics, switch-on of laser systems, and shot sign-off.

GEMINI

Gemini is a Titanium-Sapphire based dual-beam high power laser system with two synchronised Petawatt-class beams, enabling pump-probe studies at extreme light intensities (>10^{21} Wcm^{-2}). Many experiments in Gemini focus on the study and development of laser-driven plasma accelerators, with a view to employing these unique sources in a wide range of applications. Operations in Gemini this year were significantly affected by COVID-19 as it took over three-and-a-half months to get the facility back to being operational in mid-August 2020, following the initial nationwide lockdown in March 2020. Despite this interruption, the experiments in Gemini were quite successful. Highlights include using the x-rays from a laser-driven accelerator for study of extreme conditions through X-ray Near-Edge Spectroscopy, and testing out liquid-based targetry for laser-driven plasma accelerators, which will be invaluable for operations in EPAC.

TARGET FABRICATION

The Target Fabrication Group made the majority of the solid targets shot on the CLF's high-power lasers, and also supported target design for the academic access on the Orion Facility at AWE. Commercial access to target fabrication capabilities was available to external laboratories and experimentalists via the spinout company Scitech Precision Ltd.

A range of microtarget types were produced to enable the exploration of several experimental regimes. Fabrication techniques included thin film coating, precision micro-assembly, laser micromachining, and chemistry processes, all verified by sophisticated characterisation. STFC's advanced capabilities in both high precision micromachining and MEMS microfabrication were also utilised. The Group's

processes and component tracking system provided a high level of traceability.

Further progress was made in developing a high stability, high rep-rate (HRR) tape drive, which was tested on Gemini. By collaboration with several Indian institutions through EPIC, advances were made in the production of complex tapes for novel HRR applications and experiments. Progress continued in the robotic assembly of target arrays. Work with Octopus on the assembly of advanced micro optics enabled a number of high profile publications.

THEORY AND MODELLING

The Plasma Physics Group supports scheduled experiments throughout the design, analysis and interpretation phases, as well as users who need theoretical support in matters relating to CLF science. We support principal investigators using radiation hydrodynamics, particle-in-cell, hybrid and Vlasov-Fokker-Planck codes, as well as by providing access to large-scale computing (SCARF).

Despite the on-going problems with the COVID-19 pandemic, the PPG staff endeavoured to continue to fulfil this mission, as the nature of the group's work is largely compatible with remote working.

The elements of support for users that involve students have all had to be carried out remotely, but this has largely been successful. The provision of the PRISM suite and other such resources have allowed us to continue strong support for users even in this difficult time.

ARTEMIS

(Research Complex at Harwell)
Artemis is the CLF's facility for ultrafast laser and XUV science. It offers ultrashort pulses at high repetition rate, tuneable over the spectral range from the XUV (10-100 eV) to the far-infrared, and with pulselengths down to a few optical cycles. Ultrafast, coherent XUV pulses are produced through high harmonic generation and delivered through vacuum beamlines to end-stations for gas-phase chemistry, materials science and imaging. Experiments in Artemis use XUV to investigate ultrafast dynamics in experiments on gas and solid materials, and for coherent lensless imaging.

Artemis has recently moved across campus to newly refurbished labs in the Research Complex at Harwell (RCaH), and undergone a major upgrade, adding a new laser system and a third XUV beamline. Over 2020-21, commissioning started on the new laser system, which produces 1700 nm and 3000 nm pulses at 100 kHz repetition rate, and is a joint purchase with Ultra. A new XUV beamline for this laser was designed and procured. The existing 1 kHz Ti:Sapphire system and XUV beamline have been upgraded and refurbished for higher XIV flux, and these were commissioned. The first user experiment in the new labs has also taken place.

OCTOPUS AND ULTRA

(Research Complex at Harwell)
The CLF operates two other facilities in the RCaH: Ultra, for ultrafast molecular dynamics measurements in chemistry and biology, and Octopus, a cluster of advanced laser microscopes for life science research.

Ultra provides state-of-the-art structural dynamics facilities, to explore reactions in nature, energy capture and storage, catalysis and fundamental quantum level research on molecular and bio-molecular electronics, probes, therapeutics, enzymes and DNA. By utilising unique multiple laser amplifier combinations, the facility can address a wide range of problems, having the capability to access UV to IR or narrowband and broadband energy transitions, measuring dynamics across femtoseconds to seconds. A wide range of techniques are available, based on the ultrafast laser systems, providing highly sensitive time-resolved vibrational and electronic spectroscopies, as well as advanced steady-state vibrational spectroscopy techniques to observe specific interface species, with sum-frequency-generation, or weak signals obscured by strong emission from samples, with Kerr-gated

Raman. Recent developments have incorporated new high-speed spectrometers and data processing, and explored novel high average power Raman systems.

In the imaging area, the Octopus cluster offers a range of microscopy stations linked to a central core of pulsed and CW lasers, offering "tailor-made" illumination for imaging. Optical resolution techniques offered include total internal reflection (TIRF) and multi-wavelength single-molecule imaging, confocal microscopy (including multiphoton), fluorescence energy transfer (FRET), fluorescence lifetime imaging (FLIM), and Light Sheet Microscopy. Super-resolution techniques are also available: 2D and 3D Stochastic Optical Reconstruction Microscopy (STORM) with adaptive optics, Photoactivated Localization Microscopy (PALM), Structured Illumination Microscopy (SIM), gated 3D Stimulated Emission Depletion Microscopy (STED), 3D MINFLUX, and super-resolution cryo-microscopy. Laser tweezers are available for combined manipulation/trapping and imaging with other Octopus stations, and can also be used to study Raman spectra and pico-Newton forces between particles in solution for bioscience and environmental research. A cryo focused ion beam scanning electron microscope (FIB-SEM) is also available for 3D volume electron imaging. This forms part of a correlative light and electron microscopy (CLEM) workflow currently under development.

Chemistry, biology, and spectroscopy laboratories support the laser facilities, and the CLF offers access to a multidisciplinary team providing advice to users on all aspects of imaging and spectroscopy, including specialised biological sample preparation, data acquisition, and advanced data analysis techniques. Access is also available to shared facilities in the Research Complex, including cell culture, scanning and transmission electron microscopy, NMR, and x-ray diffraction.

ENGINEERING SERVICES

Engineering is fundamental to all the operations and developments in the CLF. The engineering division operates across all of the CLF's facilities. Mechanical, electrical and software support is provided to deliver the experimental programmes, and the research and development activities. Support can range from making small-scale modifications to existing equipment to improve its performance, through to carrying out larger scale projects, such as the design and development of commercial projects. In addition, there are active engineering collaborations with regional and international partners such as, HiLASE (Prague, Czech Republic), XFEL (Hamburg, Germany) and TIFR (Hyderabad, India).

This year, we have commissioned the design of a new building for Engineering, which will bring all the engineering lab spaces together into a central hub. Not only will this building provide increased space to build and test infrastructures, but it will also offer space to upskill the existing teams and support the training and development of apprentices. The ground floor of the new building will focus on manufacturing from raw materials, and the building of large structures and systems. This floor is expected to become operational in autumn 2022, once machinery has been relocated and recommissioned. The first floor will come online later, and will support the more delicate and intricate building and testing of components and sub-assemblies/sub-systems.

CENTRE FOR ADVANCED LASER TECHNOLOGY AND APPLICATIONS (CALTA)

The Centre for Advanced Laser Technology and Applications (CALTA) is developing a new class of laser, capable of delivering high energy, high peak power pulses at high repetition rate and high efficiency. Based on laser diode pumped Ytterbium-YAG in the form of a transparent ceramic, CALTA's DiPOLE Diode Pumped Solid State Laser (DPSSL) architecture has demonstrated stable 1 kW operation for extended periods in 150 J, 10 ns pulses delivered at 10 Hz. With an overall optical efficiency of >20%, DiPOLE systems have the potential to transform single shot demonstrations of effects into real world applications.

Following construction and commissioning at RAL in 2019, CALTA's most advanced 1 kW D-100X DiPOLE laser, was delivered to the HZDR laboratory in Hamburg as a UK contribution to the European XFEL facility. There it will be used to drive materials to high energy density states, to be diagnosed using the XFEL X-ray beam.

Commissioning of D-100X by CLF and HZDR staff has made progress, but COVID lockdowns and travel restrictions have inevitably delayed things. It is hoped that this phase of the project will be completed in the first few months of next year.

Access to CLF's development laboratories has been severely limited during the year, but the opportunity has been taken to continue the design work, computer modelling and simulations that underpin CALTA technology.

EXTREME PHOTONICS APPLICATIONS CENTRE (EPAC)

The Extreme Photonics Applications Centre (EPAC), which is under construction at the CLF, will enable the development of a transformational generation of laser-driven radiation sources and accelerators, and will maximise their scientific and economic exploitation through engagement of multiple end-user communities.

EPAC will initially deliver a PW laser operating at 10 Hz to three dedicated experimental areas housed in a stand-alone building. In order to achieve this high peak power and repetition rate, DiPOLE technology will be used to pump a high energy Titanium Sapphire amplifier operating at 10 Hz.

The first experimental area (EA1) will be especially designed for Laser Wakefield Acceleration (LWFA), where multi-GeV electron beams and synchrotron-like x-ray beams can be generated. The second experimental area (EA2) will be a very versatile area for fundamental science and applications with flexible focusing geometries, with a third area still to be specified.

ECONOMIC IMPACT OVERVIEW 2020-2021

This year the facilities were significantly impacted by COVID-19. To ensure the safety of our staff, restrictions were put in place, but these directly affected our operational delivery. This year industry contract-access projects amounted to 14 facility access weeks, delivering experimental access to Gemini, Ultra and Octopus, and access to CLF scientific expertise.

New to this year, the Lasers for Science division introduced a COVID-10 Rapid Access mechanism to provide facility access for R&D related to the fight against COVID-19. This facility access 'rapid response' route was a particular success, with most projects led by or including an industry partner. The rapid nature of this unique call enabled the laser facilities to respond quickly to the needs of COVID-19 research, both diagnostic and R&D. The call delivered an additional six weeks of facility access with an industrial partner.

Internationally, the CLF is a project partner organisation on the European Horizon 2020 project IMPULSE (Integrated Management and Reliable Operations for User-based Laser Scientific Excellence) that kicked off this year. This year, a project team was also established with the Extreme Photonics Innovation Centre (EPIC), CLF's partner centre in India, and work has already begun on target fabrication design and developments to advance the capabilities of our facilities.

Despite the effects of COVID-19 on the facilities, CLF scientists continued to be creative and drive forward the innovation portfolio. An additional four proof-of-concept projects were introduced and the CLF filed two new patent families this year, giving a current total of 23 active patent families.

ACCESS TO FACILITIES

The CLF operates "free at the point of access", available to any UK academic or industrial group engaged in open scientific research, subject to external peer review. European collaboration is fully open for the high power lasers, whilst European and International collaborations are also encouraged across the CLF suite for significant fractions of the time. Dedicated access to CLF facilities is awarded to European researchers via the Laserlab-Europe initiative (www.laserlab-europe.net) funded by the European Commission.

Hiring of the facilities and access to CLF expertise is also available on a commercial basis for proprietary or urgent industrial research and development.

Please visit **www.clf.stfc.ac.uk** for more details on all aspects of the CLF.

Industry engagement and innovation

Kathryn Welsby
Central Laser Facility, STFC Rutherford Appleton Laboratory, Harwell Campus, Didcot, UK
Email address: **kathryn.welsby@stfc.ac.uk** Website: **www.clf.stfc.ac.uk**

Introduction

This article highlights the industrial user engagement, industry partnerships, and innovation activities of the Central Laser Facility for the reporting period April 2020 to March 2021.

Industrial users and engagement

The COVID-19 lockdowns of 2020 directly affected the facility delivery, with an initial complete shutdown of all of our facilities. With safe working practices in place, and the majority of our staff working from home, our operational delivery was significantly reduced during the year. Prioritisation of academic operations had a significant impact on our industry user programme and we anticipate this to continue through 2021 and 2022.

The CLF delivered 14 facility access weeks with industrial users this year, delivering experimental access to Gemini, Octopus and Ultra facilities, and access to CLF scientific expertise. With the effect of COVID, we prioritised the utilisation of the CLF's expertise in combination with the world-class facilities. The CLF has continued to drive impact across a wide variety of industrial sectors and to contribute advanced characterisation in industrial R&D, despite the reduced operational delivery.

Over the past year, the CLF's Industry Partnerships and Innovation (IPI) group have delivered multiple expertise consultations with industry partners. In the food technology sector, we have shared our expertise in spectroscopy and microscopy with companies such as Quorn, Intellidigest and PepsiCo; some in further collaboration with STFC's Food Network. We have also worked with the biotechnology and pharmaceutical sectors, and chemical and manufacturing industry.

During 2020, the Lasers for Science division provided a COVID-19 Rapid Access mechanism for facility access for R&D related to the fight against COVID-19. A large proportion of the successful projects were led by or included an industry partner. The rapid nature of this unique call enabled the laser facilities to respond quickly to the needs of COVID-19 research, both diagnostic and R&D. The rapid access worked with SMEs that utilised an additional six weeks facility access to look at everything from drug delivery mechanisms to improving fluorescence markers for increased sensitivity of lateral flow testing.

This year saw the close of the STFC Bridging for Innovators (B4I) programme – an ISCF-funded scheme that was introduced to boost industrial collaboration with national facilities. The programme was highly successful for the CLF, with the laser facilities delivering the most funded projects across any of the facilities at Harwell.

Despite the effects of COVID, the construction of EPAC, our new application based facility, continued with only minor delays. The critical and extensive concrete pour was completed to schedule in November 2020. EPAC will drive the development and application of a completely new class of compact accelerators and advanced sources of laser-based radiation. This will lead to a step change in a number of fields, for example the rapid, 3D imaging of complex or moving structures, or systems under load like engines or turbines.

Industry Partnerships

The CLF's Dr Andy Ward has become a facilities ambassador for the STFC Air Quality Network (SAQN). This network facilitates the exploitation of currently untapped STFC capabilities to enhance and progress

research into air pollution, particularly with relevance to its impact on human health and the environment. Dr Ward's expertise in pollution, micro-plastics and studying droplets using the CLF's state-of-the-art optical trapping capabilities. are an excellent addition to the SAQN.

The CLF's long-standing laser fellowship programme with Johnson Matthey (JM) continued during this year, successfully delivering industrial access to both Ultra and the Octopus facilities. UKRI-EPSRC Innovation Fellow Dr Chris Thornton in partnership with JM, Manufacturing Technology Centre and Warwick Manufacturing Group successfully finished their fellowship, with the additional award of LaserNET US experimental facility access. The fellowship highlighted the importance of the work that the CLF does as a knowledge transfer body for technology innovation.

Innovation

The CLF's IPI group continue to scan for innovative concepts and technology transfer opportunities, to capture and drive forward the most impactful ideas and inventions.

This year the CLF filed two new patent families, giving a current total of 23 active patent families, and eight invention disclosure forms were submitted for consideration for future patent filing. Additionally, four proof-of-concept projects were funded or ongoing, and two CLASP projects have been advanced.

A proof-of-concept project with the CLF's CALTA division was awarded to develop a simple and low cost pulse compression scheme for the CALTA DiPOLE laser technology. The design has the potential to offer a more compact amplifier stage that will reduce the current laser system footprint by half. This reduction in size is an important phase to commercialisation of the novel DiPOLE laser.

Another of our Innovation Projects is looking to develop a prototype super-resolution fluorescence microscope, which will enable cryo correlative light-electron microscopy for a wide range of science applications across the life sciences. This commercialisation opportunity is being carried out in collaboration with the CLF's Target Fabrication group, who are assisting with the manufacture.

This past year, the operations of CLF spinout company Scitech Precision Ltd (SPL) were heavily hit by COVID-19, with many of its core customers experiencing a reduction in operations, subsequently leading to a reduction in orders and turnover. Some 21 institutions engaged with SPL for a total of 63 individual contracts, with a turnover of £182k. During this time SPL moved to a new, dedicated laser machining laboratory on the RAL site, offering improved infrastructure. SPL also engaged in a programme of upgrades to its laser, adding a femto-second laser machining system and upgraded control systems and stages, which will allow it to carry out more processes at a higher level of accuracy.

International Impact

IMPULSE (Integrated Management and Reliable Operations for User-based Laser Scientific Excellence), an ambitious project financed under Horizon 2020 kicked off on 16 December 2020. The project aims to support organisational development, sustainability and excellent science at ELI. Representatives of 15 Consortium partners from 10 European countries plus the UK are participating in this 42-month project, and the CLF is a key advisory partner in the consortium. Initial meetings have been scoping out the collaborations between STFC and the ELI partners.

The hub for innovation called the Extreme Photonics Innovation Centre (EPIC) in India, jointly-funded by the CLF and the Tata Institute of Fundamental Research (TIFR), was also affected by COVID-19. Whilst working remotely, the team focused on setting specifications for the tape-drive coating system in collaboration with the CLF's Target Fabrication group. The EPIC team also developed detailed project plans. Project teams have since been set up, allowing initial collaborations to develop.

Communication and outreach activities within the CLF

Helen Towrie
Central Laser Facility, STFC Rutherford Appleton Laboratory, Harwell Campus, Didcot, UK
Email address: **helen.towrie@stfc.ac.uk** Website: **www.clf.stfc.ac.uk** Twitter: **@CLF_STFC**

The CLF's Communication Strategies

The role of the CLF's Impact and Engagement team is to promote CLF science and technology to some of our key audiences and share what we are capable of, to engage with our community and recruit new people. Different audiences require different types of interaction, and we have worked to develop and harness the tools needed to communicate with each effectively.

We are responsible for internal and external engagement functions, including: the CLF website and twitter for our general science audience, staff and user community; talks, tours and activities for our general and next gen audiences; and a fortnightly newsletter for staff.

In 2020/21, the COVID-19 pandemic restricted almost all of our usual operations. Despite this, the team achieved substantial communications projects, campaigns and successes, as summarised below.

Social Media:

Social media continues to be a key part of how we share our stories directly with users and the public. The CLF twitter, which was created in 2018, now has 850 followers and we regularly use it to interact with PIs, users and staff.

We are pleased to see that the amount of new followers we gained almost doubled this year compared to last year, as our efforts have been focused on growing a larger following.

2019/20	**587**	(187 more than the year before)
2020/21	**850**	(263 more than the year before)

This year, the Impact and Engagement team has held monthly meetings to analyse the CLF twitter's growth, looking in particular at what tweets worked, what did not, and who is following or interacting with us. This analysis has proved invaluable, as it has allowed us to make informed decisions to help grow the twitter's followers.

One of our larger campaigns was to celebrate the Octopus Laser Facility's 10 year anniversary in late 2020. With lockdowns preventing in-person events, we relied on social media more than ever to share milestones like this. With the help of Octopus staff, we published a series of tweets highlighting some of Octopus' many successes over the years. To help boost this campaign, we also created an illustration to show Octopus' diverse set of labs and applications.

Pictured here is Phil Rice with the Ventilator

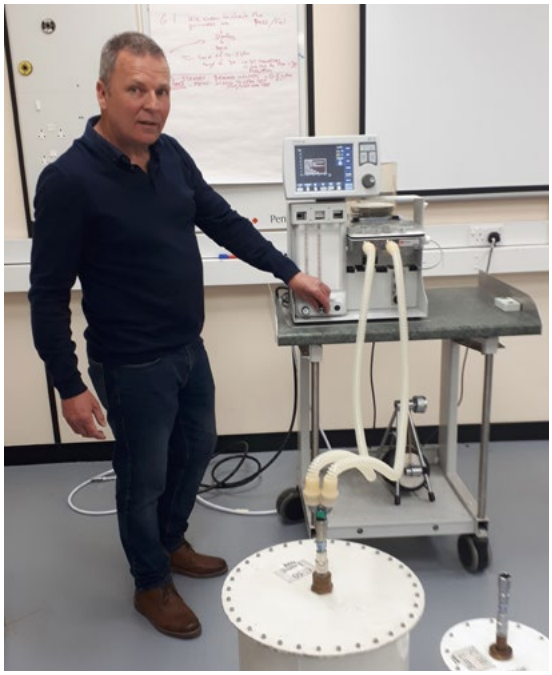

Another campaign that we had the privilege of reporting on during lockdown was the Ventilator Challenge. Engineers at the CLF along with other departments at RAL helped lead the way towards the production of new ventilators, easing the national ventilator shortage. Applying their expertise in this way was a huge act of selflessness, and CLF engineer Phil Rice ended up on BBC South Today!

We continue to keep in close contact with the STFC twitter and Instagram team, through whom we can reach a more general public audience as opposed to the general scientific audience that the CLF twitter aims to attract. To aid these discussions and others, a CLF representative attends a monthly Social Media meeting where all the departments can communicate new ideas, campaigns and best practices.

The CLF website:
Summary Financial Year: 2020/21

Amount of people who visited the website
29,000

Unique page views
(Bots subtracted)
79,649

Social referrals out of 29,000 users:

Twitter
971

Facebook
673

LinkedIn
149

YouTube
17

Instagram
3

As we expected, due to the COVID-19 pandemic, we have had fewer people visiting our website (32,000 in 2019/20). This could be due to a number of prohibiting factors, such as lockdowns halting experiments and users (our main audience) being furloughed.

It is, however, good to see that we have had more people coming from twitter (935 in 2019/20). This suggests that the growth of our twitter is also leading more people to our website through this channel.

Attracting a wider audience

And maintaining all avenues of communication

This year has stifled our opportunities to connect face-to-face, but it has given us an opportunity to embark on innovative new ways to engage with virtual audiences.

A small, but not unimportant, contribution from the CLF happened right at the beginning of lockdowns, when it became clear that children from underserved communities may not have the same computer access as others. Through the STFC's Wonder Initiative, the CLF Impact and Engagement team contributed science-focused illustrations to colour in for "Wonder Packs", which were posted physically to underserved communities in the most socioeconomically-deprived areas of the UK.

We also debuted our first CLF "story", based on the creation of a Supernova using the Vulcan Laser. Designed for young audiences, this story was first told at RAL Stargazing, and has been retold multiple times since by popular demand. The story was also featured amongst other talks at a virtual event organised by the CLF to celebrate International Day of Light.

International Day of Light

82
people joined the event

From the feedback
(about a quarter of people completed the feedback):

30% **of the audience were 8-14 year olds**

23% **were from Wonder audiences**
(in the 40% most deprived areas of the country, by the indices of multiple deprivation)

4.9/5 **Average satisfaction rating**

Comments:

"This is the first of your events that I have connected to and, as an amateur astronomer who has taken images of the residue from Black Hole formation, I was especially intrigued with your simulation just down the road from where I live!!"

"Even with the technical problems it was a well thought and delivered webinar, all speakers explained everything In a way we all could understand."

"Excellent thanks - I learnt lots of things about lasers that I didn't know I didn't know!"

"Fantastic inspiring range speakers and wonderful science. Speakers were able to respond to children's questions clearly and with ease."

"I loved being able to join from the U.S. My kids attend school online on Fridays and they had just finished their lesson so this was a great thing for them to watch. They were both interested! Thanks for inviting us!"

Public Engagement Overview:

Overall, the CLF has taken part in multiple events, despite lockdowns. These events have been well attended and we have engaged with a key audience – 8-14 year olds. This is the age where children are starting to think about their future careers, and is also around the age when many young girls unfortunately decide that science and engineering is not for them. The headline stats for 2020/21 Public Engagement relating to the CLF include:

- Total people engaged via public engagement programme: 1156, of which:
  - 1063 public (family audiences, so estimate ~30% were age 8-14, a key target)
  - 17 secondary school (teachers and students) at school events
  - 9 confirmed work experience placements – placements did not go ahead, but students attended a series of webinars instead
- This was at 9 events, plus work experience students placed with CLF
- 9 CLF staff volunteered at least once (note that some staff volunteered at non-CLF events)

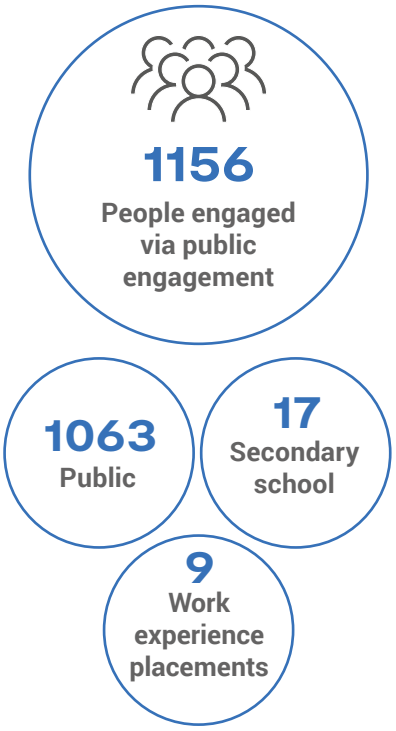

COVID-19 Response:

As we all know, 2020/21 was hit by worldwide lockdowns due to the novel virus COVID-19. From day one, the Impact and Engagement team worked to keep the website up to date with guidelines for users and other key information.

As no tours or face-to-face events have been possible, we have focused our efforts on connecting with the public digitally, which has included creating a story about an experiment, having people live broadcast a tour of their labs, and even 'hosting' a full virtual event to celebrate International Day of Light.

Our dedicated CLF in.brief that began during lockdown blossomed into a fantastic way to share light-hearted news and updates to all CLF staff. This has not only helped us share important updates and information with staff, but it has also enabled us to maintain the community feel and the personal connections between staff, despite the majority of staff working remotely during this time.

In memory of an outstanding experimental plasma physicist, and pioneer of laser plasma interactions

Professor David Neely

1965 - 2020

Professor David Neely, a pioneer in experimental High Energy Density Plasmas (HEDP), internationally recognised experimental physicist and a community champion, passed away after a short and sudden illness in August 2020.

David was born in Londonderry, Northern Ireland. He studied physics at Queen's University Belfast (QUB), and completed his PhD there on the generation of soft x-ray laser pulses, under the supervision of Professor Ciaran Lewis. He worked as a Research Assistant at QUB, teaching and supporting the undergraduate research laboratories, before joining the CLF in 1993.

David's passion for his research always shone through, proving instrumental in developing ideas and concepts that have kept the CLF at the forefront of scientific achievements. He was a strong advocate for the new EPAC facility and Vulcan 20-20 upgrade, recognising their potential to enhance research in his many areas of interest. Over the years, David pioneered experiments exploring laser driven ion and electron acceleration, fusion studies, high harmonic production, shocks, plasma diagnostics and industrial applications. As short pulse laser power steadily increased and attained PW performance, this enabled him to carry out experiments fully in the relativistic interaction regime. His interest in pre-plasma free interactions led to the utilisation of plasma mirrors in 2005 to enhance the laser contrast. This made it possible to accelerate protons to energies in the 100 MeV range using a technique called radiation transparency acceleration that depends on relativistic effects. Working with colleagues from Dstl, David

developed the idea of an x-ray "radar" that could potentially be used to probe the contents of containers remotely, and investigated using muons as a potential probe. His expertise was sought by space scientists to see how lasers could be used to de-orbit space debris, a potential hazard to satellites.

In 2005, David was promoted to lead the CLF's Experimental Science Group ,and in 2010 he became the Head of High Power Laser Science. In 2012, he was awarded an STFC Research Fellowship, to carry out independent research in high energy density science. David was a natural communicator, who formed collaborations and friendships around the world. Working with his extensive network of colleagues, he was able to carry out experiments on high power laser facilities throughout Europe, Asia and the USA. He held a Visiting Mitsuyuki Abe Chair position at the Proton Medical Research Centre, Japan Atomic Energy Agency, and was awarded the Medal of International Collaboration of the Chinese Academy of Sciences for setting up a government funded UK-China collaboration, giving him an even greater international profile. David's appointment to a Visiting Professorship at the University of Strathclyde in 2012 enabled him to co-supervise PhD students and enhance his research portfolio. He formed close and successful working relationships with his students, many of whom have gone on to take up positions at national and international laser facilities. David also took a very active role on the Editorial Board of ***High Power Laser Science and Engineering (HPLSE)***.

David's passing continues to be felt within the CLF and across the high energy density physics community. His contribution will never be forgotten.

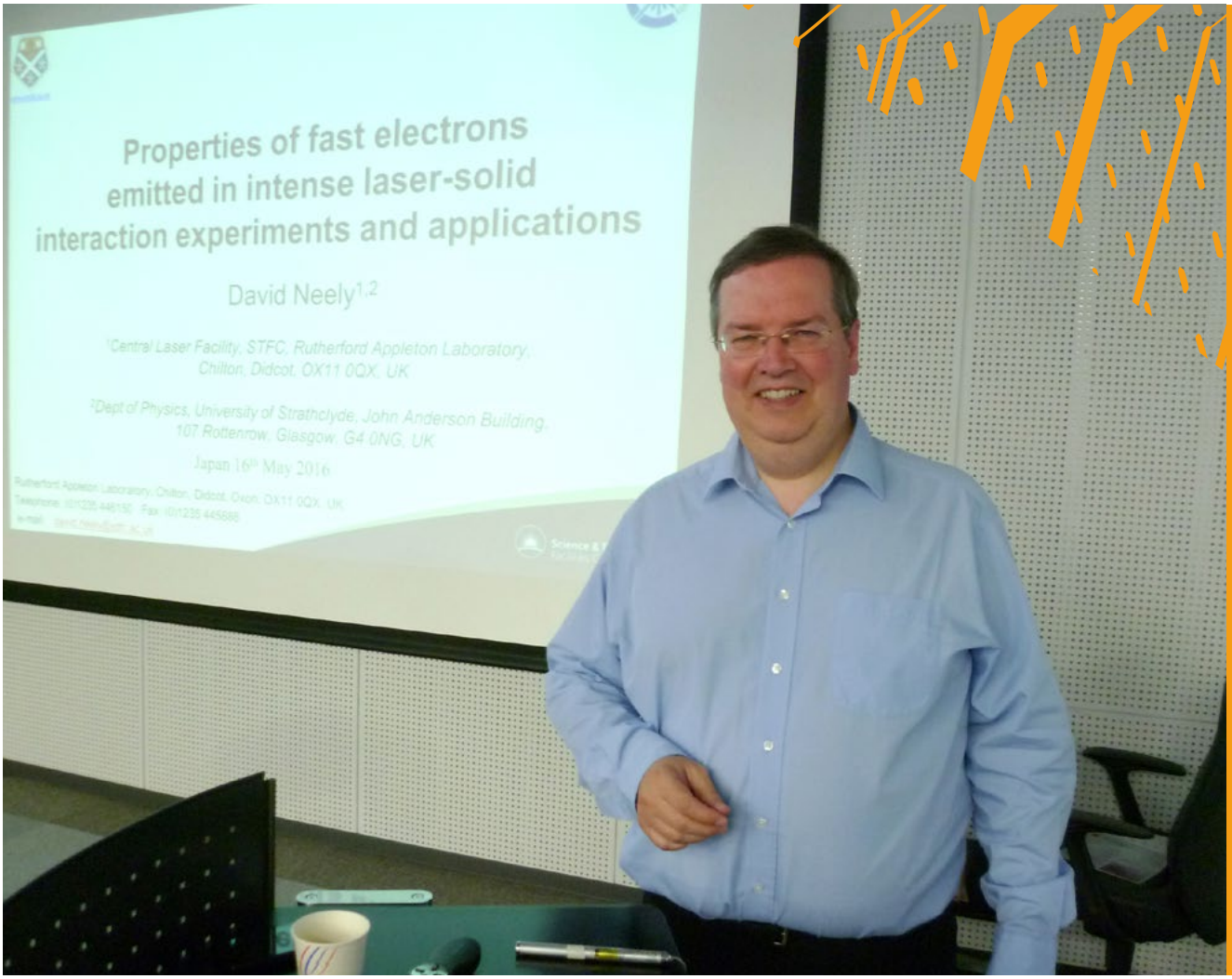

EPAC takes shape on the RAL Campus

Exciting progress has been made during the year on construction of the CLF's pioneering Extreme Photonics Applications Centre (EPAC).

Despite the on-going restrictions and work controls arising from the Coronavirus pandemic, construction work proceeded at pace. During 2020 a clear outline of the whole building envelope became visible. Some 7,500 m^3 of concrete was poured as the new building rose from the ground. The three experimental areas have two metre thick walls to provide appropriate shielding for the high energy experiments that will take place. A dedicated "test pour" and associated instrumentation gave confidence that cracking would not occur as the concrete mix dried out.

On the design side, work continued to finalise the internal building design ready for fit-out and commissioning, and to progress designs for the installed equipment. Despite the difficulties of remote working, good progress was made, and the essential tasks remained on schedule.

Professor John Collier, Director of STFC's Central Laser Facility, said:

"EPAC will drive the development and application of a completely new class of compact accelerators and advanced sources of radiation based on lasers. We expect this to lead to a step change in a number of fields, for example the rapid, 3D imaging of complex or moving structures, or systems under load like engines or turbines.

We've reached a very significant milestone for EPAC. I am delighted that this has been achieved on schedule whilst adhering to the necessary coronavirus controls, such as social distancing. This is a great credit to Mace, our construction partners, and the very effective collaboration with CLF staff."

EPAC is a new state-of-the-art high repetition rate laser-driven imaging facility that is being funded by the UK government through UKRI and partially the Ministry of Defence. Designed and hosted by the CLF on the STFC Rutherford Appleton Laboratory site, EPAC will provide a step-change in capabilities for laser-driven accelerator research in the UK, enabling cutting-edge experiments in plasma physics, laboratory astrophysics and condensed matter and material science. The unique capabilities of EPAC – combining near-light speed particles and synchronised ultra-intense electromagnetic fields – will provide a world-leading platform capable of generating extreme states of matter and the tools to probe, control and manipulate them, enabling exploration of some fundamental questions in nature including those in quantum electrodynamics. EPAC will image objects ranging from a piece of bone to complex working structures, like an engine in 3D at ultra-high contrast. These images will allow industrial and scientific users to explore and better understand both material properties and product performance at previously unreachable levels of detail, leading to better materials and products for end consumers. The facility will be open to users by 2026.

From this in April 2020…

To this in April 2021

Low carbon concrete has been used, comprising 75% Ground Granulated Blast Furnace Slag (GGBS) instead of traditional Portland Cement. This has reduced the carbon footprint by 48%, saving 1,373 tonnes compared to normal practice.

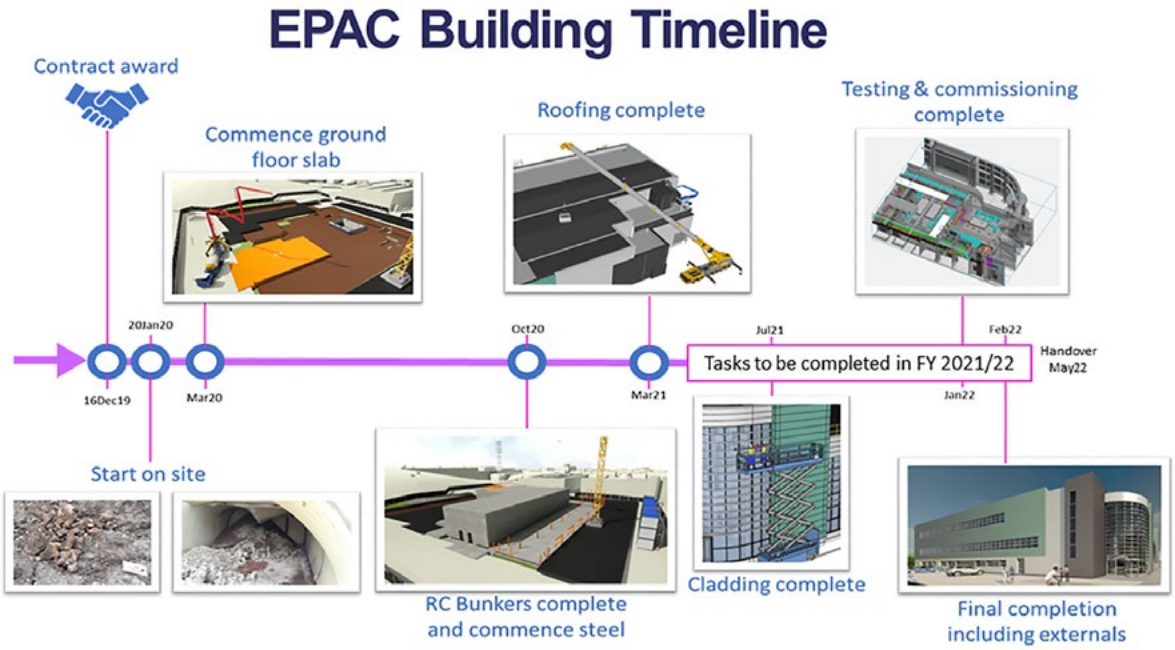

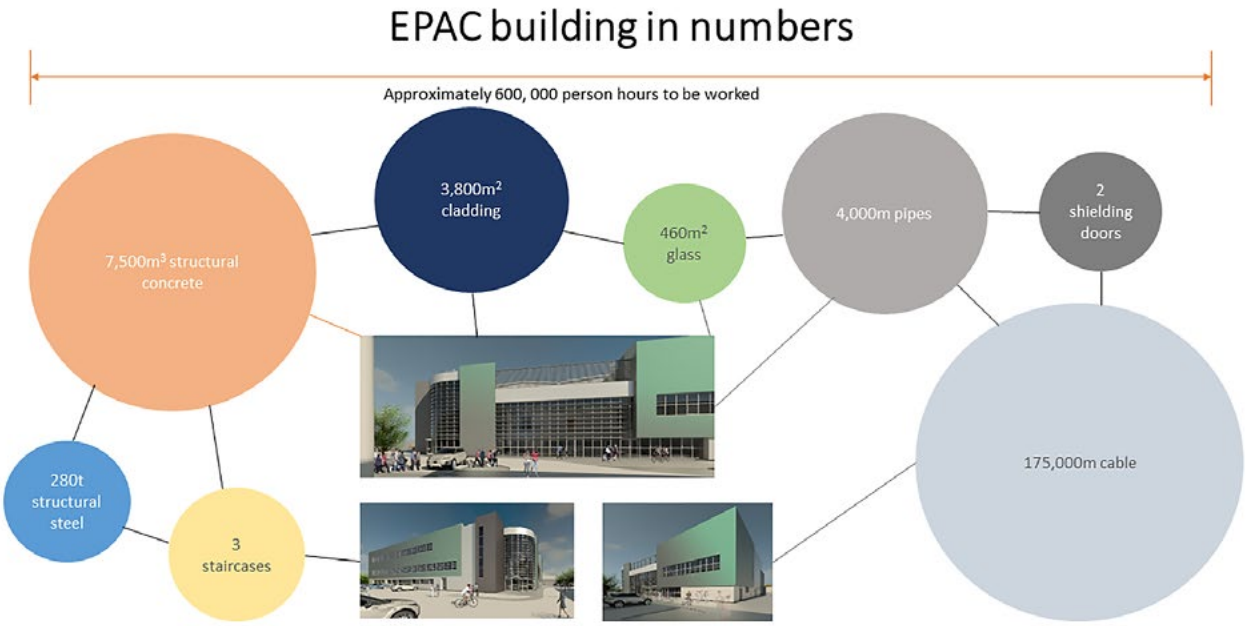

High energy density and high intensity physics

Measuring the orbital angular momentum of high-power laser pulses

R. Aboushelbaya, A.F. Savin, M. Mayr, B. Spiers, R. Wang *(Clarendon Laboratory, University of Oxford, UK)*
K. Glize, N. Bourgeois, R. Bingham *(Central Laser Facility, STFC Rutherford Appleton Laboratory, Harwell Campus, Didcot, UK)*
C. Spindloe *(Scitech Precision Ltd, STFC Rutherford Appleton Laboratory, Didcot, UK)*
P. Norreys *(Clarendon Laboratory, University of Oxford, UK; Central Laser Facility, STFC Rutherford Appleton Laboratory, Harwell Campus, Didcot, UK; John Adams Institute for Accelerator Science, University of Oxford, UK)*

In this article, we showcase the experimental results of methods to produce and characterise orbital angular momentum (OAM) carrying high-power lasers. The OAM pulses were produced on the Gemini laser of the Central Laser Facility using a continuous spiral phase plate.

Three different characterisation methods were then used to measure the OAM content of the beam. The methods that were used were a cylindrical lens diagnostic, an interferometric diagnostic, and a projective diagnostic. We further discuss the relative advantages and disadvantages of each method in the context of high-power laser experiments.

Reprinted with permission from R. Aboushelbaya, K. Glize, A.F. Savin et al. Measuring the orbital angular momentum of high-power laser pulses, Phys. Plasmas 27, 053107 (2020); doi: 10.1063/5.0005140

Contact: R. Aboushelbaya
(ramy.aboushelbaya@physics.ox.ac.uk)

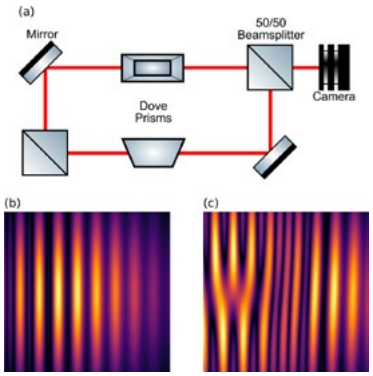

Figure 1

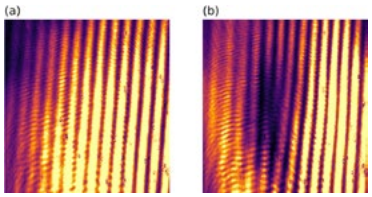

Figure 2

Figure 1: (a) Basic schematic showing the optical setup for the OAM interferometer.(b) and (c) Simulated results for the output of the interferometer in the case of a normal Gaussian profile and a LG with l = 1, respectively.

Figure 2: Experimental results for the interferometric diagnostic on the Gemini laser. (a) The result for the standard beam without the SPP, so l = 0, shows the typical fringes usually seen in interferometers. (b) When the SPP is placed in the beam path, the profile of the fringes changes and a discontinuity similar to the one in Figure 1 (c) is seen, indicating the presence of OAM

Application of compact laser-driven accelerator X-ray sources for industrial imaging

J-N. Gruse, S.P.D. Mangles, Z. Najmudin, J.C. Wood *(The John Adams Institute for Accelerator Science, Imperial College London, UK)*
M.J.V. Streeter *(The John Adams Institute for Accelerator Science, Imperial College London, UK; Physics Department, Lancaster University, UK)*
C. Thornton, C.D. Armstrong, N. Bourgeois, C.D. Gregory,, Y. Katzir, D. Neely, P.P. Rajeev, D.R. Rusby, C.M. Brenner, D.R. Symes *(Central Laser Facility, STFC Rutherford Appleton Laboratory, Harwell Campus, Didcot, UK)*
C.D. Baird *(York Plasma Institute, Department of Physics, University of York, UK; Central Laser Facility, STFC Rutherford Appleton Laboratory, Harwell Campus, Didcot, UK)*
S. Cipiccia *(Diamond Light Source, Harwell Science and Innovation Campus, Didcot, UK)*
O.J. Finlay *(Physics Department, Lancaster University, UK)*
N.C. Lopes *(The John Adams Institute for Accelerator Science, Imperial College London, UK; GoLP, IPFN, Instituto Superior Tecnico, U. Lisboa, Portugal)*
L.R. Pickard *(National Composites Centre, Bristol and Bath Science Park, Bristol, UK)*
K.D. Potter *(Advanced Composites Collaboration for Science and Innovation (ACCIS) University of Bristol, UK)*
C.I.D. Underwood, C.D. Murphy *(York Plasma Institute, Department of Physics, University of York, UK)*
J.M. Warnett, M.A. Williams *(WMG, University of Warwick, UK)*

X-rays generated by betatron oscillations of electrons in a laser-driven plasma accelerator were characterised and applied to imaging industrial samples. With a 125 TW laser, a low divergence beam with 5.2 ± 1.7 × 10^7 photons $mrad^{-2}$ per pulse was produced with a synchrotron spectrum with a critical energy of 14.6 ± 1.3 keV. Radiographs were obtained of a metrology test sample, battery electrodes, and a damage site in a composite material. These results demonstrate the suitability of the source for non-destructive evaluation applications. The potential for industrial implementation of plasma accelerators is discussed.

Reprinted from J.-N Gruse et al. Application of compact laser-driven accelerator x-ray sources for industrial imaging, Nucl. Instrum. Methods Phys. Res. Sect. A 983, 164369 (2020), under the terms of the Creative Commons CC-BY license. doi: 10.1016/j.nima.2020.164369

Contacts: J.-N. Gruse (j.gruse16@imperial.ac.uk)
D.R. Symes (dan.symes@stfc.ac.uk)

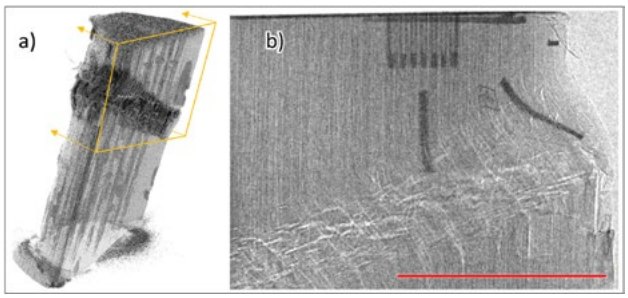

Kink band failure in a composite cylinder initiated by impact and propagated by compressive end loading. (a) tomographic reconstruction obtained using conventional lab x-ray CT (b) radiograph obtained with the laser-betatron source with carbon fibre tows visible. The red line indicates 1 cm. (For interpretation of the references to colour in this figure legend, the reader is referred to the web version of this article.)

A laser-plasma platform for ultra-fast absorption spectroscopy: measuring the electron-ion equilibration rate of warm dense matter

B. Kettle, C. Colgan, E. Los, E. Gerstmayr, R.A. Baggott, R. Watt, S.J. Rose, S.P.D. Mangles *(The John Adams Institute for Accelerator Science, Blackett Laboratory, Imperial College London, UK)*
M.J.V. Streeter, N. Cavanagh, D. Riley, G. Sarri *(Department of Physics and Astronomy, Queen's University Belfast, UK)*
F. Albert *(Lawrence Livermore National Laboratory, Livermore, California, USA)*
S. Astbury, P.P. Rajeev, C. Spindloe, D. Symes, C. Thornton *(Central Laser Facility, STFC Rutherford Appleton Laboratory, Harwell Campus, Didcot, UK)*
K. Falk, M. Šmíd *(Helmholtz-Zentrum Dresden-Rossendorf, Germany)*
O. Lundh, K. Svendsen *(Department of Physics, Lund University, Sweden)*
A.G.R. Thomas *(Center for Ultrafast Optical Science, University of Michigan, USA)*

The K-edge absorption profile of a copper sample has been measured over a 200 eV spectral window on a single shot using the ultrafast x-rays from a laser-wakefield accelerator. This provides simultaneous snapshot details of the samples electronic and ionic configurations through the XANES (X-ray Absorption Near Edge Structure) and EXAFS (Extended X-ray Absorption Fine Structure) profiles. We discuss how, when combined with an appropriate sample heating technique, this unique x-ray source could be used to measure ultrafast processes in high density matter, for example the electron-ion equilibration rates of warm dense samples.

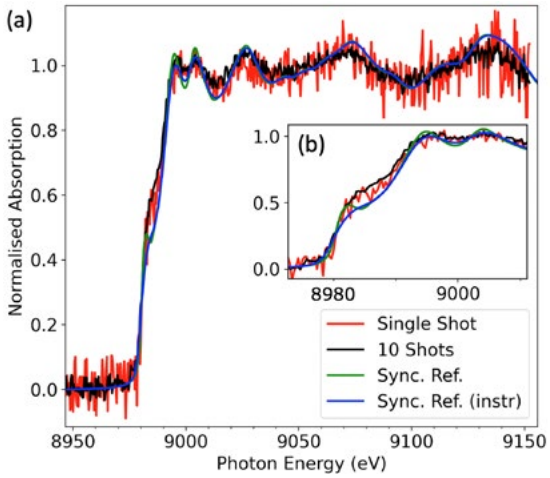

(a) Normalised absorption profile of a 4 μm copper foil. Data is shown for a single shot (red) and the average of ten shots (black). Both are compared to a synchrotron reference (green) and the same reference which has been convolved with our simulated instrument response (blue). (b) A zoomed view of the near edge profile.

Contact: B. Kettle (b.kettle@imperial.ac.uk)

Nonlinear wakefields and electron injection in cluster plasma

M.W. Mayr, B. Spiers, R. Aboushelbaya, R.W. Paddock, C. Sillett, R.H.W. Wang *(Clarendon Laboratory, University of Oxford, UK)*
J.D. Sadler *(Los Alamos National Laboratory, New Mexico, USA)*
K. Krushelnick *(Center for Ultrafast Optical Science, University of Michigan, USA)*
P.A. Norreys *(Central Laser Facility, STFC Rutherford Appleton Laboratory, Harwell Campus, Didcot, UK; Clarendon Laboratory, University of Oxford, UK; John Adams Institute for Accelerator Science and Department of Physics, University of Oxford, UK)*

Laser and beam driven wakefields promise orders of magnitude increases in electric field gradients for particle accelerators for future applications. Key areas to explore include the emittance properties of the generated beams and overcoming the dephasing limit in the plasma. In this paper, the first in-depth study of the self-injection mechanism into wakefield structures from nonhomogeneous cluster plasmas is provided using high-resolution two dimensional particle-in-cell simulations. The clusters which are typical structures caused by ejection of gases from a high-pressure gas jet have a diameter much smaller than the laser wavelength. Conclusive evidence is provided for the underlying mechanism that leads to particle trapping, comparing uniform and cluster plasma cases. The accelerated electron beam properties are found to be tunable by changing the cluster parameters. The mechanism explains enhanced beam charge paired with large transverse momentum and energy which has implications for the betatron x-ray flux. Finally, the impact of clusters on the high-power laser propagation behavior is discussed.

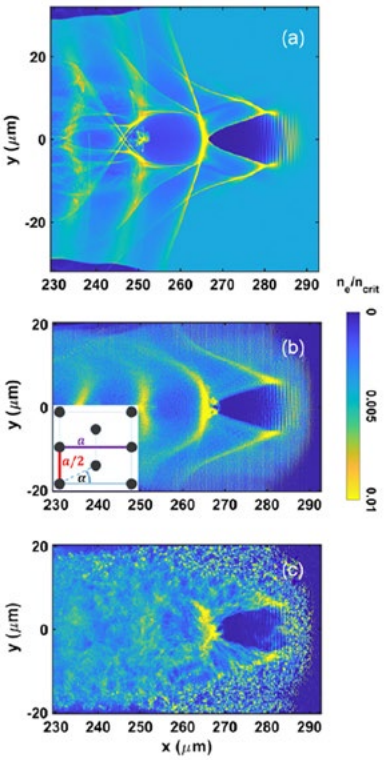

Results of PIC simulations A, B, and C (parameters according to Table I in the published paper). Electron density normalized to critical density for (a) a uniform plasma, (b) a plasma of clusters arranged in a staggered grid, and (c) a plasma of clusters with random positions after 0.76 ps.

*Reprinted from M.W. Mayr et al. Nonlinear wakefields and electron injection in cluster plasma, Rev. Accel. Beams **23**, 081303 (2020), under the terms of the Creative Commons Attribution 4.0 International License. doi: 10.1103/PhysRevAccelBeams.23.093501*

Contact: M.W. Mayr (marko.mayr@physics.ox.ac.uk)

Metre-scale conditioned hydrodynamic optical-field-ionized plasma channels

A. Picksley, A. Alejo, R.J. Shalloo, C. Arran, A. von Boetticher, J.A. Holloway, J. Jonnerby, O. Jakobsson, R. Walczak, S.M. Hooker *(John Adams Institute for Accelerator Science and Department of Physics, University of Oxford, UK)*

C. Thornton *(Central Laser Facility, STFC Rutherford Appleton Laboratory, Harwell Campus, Didcot, UK)*
L. Corner *(Cockcroft Institute for Accelerator Science and Technology, School of Engineering, University of Liverpool, UK)*

We demonstrate through experiments and numerical simulations that low-density, low-loss, metre-scale plasma channels can be generated by employing a conditioning laser pulse to ionize the neutral gas collar surrounding a hydrodynamic optical-field-ionized (HOFI) plasma channel. We use particle-in-cell simulations to show that the leading edge of the conditioning pulse ionizes the neutral gas collar to generate a deep, low-loss plasma channel which guides the bulk of the conditioning pulse itself as well as any subsequently injected pulses. In proof-of-principle experiments, we generate conditioned HOFI (CHOFI) waveguides with axial electron densities of $n_{e0} \approx 1 \times 10^{17}\,\mathrm{cm}^{-3}$ and a matched spot size of 26 μm. The power attenuation length of these CHOFI channels was calculated to be L_{att} = (21 ± 3) m, more than two orders of magnitude longer than achieved by HOFI channels. Hydrodynamic and particle-in-cell simulations demonstrate that metre-scale CHOFI waveguides with attenuation lengths exceeding 1 m could be generated with a total laser pulse energy of only 1.2 J per metre of channel. The properties of CHOFI channels are ideally suited to many applications in high-intensity light-matter interactions, including multi-GeV plasma accelerator stages operating at high pulse repetition rates.

Reprinted with permission from Picksley A, Alejo A, Shalloo RJ, et al., 2020, Meter-scale conditioned hydrodynamic optical-field-ionized plasma channels, Phys. Rev. E 102, 053201, ©2020 American Physical Society. doi: 10.1103/PhysRevE.102.053201

Contact: S.M. Hooker (simon.hooker@physics.ox.ac.uk)

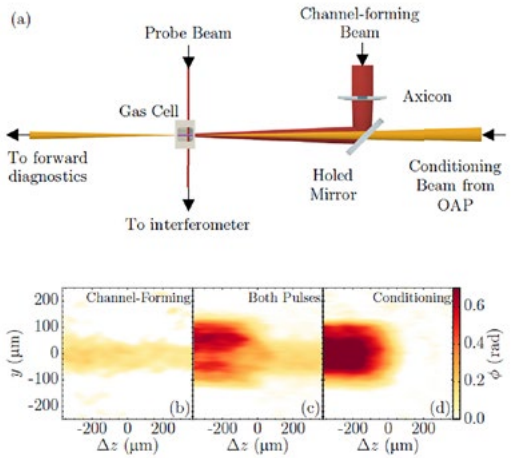

Figure 1: (a) Schematic of the experimental interaction region. [(b)–(d)] Phase shifts measured by the transverse probe beam at z ≈ 3.5 mm for (b) the channel-forming pulse alone, (c) the channel-forming pulse and the conditioning pulse at a delay τ = 1.5 ns; and (d) the conditioning pulse alone

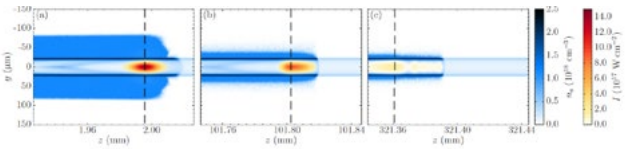

Figure 2: Transverse profiles of the electron density and the laser intensity when the peak of the conditioning pulse, indicated by the dashed line, has reached (a) z = 2 mm, (b) z = 101 mm, and (c) z = 321 mm. The input intensity of the conditioning pulse was I_{peak} = 6.0×10^{17} Wcm^{-2}

Guiding of high-intensity laser pulses in 100-mm-long hydrodynamic optical-field-ionized plasma channels

A. Picksley, A. Alejo, J. Cowley, J. Holloway, J. Jonnerby, A.J. Ross, R. Walczak, S.M. Hooker *(John Adams Institute for Accelerator Science and Department of Physics, University of Oxford, UK)*
N. Bourgeois *(Central Laser Facility, STFC Rutherford Appleton Laboratory, Harwell Campus, Didcot, UK)*
L. Corner, H. Jones, L.R. Reid *(Cockcroft Institute for Accelerator Science and Technology, School of Engineering, University of Liverpool, UK)*
L. Feder, H.M. Milchberg *(Institute for Research in Electronics and Applied Physics, University of Maryland, USA)*

Hydrodynamic optically-field-ionized (HOFI) plasma channels up to 100 mm long are investigated. Optical guiding is demonstrated of laser pulses with a peak input intensity of 6×10^{17} W cm^{-2} through 100 mm long plasma channels with on-axis densities measured interferometrically to be as low as $n_{e0} = (1.0 \pm 0.3) \times 10^{17}$ cm^{-3}. Guiding is also observed at lower axial densities, which are inferred from magneto-hydrodynamic simulations to be approximately 7×10^{16} cm^{-3}. Measurements of the power attenuation lengths of the channels are shown to be in good agreement with those calculated from the measured transverse electron density profiles. To our knowledge, the plasma channels investigated in this work are the longest, and have the lowest on-axis density, of any free-standing waveguide demonstrated to guide laser pulses with intensities above >10^{17} W cm^{-2}.

Reprinted from Picksley A, Alejo A, Cowley J, et al., 2020, Guiding of high-intensity laser pulses in 100-mm-long hydrodynamic optical-field-ionized plasma channels, Phys. Rev. Accel. Beams 23, 081303, under the terms of the Creative Commons 4.0 International License. doi: 10.1103/PhysRevAccelBeams.23.081303

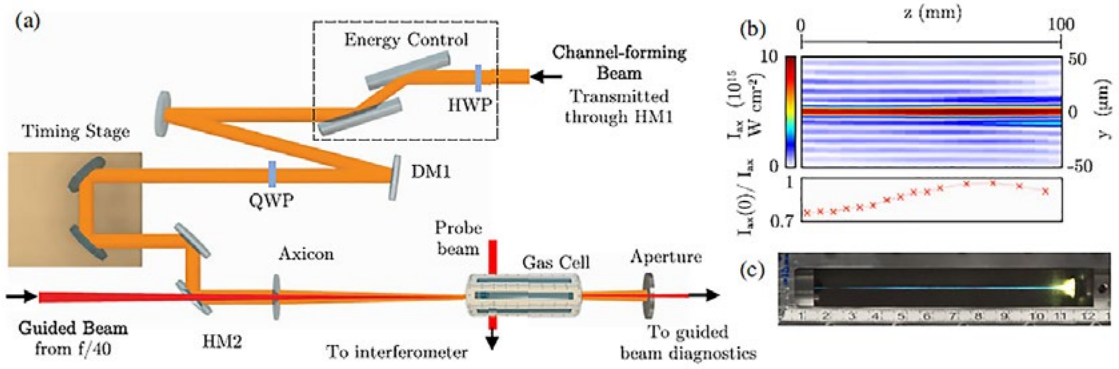

Figure 1: (a) Schematic diagram of the experiment layout. (b) Longitudinal variation of the transverse intensity profile of the axicon focus, measured in vacuo by a camera in the vacuum chamber. The red curve shows the axial intensity I_{ax} as a function of longitudinal position. (c) Time-integrated image of the visible plasma emission produced by the channel-forming beam focused into the gas cell at a fill pressure P = 26 mbar. The scale visible at the bottom of the image is in cm. Note that the apparent decrease in plasma brightness near a scale reading of 2.5 cm arises from blackening of the cell window in that region, not from non-uniformity of the plasma.

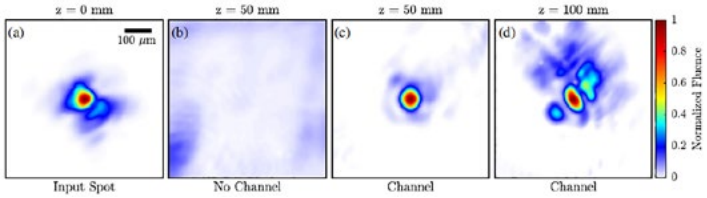

Figure 2: Measured transverse fluence profiles of the guided beam at: (a) focus, in vacuum; (b) z = 50 mm, in vacuum; (c) z = 50 mm, for P = 68 mbar and τ = 3.0 ns; (d) z = 100 mm, for P = 26 mbar and τ = 2.7 ns. The transverse scale is the same for all plots, as indicated by the scale bar shown in (a). For plots (a), (c), and (d) the fluence is normalized to the peak value in that plot; the fluence scale for (b) is the same as in (a). Compared to (a), the fluence scales of (c) and (d) were increased by factors of approximately 4 and 7 respectively.

Contact: S.M. Hooker (simon.hooker@physics.ox.ac.uk)

Spectral and spatial characterisation of GeV-scale laser-driven positron beams

M.J.V. Streeter, N. Cavanagh, T. Audet, L. Calvin, G. Sarri *(Centre for Plasma Physics, School of Mathematics and Physics, Queen's University Belfast, UK)*
C. Colgan, E. Los, B. Kettle, S.P.D. Mangles, Z. Najmudin *(The John Adams Institute for Accelerator Science, Imperial College London, UK)*
A. Antoine, M. Balcazar, J. Carderelli, Y. Ma, A.G.R. Thomas *(Center for Ultrafast Optical Science, University of Michigan, USA)*
H. Ahmed, P.P. Rajeev, D.R. Symes *(Central Laser Facility, STFC Rutherford Appleton Laboratory, Harwell Campus, Didcot, UK)*

We report here on the first comprehensive characterisation of laser-driven positron beams with near-GeV energies, generated using Gemini. This work demonstrates that sizeable positron beams with micron-scale source size and nm-scale geometrical emittance can be generated using laser parameters that are available with commercial systems. Such positron beams are of sufficient quality to be further injected in a plasma-based wakefield accelerator, demonstrating the first step towards a plasma-based positron accelerator.

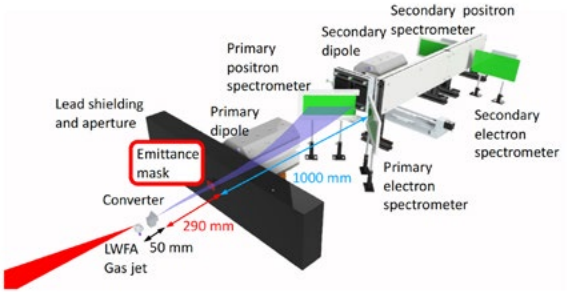

Figure 1: Schematic of the experimental setup. The laser is focused into the gas jet to drive the Laser-Wakefield Accelerator, which generates the primary electron beam. This electron beam produces electron-positron pairs in the converter which then propagate through an aperture in the lead wall. The primary dipole disperses the electron and positron beams (positrons shown in blue) onto the spectrometer screens. The emittance mask can be placed into the beam to measure the electron and positron beam spatial properties. A secondary electron spectrometer screen is used to improve the accuracy of the electron spectrum measurement. The secondary dipole and positron spectrometer screen is used to be perform energy selection.

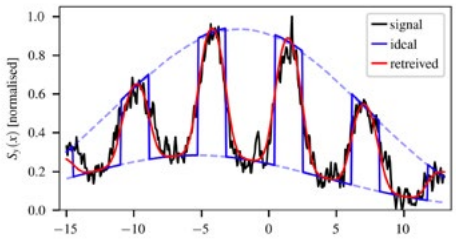

Figure 2: Example signal modulation fitting for beam parameters retrieval. The signal (black line) is taken for a central positron energy of 420MeV with a converter thickness of 8 mm. The retrieved signal (red line) corresponds to a source size of 127 μm. An ideal beam (zero source size) would produce a rectangular profile pattern (blue line) between the scattered signal and the beam amplitude (blue dashed lines).

Contact: G. Sarri (g.sarri@qub.ac.uk)

Automation and control of laser wakefield accelerators using Bayesian optimization

R.J. Shalloo, J-N. Gruse, M. Backhouse, S.P.D. Mangles, Z. Najmudin, S. Rozario, M.J.V. Streeter *(The John Adams Institute for Accelerator Science, Imperial College London, UK)*
S.J.D. Dann, N. Bourgeois, P.P. Rajeev, D.R. Symes, C. Thornton *(Central Laser Facility, STFC Rutherford Appleton Laboratory, Harwell Campus, Didcot, UK)*
C.I.D. Underwood, C.Arran, C.D. Murphy, C.P. Ridgers, M.P. Selwood *(York Plasma Institute, Department of Physics, University of York, UK)*
P. Hatfield *(Clarendon Laboratory, University of Oxford, UK)*
C.D. Baird *(York Plasma Institute, Department of Physics, University of York, UK; Central Laser Facility, STFC Rutherford Appleton Laboratory, Harwell Campus, Didcot, UK)*
A.F. Antoine, M.D. Balcazar, J.A. Cardarelli, K. Krushelnick, A.G.R. Thomas *(Center for Ultrafast Optical Science, University of Michigan, USA)*
J. Kang *(Department of Chemical Engineering, University of Michigan, USA)*
N. Lu, A.J. Shahani *(Department of Materials Science and Engineering, University of Michigan, USA)*
J. Osterhoff, K. Pöder *(Deutsches Elektronen-Synchrotron DESY, Hamburg, Germany)*

Laser wakefield accelerators promise to revolutionize many areas of accelerator science. However, one of the greatest challenges to their widespread adoption is the difficulty in control and optimization of the accelerator outputs due to coupling between input parameters and the dynamic evolution of the accelerating structure. Here, we use machine learning techniques to automate a 100 MeV-scale accelerator, which optimized its outputs by simultaneously varying up to six parameters including the spectral and spatial phase of the laser and the plasma density and length. Most notably, the model built by the algorithm enabled optimization of the laser evolution that might otherwise have been missed in single-variable scans. Subtle tuning of the laser pulse shape caused an 80% increase in electron beam charge, despite the pulse length changing by just 1%.

Shalloo, R.J., Dann, S.J.D., Gruse, JN. et al. Automation and control of laser wakefield accelerators using Bayesian optimization. Nat Commun 11, 6355 (2020), under the terms of the Creative Commons 4.0 International License. doi: 10.1038/s41467-020-20245-6

Contact: R.J. Shalloo (r.shalloo@imperial.ac.uk)

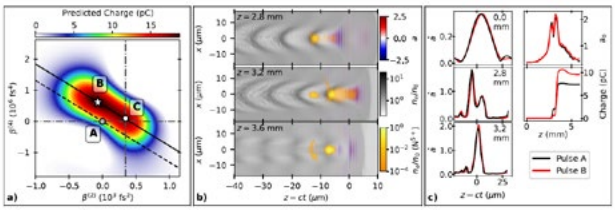

*Electron beam charge optimization through pulse shaping. **a** Surrogate model predicted charge on the $\beta^{(2)} - \beta^{(4)}$ plane at the optimal values of $\beta^{(3)}$ and f. Markers show the initial position projected onto this plane, A, and the optimal position, B. Marker C shows the likely end result of sequential 1D optimizations of $\beta^{(2)}$ and $\beta^{(4)}$ when starting from position A. The diagonal lines show the combination of $\beta^{(2)}$ and $\beta^{(4)}$ modifications that maintain an approximately constant pulse shape. **b** Snapshots from a PIC simulation showing the laser normalized vector potential a, the electron densities of the background plasma and the electrons released from the two inner ionization levels of nitrogen normalized to $n_0 = 1.2 \times 10^{19}\,cm^{-3}$. **c** Left: axial laser field envelope at the given z positions and (right) maximum laser field, and total electron beam charge as functions of z position from simulations using the input laser pulse spectral phase coefficients from points A and B from **a**.*

Electron trapping and reinjection in prepulse-shaped gas targets for laser-plasma accelerators

R.H.H. Scott, D.R. Symes, C. Hooker *(Central Laser Facility, STFC Rutherford Appleton Laboratory, Harwell Campus, Didcot, UK)*

C. Thornton, N. Bourgeois, J. Cowley, W. Ritterhofer, S.M. Hooker *(Department of Physics and John Adams Institute for Accelerator Science, University of Oxford, UK)*
T. Kleinwächter, J. Osterhoff *(DESY, Hamburg, Germany)*

A novel mechanism for injection, emittance selection, and postacceleration for laser wakefield electron acceleration is identified and described. It is shown that a laser prepulse can create an ionized plasma filament through multiphoton ionization and this heats the electrons and ions, driving an ellipsoidal blast-wave aligned with the laser-axis. The subsequent high-intensity laser-pulse generates a plasma wakefield which, on entering the leading edge of the blast-wave structure, encounters a sharp reduction in electron density, causing density down-ramp electron injection. The injected electrons are accelerated to ~2 MeV within the blast-wave. After the main laser-pulse has propagated past the blast-wave, it drives a secondary wakefield within the homogenous background plasma. On exiting the blast-wave structure, the preaccelerated electrons encounter these secondary wakefields, are retrapped, and accelerated to higher energies. Due to the longitudinal extent of the blast-wave, only those electrons with small transverse velocity are retrapped, leading to the potential for the generation of electron bunches with reduced transverse size and emittance.

Reprinted from Scott RHH, Thornton C, Bourgeois N, et al. 2020 Phys. Rev. Accel. Beams 23, 111301, under the terms of the Creative Commons 4.0 International License
doi: 10.1103/PhysRevAccelBeams.23.111301

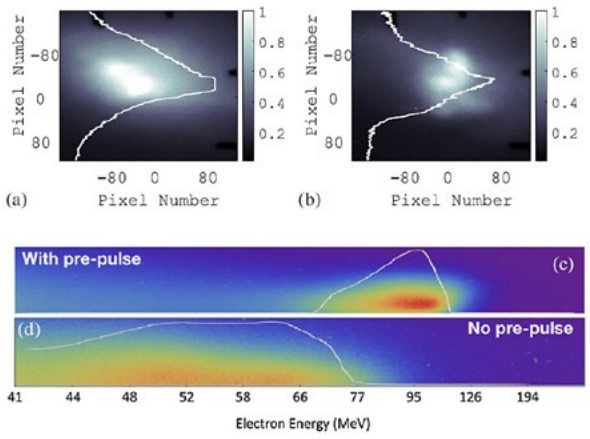

Figure 1: Electron beam energy deposition on a lanex screen, indicative of beam divergence (a) with prepulse, and (b) without. Note (a) is unfortunately saturated. Lines depict the relative signal and show both increased total signal (charge) and reduced divergence. Representative electron spectra with prepulse (c) and without (d). Spectra are imaged in the vertical direction corroborating (a) and (b).

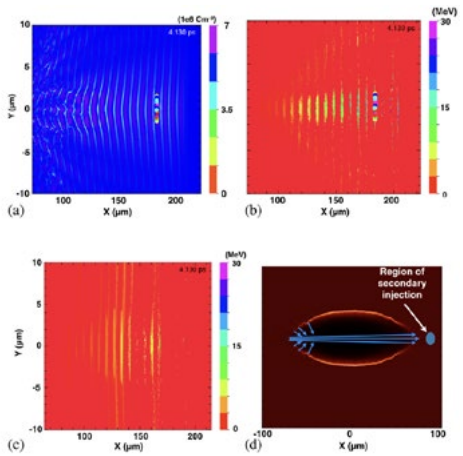

Plasma parameters after the laser has propagated to X = 205 μm. The blast-wave ends at X = 70 μm. (a) The charge density distribution shows the wakefield structures created after the blast-wave; these wakes trap those electrons which are pre-accelerated within the blast-wave. (b) This plot of cell-averaged particle kinetic energy shows multiple bunches are accelerated to higher energies by the multiple wakes trailing the laser. The laser is not shown, but is centred at X = 205 μm. Only those electrons originating from the nitrogen atoms are shown. (c) As per (b) but with a density profile which only varies as a function of x. Here the lateral extent of the bunches is significantly increased from ~2 μm to 10 μm. (d) Blue arrows illustrate the initial propagation directions of those electrons injected at the blast-wave. The electrons are injected approximately perpendicularly to the blast-wave at a given location, so only those with small divergence (near y = 0) enter the region of secondary injection.

Contact: R.H.H. Scott (robbie.scott@stfc.ac.uk)

Development of control mechanisms for a laser wakefield accelerator-driven bremsstrahlung x-ray source for advanced radiographic imaging

C.I.D. Underwood, C.D. Murphy, M.P. Selwood *(York Plasma Institute, Department of Physics, University of York, UK)*
C.D. Baird *(York Plasma Institute, Department of Physics, University of York, UK; Central Laser Facility, STFC Rutherford Appleton Laboratory, Harwell Campus, Didcot, UK)*
C.D. Armstrong, C. Thornton, D. Rusby, D.R. Symes, C.M. Brenner *(Central Laser Facility, STFC Rutherford Appleton Laboratory, Harwell Campus, Didcot, UK)*
O.J. Finlay *(The Cockcroft Institute, Keckwick Lane, Daresbury, UK)*
M.J.V. Streeter, J-N. Gruse, Z. Najmudin *(The John Adams Institute for Accelerator Science, Imperial College London, UK)*
N. Brierley *(The Manufacturing Technology Centre, Ansty Park, Coventry, UK)*
S. Cipiccia *(Diamond Light Source, Harwell Science and Innovation Campus, Didcot, UK)*
P. McKenna *(SUPA Department of Physics, University of Strathclyde, Glasgow, UK)*
D. Neely *(Central Laser Facility, STFC Rutherford Appleton Laboratory, Harwell Campus, Didcot, UK; SUPA Department of Physics, University of Strathclyde, Glasgow, UK)*

A high power laser was used to accelerate electrons in a laser-driven wakefield accelerator. The high energy electrons were then used to generate an x-ray beam by passing them through a converter target. This bremsstrahlung source was characterised and used to perform penetrative imaging of industrially relevant samples. The photon spectrum had a critical energy in excess of 100 MeV and a source size smaller than the resolution of the diagnostic (≲150 μm). Simulations indicate a significantly smaller source is achievable. Variations in the x-ray source characteristics were realised through changes to the plasma and converter parameters while simulations confirm the adaptability of the source. Imaging of high areal density objects with 150 μm resolution was performed, demonstrating the unique advantages of this novel source.

Reprinted from C I D Underwood et al 2020 Plasma Phys. Control. Fusion 62 124002, under the terms of the Creative Commons 4.0 International License. doi: 10.1088/1361-6587/abbebe

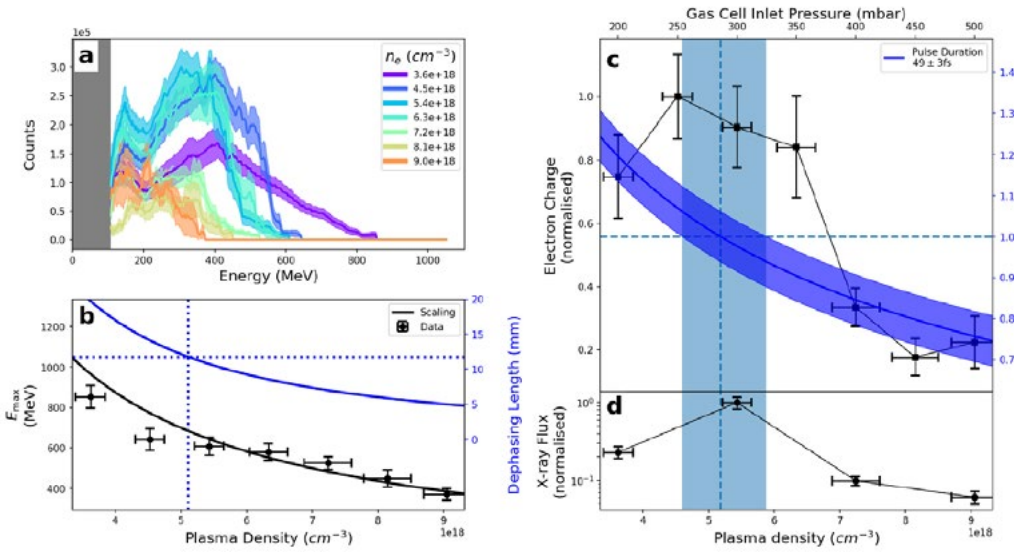

The measured source characteristics with respect to electron plasma density (n_e). (a) The average electron spectrum for the different plasma densities used. The shaded regions correspond to one standard error. (b) The maximum electron energy, showing that when the dephasing length (solid blue line) is shorter than the gas cell (dotted blue line) then the maximum energy follows the inverse scaling (solid black line). (c) Total electron charge (normalised) vs. ne shown in black. The blue line represents $\lambda_p/c\tau$ for the measured pulse length of 49 ± 3 fs. The point where the pulse duration is matched to the plasma wavelength is shown (marked with the blue dashed line, and the shaded region the error in this value). (d) The x-ray flux (normalised) measured with the caesium iodide (CsI) array for the 1 mm iron converter target. The x-ray flux maximum corresponds to the electron beam with peak charge.

Contact: C.I.D. Underwood (christopher.underwood@york.ac.uk)

Self-Referencing Spectral Interferometric Probing of the Onset Time of Relativistic Transparency in Intense Laser-Foil Interactions

S.D.R. Williamson, R. Wilson, M. King, M. Duff, B. Gonzalez-Izquierdo, Z.E. Davidson, A. Higginson, R.J. Gray, P. McKenna *(SUPA Department of Physics, University of Strathclyde, Glasgow, UK)*

N. Booth, S. Hawkes *(Central Laser Facility, STFC Rutherford Appleton Laboratory, Harwell Campus, Didcot, UK)*
D. Neely *(SUPA Department of Physics, University of Strathclyde, Glasgow, UK; Central Laser Facility, STFC Rutherford Appleton Laboratory, Harwell Campus, Didcot, UK)*

Irradiation of an ultrathin foil target by a high-intensity laser pulse drives collective electron motion and the generation of strong electrostatic fields, resulting in ultrabright sources of high-order harmonics and energetic ions. The ion energies can be significantly enhanced if the foil undergoes relativistic self-induced transparency during the interaction, with the degree of enhancement depending in part on the onset time of transparency. We report on a simple and effective approach to diagnose the time during the interaction at which the foil becomes transparent to the laser light, providing a route to optically controlling and optimizing ion acceleration and radiation generation. The scheme involves a self-referencing approach to spectral interferometry, in which coherent transition radiation produced at the foil rear interferes with laser light transmitted through the foil. The relative timing of the onset of transmission with respect to the transition-radiation generation is determined from spectral fringe spacing and compared to simultaneous frequency-resolved optical-gating measurements. The results are in excellent agreement, and are discussed with reference to particle-in-cell simulations of the interaction physics and an analytical model for the onset time of transparency in ultrathin foils.

Reprinted with permission from Williamson SDR, Wilson R, King M, et al., 2020, Self-Referencing Spectral Interferometric Probing of the Onset Time of Relativistic Transparency in Intense Laser-Foil Interactions, Phys. Rev. Applied 14, 034018, ©2020 American Physical Society. doi: 10.1103/PhysRevApplied.14.034018

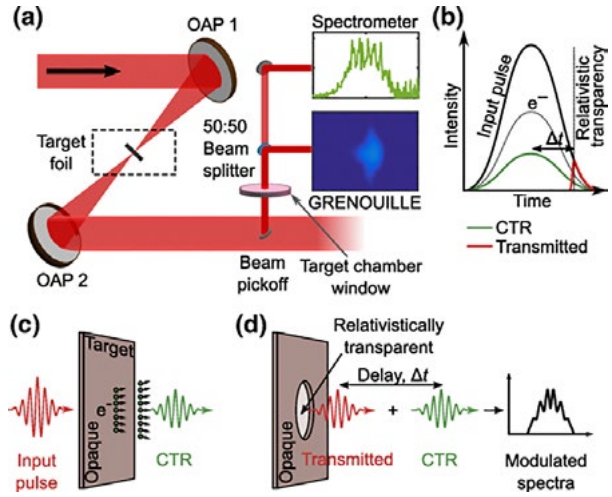

Figure 1: (a) Schematic of the experiment showing the laser-focusing geometry and diagnostic channel. The drive laser pulse is focused using off-axis parabola OAP 1 and the light collected at the target rear, using OAP 2, is directed for simultaneous measurement using a GRENOUILLE and an optical spectrometer. (b) Schematic illustrating the timing of the CTR generation and transmitted part of the laser pulse, where the temporal separation (Δt) relates to the onset time of RSIT relative to the peak of the laser pulse interacting and fast electron generation. (c,d) Schematic of the laser-plasma interaction before, (c), and after, (d), RSIT, resulting in a generated pulse of CTR light and the transmitted laser pulse, with a temporal delay defined by the onset time for RSIT.

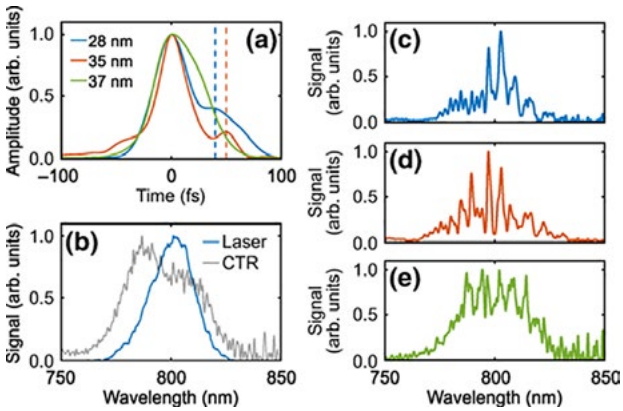

Figure 2: (a) Temporal-intensity profile extracted from GRENOUILLE measurements for three given target thicknesses, for fixed drive laser pulse duration τ_L = 40 fs. (b) Representative measurements of the input laser spectrum and the generated CTR spectrum. (c)–(e) Spectral measurements for (c) d = 28 nm, (d) d = 35 nm, and (e) d = 37 nm targets.

Contact: P. McKenna (paul.mckenna@strath.ac.uk)

Influence of target-rear-side short scale length density gradients on laser-driven proton acceleration

A. Higginson, R. Wilson, J. Goodman, R.J. Dance, N.M.H. Butler, R.J. Gray *(SUPA, Department of Physics, University of Strathclyde, Glasgow, UK)*
M. King, P. McKenna *(SUPA, Department of Physics, University of Strathclyde, Glasgow, UK; The Cockcroft Institute, Sci-Tech Daresbury, Warrington, UK)*
C.D. Armstrong, D. Neely *(SUPA, Department of Physics, University of Strathclyde, Glasgow, UK; (Central Laser Facility, STFC Rutherford Appleton Laboratory, Harwell Campus, Didcot, UK)*
M. Notley, D.C. Carroll *(Central Laser Facility, STFC Rutherford Appleton Laboratory, Harwell Campus, Didcot, UK)*
Y. Fang, X.H. Yuan *(Key Laboratory for Laser Plasmas and CICIFSA, School of Physics and Astronomy, Shanghai Jiao Tong University, People's Republic of China)*

In this article the influence of a short plasma density scale length on laser-driven proton acceleration, in the TNSA regime, is investigated experimentally by heating and driving the expansion of a large area on the target rear. Key parameters of the generated protons, such as maximum proton energy, proton flux and divergence, are all measured to decrease with increasing plasma expansion. Even for a small plasma scale length of the order of the laser wavelength (~1 μm), a substantial decrease in the number of protons over a wide spectral range is measured. Through a combination of radiation-hydrodynamic and particle-in-cell simulations new insight into the underlying physics is observed, providing new understanding of the strong influence even a small plasma density gradient can have on laser-driven ion acceleration. The findings have implications for applications that require efficient laser energy conversion to ions, such as the proton-driven fast-ignition scheme of inertial confinement fusion (ICF).

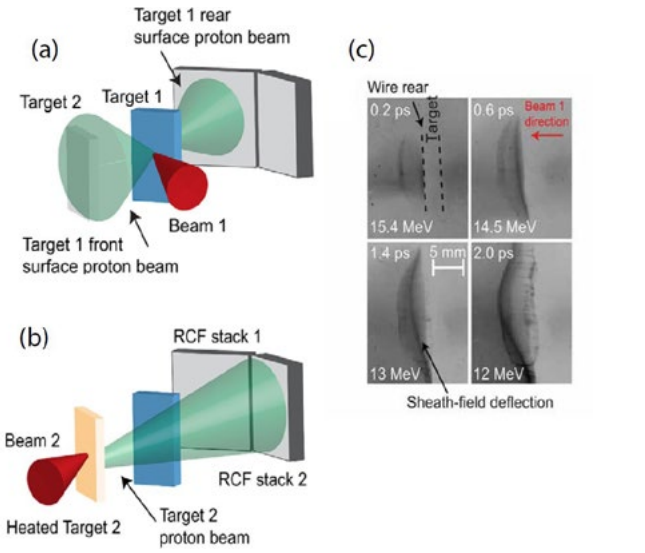

Schematic of the experimental set-up, showing the two steps corresponding to the dual beam interaction. (a) interaction between laser beam 1 and target 1, with the rear-surface-accelerated (TNSA) protons characterised using RCF 1 and the front-surface-accelerated protons irradiating and heating target 2. (b) Second interaction, between laser beam 2 and target 2, which occurs after a controlled temporal delay relative to the protons from the first interaction arriving at the rear of target 2. (c) Example RCF measurements of TNSA protons from target 2 probing the spatio-temporal evolution of the sheath-field on Target 1.

Contact: P. McKenna (paul.mckenna@strath.ac.uk)

Narrow-band acceleration of gold ions from ultra-thin foils

P. Martin, F. Hanton, D. Gwynne, M. Borghesi, S. Kar *(Centre for Plasma Physics, Queen's University Belfast, UK)*
H. Ahmed, J. S. Green *(Central Laser Facility, STFC Rutherford Appleton Laboratory, Harwell Campus, Didcot, UK)*
D. Doria *(ELI NP, Magurele, Romania)*
A. Alejo *(IGFAE, Universidade de Santiago de Compostela, Spain)*
A. Macchi *(Istituto Nazionale di Ottica, Consiglio Nazionale delle Ricerche (CNR/INO), Laboratorio Adriano Gozzini, Pisa, Italy)*
M. Cerchez, M. Swantusch, O. Willi *(Institut für Laser-und Plasmaphysik, Heinrich-Heine-Universität, Düsseldorf, Germany)*
J. Fernandez-Tobias, J. A. Ruiz *(Instituto de Fusion Nuclear, Universidad Politécnica de Madrid, Spain)*
D. Maclellan, P. McKenna *(Department of Physics, University of Strathclyde, UK)*
S. Zhai *(Shanghai Normal University, China)*

In this paper we demonstrate, for the first time, the laser-driven acceleration of extremely heavy gold ions to a narrow-band spectral bunch. The Au ion energies are the highest reported to date, and the flux achieved exceeds other notable works by orders of magnitude. Simulations reveal an interplay of multiple acceleration mechanisms, whereby the high flux Au bunch is generated from the influence of strong radiation pressure acceleration. We also demonstrate scalability of this phenomenon for multi-PW laser systems. Such high flux, energetic Au ion beams would be of profound interest for applications in laboratory astrophysics, and nuclear physics research.

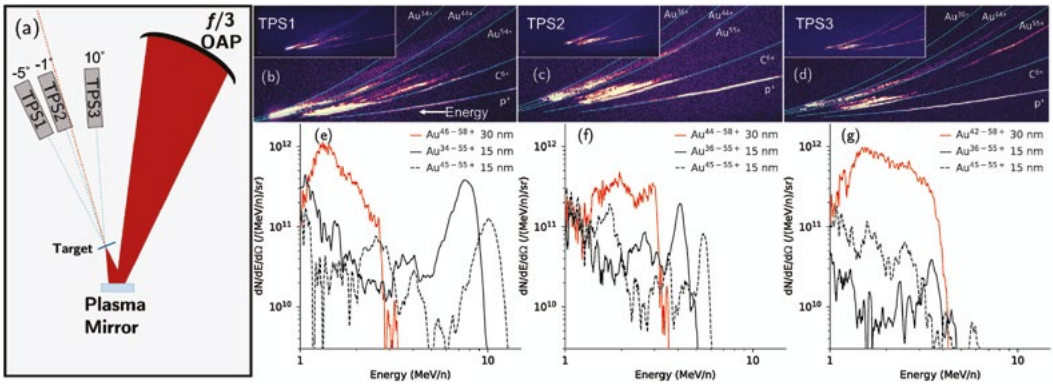

Figure 1

Figure 1: (a) Schematic of the experimental setup, TPS1–3 represents the three high resolution Thomson parabola spectrometers (TPS) deployed at different angles (as labelled) with respect to target normal (red dashed line). (b, c, d) Raw image plate data from each TPS on 15 nm gold foil, with example ion traces indicated in cyan, where ion energies increase going from right to left on each image. Au ion traces (as labelled) represent the bounds of the charge ranges over which spectra were integrated. The insets show the full IP image. (e, f, g) Au ion spectra, in order from TPS1 to TPS3, for 15 nm (black) and 30 nm (red) targets. For both thicknesses, spectra are shown representing signal integration over the entirety of the charge states observed (solid lines, charge ranges are as labelled in the legend), and energies calculated assuming a central charge of 44+ and 51+ for the 15 and 30 nm targets, respectively. Additionally, for the 15 nm target, a second spectrum was generated integrating signal only for charges above 45+ (dashed lines), representing most of the ion signal, at a central charge of 51+. The difference in ion energy at the spectral peak of solid and dashed black lines is due to the chosen charge states for energy calculation. The Au ion flux in the spectrum was calculated by using the absolute calibration of the detector (BAS-TR image plate) response to laser driven Au ions shown in doi: 10.1063/5.0079564.

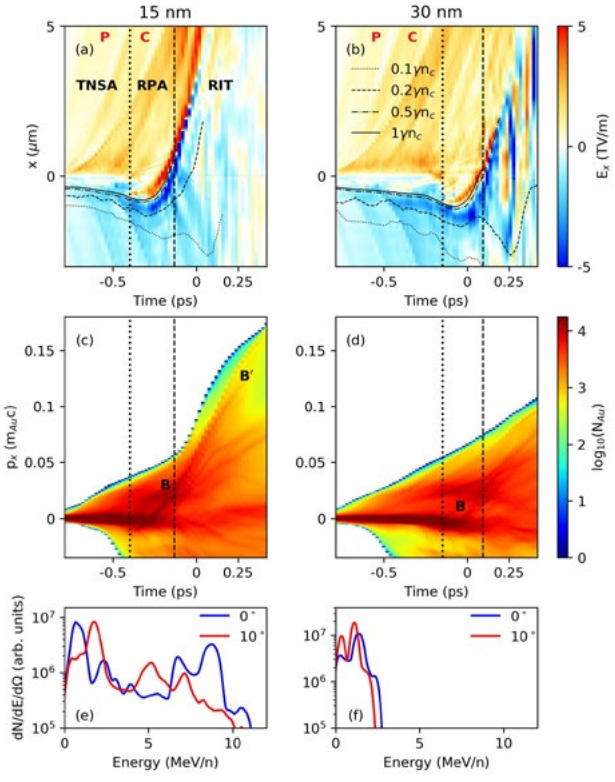

Figure 2

Figure 2: 2D PIC simulations comparing two target thicknesses, showing (a,b) the time evolution of the cycle averaged longitudinal electric field along the laser axis for 15 nm and 30 nm thick targets, respectively. The black curves indicate the positions of (relativistically corrected) electron density fronts at 0.1, 0.2, 0.5, and 1 times critical, while the vertical dotted and dashed lines indicate the transitions between each acceleration phase: TNSA, RPA, and RIT. (c,d) The time evolution of the Au ion momentum spectrum (integrated over all charge states, to account for ionisation during the pulse) along the laser axis, for each thickness. Time is measured relative to the incidence of the pulse peak at the initial target front surface (x=0 μm). Au^{40-51+} ion energy spectra from the 15 nm (e) and 30 nm (f) targets are shown, taken at t = 270 fs, inside 1 degree half-angle cones directed on-axis (blue — 0°) and off-axis (red — 10°).

Contact: P. Martin (p.martin@qub.ac.uk)

Determining the short laser pulse contrast based on X-Ray emission spectroscopy

A.S. Martynenko *(Joint Institute for High Temperatures of Russian Academy of Sciences, Moscow, Russia)*
I.Yu. Skobelev, S.A. Pikuz, S.N. Ryazantsev *(Joint Institute for High Temperatures of Russian Academy of Sciences, Moscow, Russia; National Research Nuclear University MEPhI, Moscow, Russia)*
C. Baird, L. Doehl, P. Durey, D. Farley, K. Lancaster, C.D. Murphy, N. Woolsey *(York Plasma Institute, Department of Physics, University of York, UK)*
N. Booth, C. Spindloe *(Central Laser Facility, STFC Rutherford Appleton Laboratory, Harwell Campus, Didcot, UK)*
R. Kodama *(Open and Transdisciplinary Research Initiative, Osaka University, Japan)*
P. McKenna *(Department of Physics, SUPA, University of Strathclyde, Glasgow, UK)*
T.A. Pikuz *(Joint Institute for High Temperatures of Russian Academy of Sciences, Moscow, Russia; Open and Transdisciplinary Research Initiative, Osaka University, Japan)*

The interaction of high-power short lasers with solid density targets is an important application of modern solid state lasers. However, uncertainties in measurements due to lack of information on the laser pedestal-to-peak contrast limits the validity of many conclusions. We show that X-ray spectral measurements can provide a straightforward way for accessing the laser pedestal-to-peak contrast. The experiments use silicon targets and relativistic laser intensities of 3×10^{20} W/cm^2 with a pulse duration of 1 ps. By not using or using a plasma mirror we compare low and high contrast measurements of the Ly-α line and its satellites to show that these lines are an effective laser contrast diagnostic. This diagnostic has potential to reduce uncertainty in future laser-solid interaction studies.

Reproduced from the Accepted Version (https://eprints.whiterose.ac.uk/170892/) of Martynenko, A. S., Skobelev, I. Yu, Pikuz, S. A. et al. (13 more authors) (2021) Determining the short laser pulse contrast based on X-Ray emission spectroscopy. HIGH ENERGY DENSITY PHYSICS. 100924. ISSN 1574-1818 under the terms of the Creative Commons licence CC-BY-NC-ND 2.5. A definitive version was subsequently published in High Energy Density Physics, 38:100924 (2021) © 2021, Elsevier. doi: 10.1016/j.hedp.2021.100924

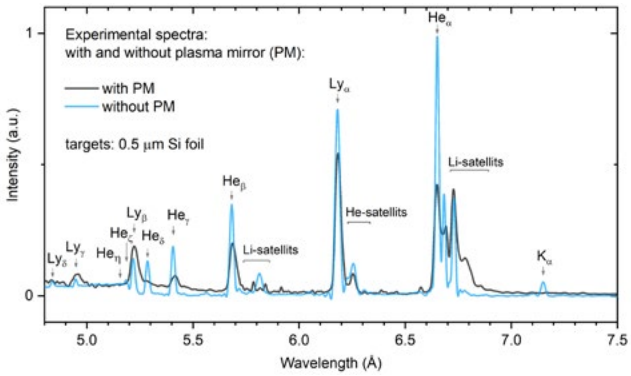

Spectra of the picosecond laser plasma formed by laser pulses of different contrasts: a spectrum from a relatively high contrast is shown by the orange curve and compared to a spectrum from a relatively low contrast interaction by the black curve.. The spectra allow an estimation of the plasma density at the time of arrival of a main laser beam.

Contact: S.A. Pikuz (spikuz@gmail.com)

Optimization of a laser plasma-based x-ray source according to WDM absorption spectroscopy requirements

A.S. Martynenko *(Joint Institute for High Temperatures of Russian Academy of Sciences, Moscow, Russia)*
S.A. Pikuz, I.Yu. Skobelev, S.N. Ryazantsev *(Joint Institute for High Temperatures of Russian Academy of Sciences, Moscow, Russia; National Research Nuclear University MEPhI, Moscow, Russia)*
C. Baird, L. Döhl, P. Durey, D. Farley, K. Lancaster, C. D. Murphy, N. Woolsey *(York Plasma Institute, Department of Physics, University of York, UK)*
N. Booth, C. Spindloe *(Central Laser Facility, STFC Rutherford Appleton Laboratory, Harwell Campus, Didcot, UK)*
R. Kodama *(Open and Transdisciplinary Research Initiative, Osaka University, Japan; Institute of Laser Engineering, Osaka University, Japan)*
P. McKenna *(Department of Physics, SUPA, University of Strathclyde, Glasgow, UK)*
T.A. Pikuz, A.Ya. Faenov *(Joint Institute for High Temperatures of Russian Academy of Sciences, Moscow, Russia; Open and Transdisciplinary Research Initiative, Osaka University, Japan)*

X-ray absorption spectroscopy is a recognised diagnostic technique for experimental studies of warm dense matter. It requires a short-lived X-ray source with a sufficiently high emissivity and without characteristic lines in a spectral range of interest. In the present work, we discuss the choice of the optimal material and thickness to obtain a bright source in the wavelength range of 2 - 6 Å (~2 - 6 keV) considering relatively low Z elements. We demonstrate that the highest emissivity of solid aluminium and silicon foil targets irradiated with a high-contrast sub-kJ laser pulse of 1 ps is obtained when the thickness of the target is close to 10 μm. An outer plastic layer can further increase the emissivity.

Reproduced from Matter Radiat. Extremes 6, 014405 (2021), under the terms of a Creative Commons Attribution (CC BY) license. doi: 10.1063/5.0025646

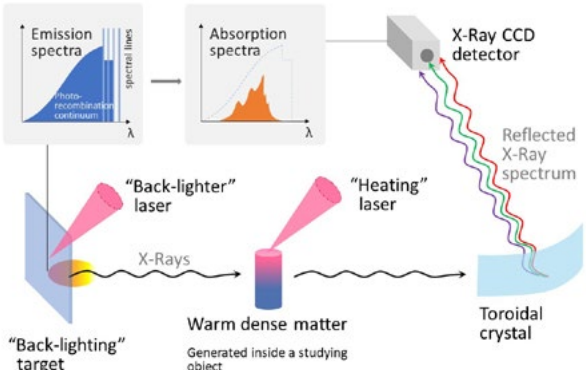

Principle scheme of absorption spectroscopy with a laser-based X-ray source. The focus is on the photorecombination continuum emission from solid- density plasmas to produce a featureless spectral continuum of high intensity that can be used e.g. for X-ray absorption spectroscopy studies of warm dense matter.

Contacts: A.S. Martynenko (artmarty@mail.ru)
S.A. Pikuz (spikuz@gmail.com)

Effect of plastic coating on the density of plasma formed in Si foil targets irradiated by ultra-high-contrast relativistic laser pulses

A.S. Martynenko, S.A. Pikuz, I.Yu. Skobelev, S.N. Ryazantsev *(Joint Institute for High Temperatures of Russian Academy of Sciences, Moscow, Russia; National Research Nuclear University MEPhI, Moscow, Russia)*
C. Baird, L. Doehl, P. Durey, D. Farley, K. Lancaster, C.D. Murphy, N. Woolsey *(York Plasma Institute, Department of Physics, University of York, UK)*
N. Booth, C. Spindloe *(Central Laser Facility, STFC Rutherford Appleton Laboratory, Harwell Campus, Didcot, UK)*
R. Kodama *(Open and Transdisciplinary Research Initiative, Osaka University, Japan; Institute of Laser Engineering, Osaka University, Japan)*
P. McKenna *(Department of Physics, SUPA, University of Strathclyde, Glasgow, UK)*
T.A. Pikuz, A.Ya. Faenov *(Joint Institute for High Temperatures of Russian Academy of Sciences, Moscow, Russia; Open and Transdisciplinary Research Initiative, Osaka University, Japan)*

The formation of matter with high energy density occurs in inertial fusion and in astrophysical and geophysical systems. In this context, it is important to couple as much energy as possible into a target while maintaining a high density. A recent experimental campaign using buried layer (or "sandwich" type) targets and the Vulcan PW ultra-high laser contrast resulted in 500 Mbar pressures in near-solid density plasmas (corresponding to an energy density of about 4.6 × 10^7 J/cm^3). The densities and temperatures of the generated plasma were measured by analysing the X-ray spectral line profiles and relative intensities.

Reprinted with permission from A Martynenko et al. Effect of plastic coating on the density of plasma formed in Si foil targets irradiated by ultra-high-contrast relativistic laser pulses, Phys. Rev. E 101, 043208, © American Physical Society 2020. doi: 10.1103/PhysRevE.101.043208

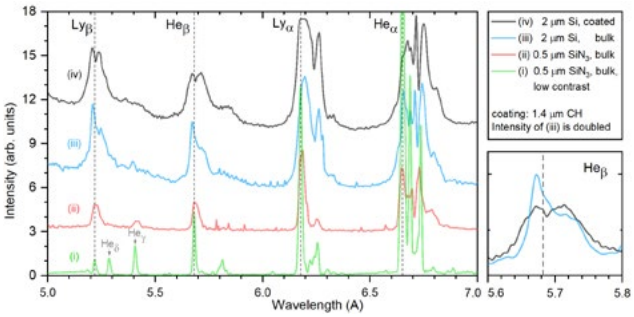

Experimental X-ray spectra obtained by laser pulse irradiation of (i) 0.5 μm SiN_3 uncoated film without plasma mirror, (ii) 0.5 μm SiN_3 uncoated film with plasma mirror, (iii) 2 μm Si film coated on both sides with 1.4 μm CH plastic layers, and (iv) 2 μm Si uncoated film. The intensity of curve (i) is divided by a factor of 2 and the intensity of curve (iii) is doubled. One can see an influence of the plastic coating and the plasma mirror on the plasma density.

Contact: S.A. Pikuz (spikuz@gmail.com)

Influence of spatial-intensity contrast in ultraintense laser-plasma interactions

R. Wilson, N.M.H. Butler, T.P. Frazer, M.J. Duff, A. Higginson, R.J. Dance, J. Jarrett, Z.E. Davidson, R.J. Gray *(SUPA Department of Physics, University of Strathclyde, Glasgow, UK)*
M. King, P. McKenna *(SUPA Department of Physics, University of Strathclyde, Glasgow, UK; The Cockcroft Institute, Sci-Tech Daresbury, Warrington, UK)*
D.C. Carroll, S.J. Hawkes, R.J. Clarke *(Central Laser Facility, STFC Rutherford Appleton Laboratory, Harwell Campus, Didcot, UK)*
C.D. Armstrong, D. Neely *(SUPA Department of Physics, University of Strathclyde, Glasgow, UK; Central Laser Facility, STFC Rutherford Appleton Laboratory, Harwell Campus, Didcot, UK)*
H. Liu *(Central Laser Facility, STFC Rutherford Appleton Laboratory, Harwell Campus, Didcot, UK; Beijing National Laboratory for Condensed Matter Physics, Institute of Physics, Chinese Academy of Sciences, Beijing, China)*

There has been continual drive to increase the achievable peak intensity of laser light, resulting in an average increase of two to three orders of magnitude per decade. Further increase is achievable via tighter focusing, however the influence the focal spot spatial profile plays is not fully understood. In this article it is demonstrated that the spatial-intensity distribution, specifically the ratio of the intensity in the peak of the spot to the surrounding halo of light, is important in the interaction of ultraintense laser pulses with solid targets. Through the comparison of TNSA proton acceleration from targets irradiated by a near-diffraction-limited wavelength scale focal spot and larger F-number focusing, we find that the focal spot spatial-intensity contrast strongly influences laser energy coupling to fast electrons. From this study it is clear that for future multi-petawatt laser systems, spatial-intensity contrast is potentially as important as temporal-intensity contrast.

Reproduced from Wilson, R., King, M., Butler, N.M.H. et al. Influence of spatial-intensity contrast in ultraintense laser–plasma interactions. Sci Rep 12, 1910 (2022), under the terms of the Creative Commons Attribution 4.0 International License. doi: 10.1038/s41598-022-05655-4

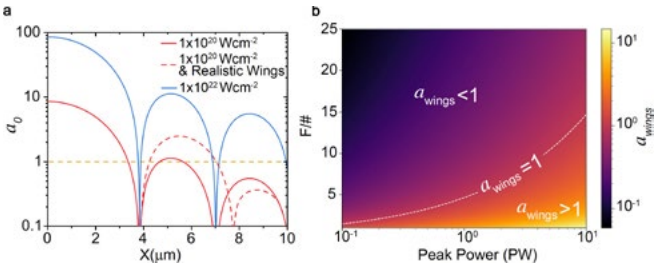

(a) Normalised vector potential (a_0) as a function of spot radius, for idealised (Airy disk) focal spots at two given peak intensities, each of the same diameter. The dashed red data illustrates a case for which the intensity distribution is non-ideal, resulting in a higher intensity in the wings (a degradation of the spatial-intensity contrast). The dashed orange line marks the relativistic threshold intensity for 1 μm light. (b) Normalised vector potential of the laser light in the focal spot wings, a_{wings} , as a function of laser pulse power and focusing geometry. The a_{wings} = 1 curve marks the threshold for which the intensity in the wings is relativistic.

Contact: P. McKenna (paul.mckenna@strath.ac.uk)

Laser science and development

Zemax OpticStudio Case Study: optical design of a finite conjugate, 4f, telecentric imaging system for re-imaging a VCSEL array

D.L. Clarke *(Central Laser Facility, STFC Rutherford Appleton Laboratory, Harwell Campus, Didcot, UK)*

The performance of a 4f imaging system for a 7.75 mm x 7.75 mm VCSEL (vertical-cavity surface-emitting laser) array is investigated for different optical configurations and magnifications by consideration of the RMS spot radius and encircled energy plots in Zemax sequential mode. In general, off-the-shelf components are preferred due to the costly nature of manufacturing bespoke lenses. While in the case of [1:1] magnification, the use of an off-the-shelf achromatic doublet requires a small compromise on performance over the use of aspheric singlet, in the case of [1:1.25] magnification, it provides the best system performance. Additionally, the use of an achromatic doublet will make for a more robust system that can be used for a range of wavelengths of light.

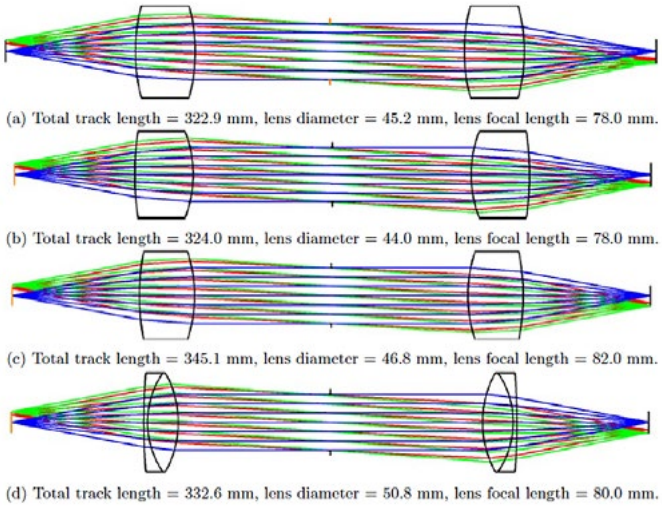

Right: Layout of an optimised telecentric, 4f imaging system for two identical (a) equiconvex, (b) biconvex, (c) aspheric singlets and (d) Thorlabs cemented achromatic doublets

Contact: D.L. Clarke (danielle.clarke@stfc.ac.uk)

Design and performance of a 100 J pump laser front-end for use in a 10 Hz PW-class amplifier

A.M. Wojtusiak, J. Spear, J.M. Smith, T. Butcher *(Central Laser Facility, STFC Rutherford Appleton Laboratory, Harwell Campus, Didcot, UK)*

We present the front-end system for a diode-pumped solid state laser (DPSSL), optimised specifically for pumping a 10 Hz PW-class amplifier. The front-end provides 150 mJ, 1 - 15 ns pulses and has spatial and temporal pulse-shaping capabilities.

DPSSLs are a better alternative to flashlamps for pumping amplifiers of PW-class lasers, as they are capable of providing much higher repetition rates and have longer lifetimes. This method is applied in the upcoming Extreme Photonics Applications Centre (EPAC), a new national facility at the STFC Rutherford Appleton Laboratory (RAL), where a Titanium-doped Sapphire (Ti:Sa) femtosecond amplifier will be pumped by a 120 J DPSSL. EPAC will house a PW-class 10 Hz laser, feeding radiation-shielded experimental areas, that will provide academia and industry with a range of applications from laser plasma acceleration to imaging with secondary sources of radiation.

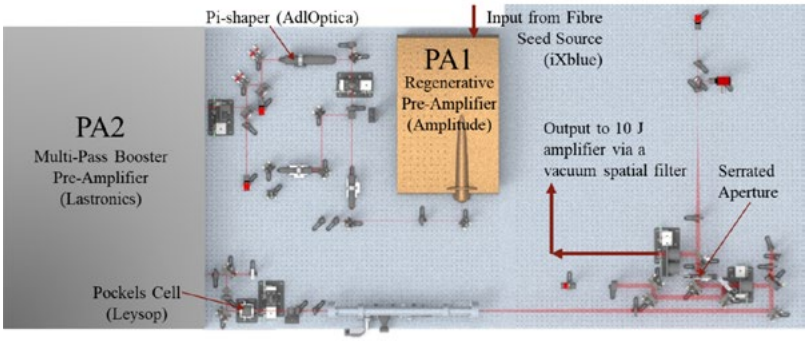

Layout of the front end of the DPSSL pump laser for the Extreme Photonics Applications Centre

Contact: A.M. Wojtusiak (agnes.wojtusiak@stfc.ac.uk)

Response of silicon nitride ceramics subject to laser shock treatment

P. Shukla, X. Shen, P. Swanson, M.E. Fitzpatrick *(School of Mechanical, Aerospace and Automotive Engineering, Coventry University, UK)*
R. Allott, K. Ertel *(Central Laser Facility, STFC Rutherford Appleton Laboratory, Harwell Campus, Didcot, UK)*

S. Robertson, R. Crookes, H. Wu *(Department of Materials, Loughborough University, UK)*
A. Zammit *(Department of Metallurgy and Materials Engineering, Faculty of Engineering, University of Malta, Malta)*

A comprehensive and novel investigation on multiple-layer, square-beam laser shock treatment ("laser peening") of Si_3N_4 ceramics is reported in this work. Surface topography, hardness, fracture toughness (K_{Ic}), residual stresses, and microstructural changes were investigated. The evaluation of fracture toughness via the Vickers hardness indentation method revealed a reduction in crack lengths produced by the indenter after laser shock treatment. Upon appropriate calculation, this revealed an increase in K_{Ic} of 60%, this being attributed to a near-surface (50µm depth) compressive residual stress measured at –289 MPa. Multiple layer laser shock treatment also induced beneficial residual stresses to a maximum measured depth of 512µm. Oxidation was evident only on the top surface of the ceramic post laser shock treatment (<5µm depth) and was postulated to be due to hydrolyzation. The surface enhancement in K_{Ic} and flaw-size reduction was assigned to an elemental change on the surface, whereby, Si_3N_4 was transformed to SiO_2, particularly, with multiple layers laser shock treatment. Compressive residual stresses measured in the sub-surface were attributed to mechanical effects (below sub-surface elastic constraint) and corresponding shock-wave response of the Si_3N_4. This work has led to a new mechanistic understanding regarding the response of Si_3N_4 ceramics subject to laser shock treatment (LST). It is significant because inducing deep compressive residual stresses and corresponding enhancement in surface K_{Ic} are important for the enhanced durability in many applications of this ceramic including cutting tools, hip and knee implants, dental replacements, bullet-proof vests and rocket nozzles in automotive, aerospace, space and biomedical industries.

A definitive version was subsequently published in Ceramics International, 47:24, (2021)
 doi: 10.1016/j.ceramint.2021.08.369

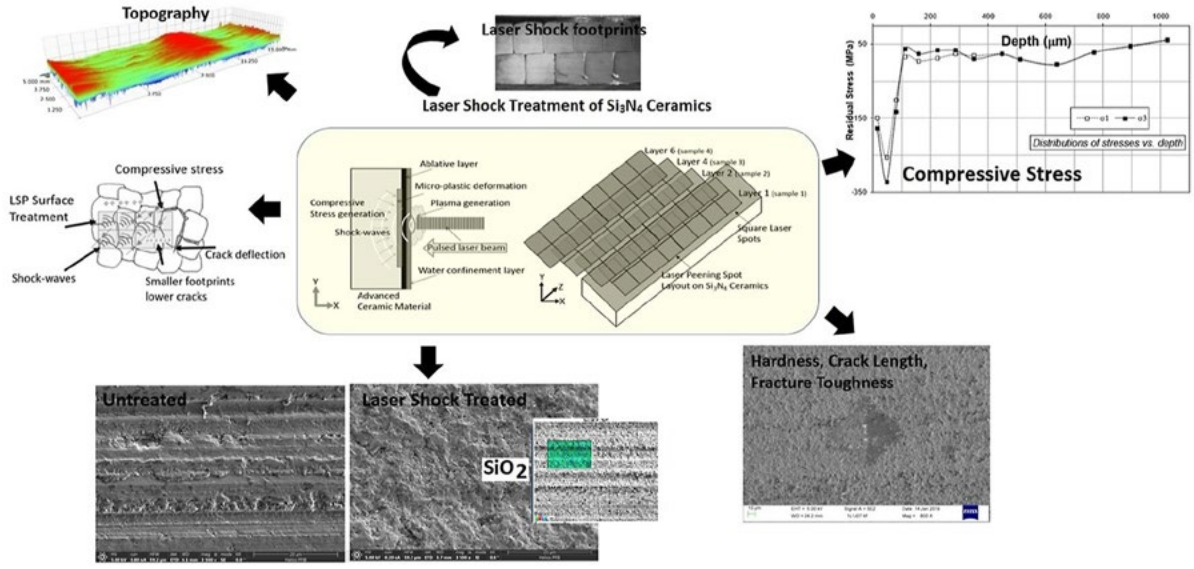

Graphical abstract from https://www.sciencedirect.com/science/article/pii/S0272884221027711

Contact: P. Shukla (pratik.shukla@talk21.com)

Stable high-energy, high-repetition-rate, frequency doubling in a large aperture temperature-controlled LBO at 515 nm

J. Phillips, S. Banerjee, K. Ertel, P. Mason, J. Smith, T. Butcher, M. De Vido, C. Edwards, C. Hernandez-Gomez, J. Collier *(Central Laser Facility, STFC Rutherford Appleton Laboratory, Harwell Campus, Didcot, UK)*

We report on frequency doubling of high-energy, high-repetition-rate ns pulses from a cryogenically gas cooled, multi-slab Yb:YAG laser system, using a type-I phase-matched lithium triborate (LBO) crystal. Pulse energy of 4.3 J was extracted at 515 nm for a fundamental input of 5.4 J at 10 Hz (54 W), corresponding to a conversion efficiency of 77%. However, during long-term operation, a significant reduction of efficiency (more than 25%) was observed owing to the phase mismatch arising due to the temperature-dependent refractive index change in the crystal. This forced frequent angle tuning of the crystal to recover the second-harmonic generation (SHG) energy. More than a five-fold improvement in energy stability of SHG was observed when the LBO crystal was mounted in an oven, and its temperature was controlled at 27°C. Stable frequency doubling with 0.8% rms energy variation was achieved at a higher input power of 74 W when the LBO temperature was controlled at 50°C.

Reproduced from J. Phillips et al. "Stable high-energy, high-repetition-rate, frequency doubling in a large aperture temperature-controlled LBO at 515 nm," Opt. Lett. 45, 2946-2949 (2020), © 2020 Optical Society of America, under the terms of the OSA Open Access Publishing Agreement. doi: 10.1364/OL.383129

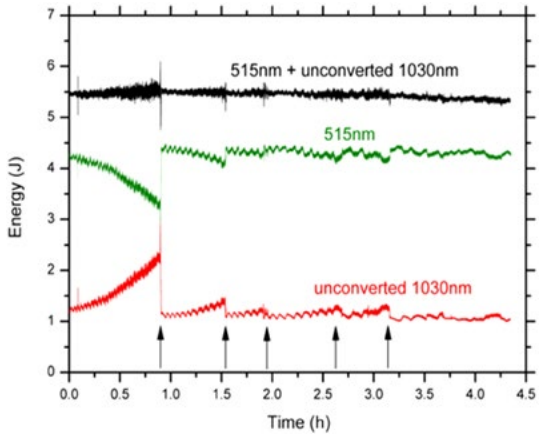

Figure 1: Long-term energy stability of type-I SHG in LBO in a thermally isolated mount using a 1 cm² beam. The black line shows total energy (515 nm + unconverted 1030 nm), the green line shows frequency converted energy (515 nm), and the red line shows the unconverted fundamental (1030 nm). The arrows indicate the times at which the crystal angle (theta) was changed to restore the second-harmonic energy.

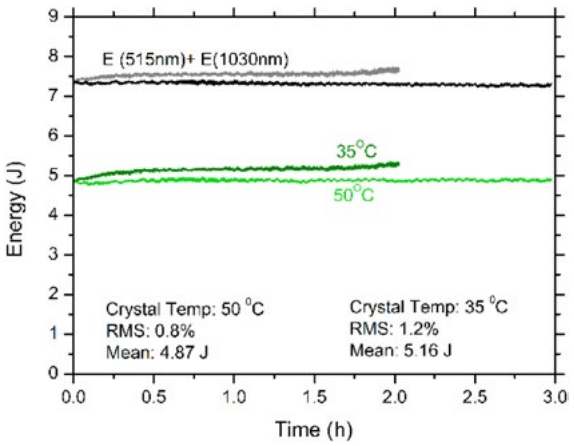

Figure 2: Long-term energy stability of type-I SHG in LBO in an oven set to 35°C and 50°C using a 1.4 cm² beam. Total input energy of 7.4 J (grey and black lines) and average power of 74 W, 515 nm energy 5.0 J (green lines), 50 W average power.

Figure 3: Photographs of LBO crystal oven components: (left) spring-loaded metallic crystal holder with the crystal in place. This is placed inside the oven unit (right). The oven is then connected to a separate temperature control unit.

Contact: P.J. Phillips (jonathan.phillips@stfc.ac.uk)

Modelling and measurement of thermal stress-induced depolarisation in high energy, high repetition rate diode-pumped Yb:YAG lasers

M. De Vido, G. Quinn, D. Clarke *(Central Laser Facility, STFC Rutherford Appleton Laboratory, Harwell Campus, Didcot, UK; Institute of Photonics and Quantum Sciences, Heriot-Watt University, Edinburgh, UK)*

P. Mason, M. Fitton, K. Ertel, T.J. Butcher, P.J. Phillips, S. Banerjee, J. Smith, J. Spear, C. Edwards, J. Collier *(Central Laser Facility, STFC Rutherford Appleton Laboratory, Harwell Campus, Didcot, UK)*
R.W. Eardley *(University of Bath, UK)*

In this paper, we present a model to predict thermal stress-induced birefringence in high energy, high repetition rate diode-pumped Yb:YAG lasers. The model calculates thermal depolarisation as a function of gain medium geometry, pump power, cooling parameters, and input polarisation state. We show that model predictions are in good agreement with experimental observations carried out on a DiPOLE 100 J, 10 Hz laser amplifier. We show that single-pass depolarisation strongly depends on input polarisation state and pumping parameters. In the absence of any depolarisation compensation scheme, depolarisation varies over a range between 5% and 40%. The strong dependence of thermal stress-induced depolarisation on input polarisation indicates that, in the case of multipass amplifiers, the use of waveplates after every pass can reduce depolarisation losses significantly. We expect that this study will assist in the design and optimisation of Yb:YAG lasers.

*Reproduced from M. De Vido et al. "Modelling and measurement of thermal stress-induced depolarisation in high energy, high repetition rate diode-pumped Yb:YAG lasers," Opt. Express **29**, 5607-5623 (2021), under the terms of the Creative Commons Attribution 4.0 License. doi: 10.1364/OE.417152*

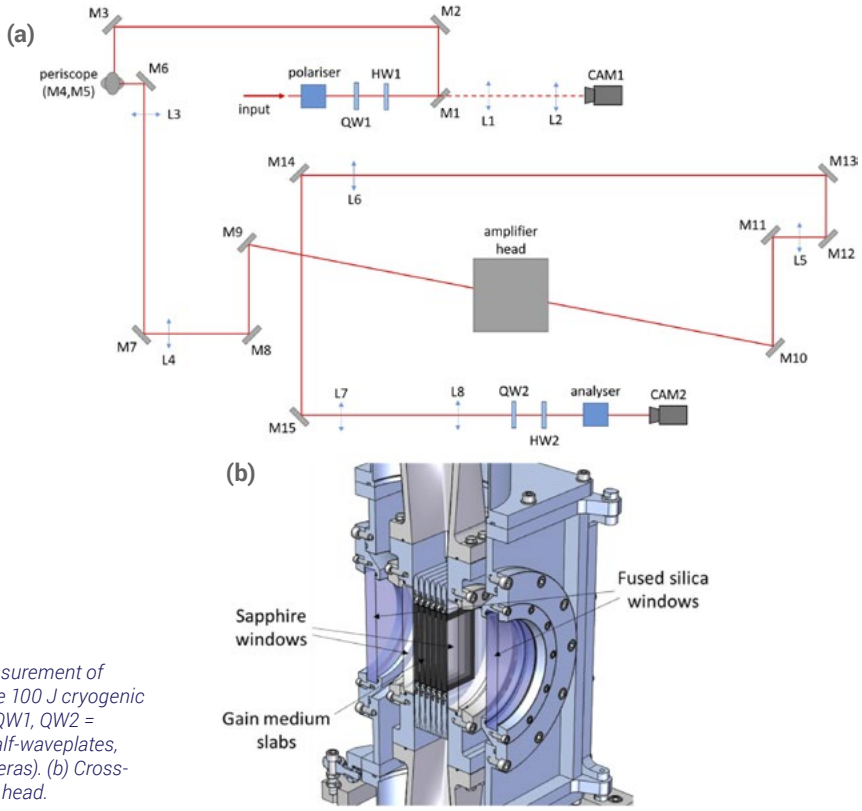

Figure 1: (a) Setup used for the measurement of stress-induced depolarisation in the 100 J cryogenic main amplifier (M1-M15 = mirrors, QW1, QW2 = quarter-waveplates, HW1, HW2 = half-waveplates, L1-L8 = lenses, CAM1, CAM2 = cameras). (b) Cross-sectional rendering of the amplifier head.

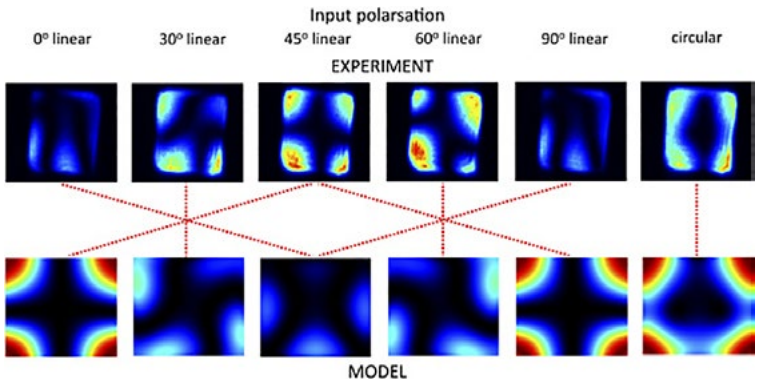

Figure 2: Experimental (upper row) and theoretical (lower row) depolarisation patterns for the "180 g/s, 3.77 kW" scenario and for a number of input polarisation states. Red dashed lines link images with similar depolarisation patterns. The colour scales for experimental and theoretical patterns are the same for all experimental and theoretical images, respectively.

Contact: M. De Vido (mariastefania.de-vido@stfc.ac.uk)

Use of Recast3D for real-time reconstruction

Z. Huang, T. Zata *(Central Laser Facility, STFC Rutherford Appleton Laboratory, Harwell Campus, Didcot, UK)*
T. Cobb, J. Filik *(Diamond Light Source, Harwell Science & Innovation Campus, Didcot, UK*

This paper is going to introduce our work on developing a distributed real-time tomography reconstruction platform for EPAC based on Recast3D with the collaboration of Diamond Light Source (DLS).

Recast3D is a visualization platform for tomographic imaging based on on-demand reconstruction of arbitrary slices, and is built for use in a distributed, real-time, and online construction pipeline. It is a useful real-time tomography reconstruction software toolkit that avoids the high computational cost of full 3D tomographic reconstructions. Through the work completed, we established the prototype platform and carried out performance tests. Further work is planned to reduce reconstruction time.

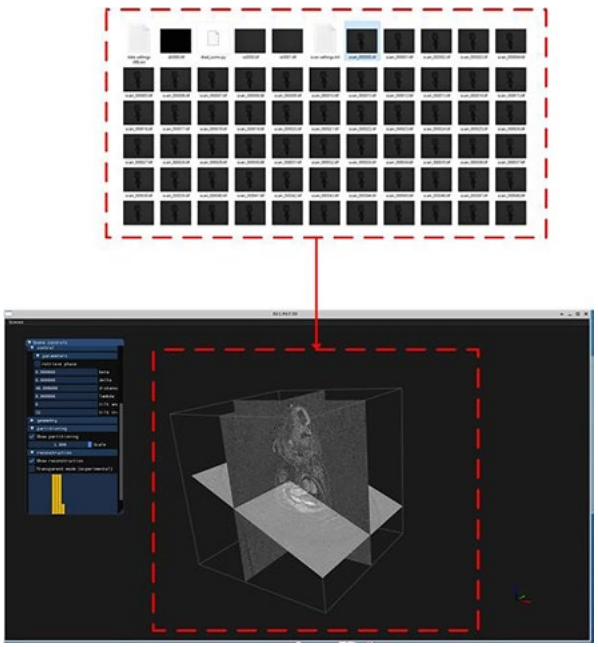

Right: The raw scanned slice images (top) and the reconstructed 3D image in Recast3D

Contact: Z. Huang (ziyu.huang@stfc.ac.uk)

Ø320 mm beam positioning mirror mount for the EPAC project with 1 µrad stability

A. Stallwood, I. Cheshire, R. Sarasola *(Central Laser Facility, STFC Rutherford Appleton Laboratory, Harwell Campus, Didcot, UK)*

For the new Extreme Phonics Application Centre (EPAC) at the Central Laser Facility (CLF) a beam positioning mirror mount was designed to propagate a laser beam measuring up to 320 mm in diameter with 1 µrad stability under vacuum.

The end design consisted of the novel approach to integrate the mechanics within a solid aluminium vacuum chamber. This improved the rigidity of the mirror mount and exceeded the stability specification by offering less than 500 nano-radians peak to peak.

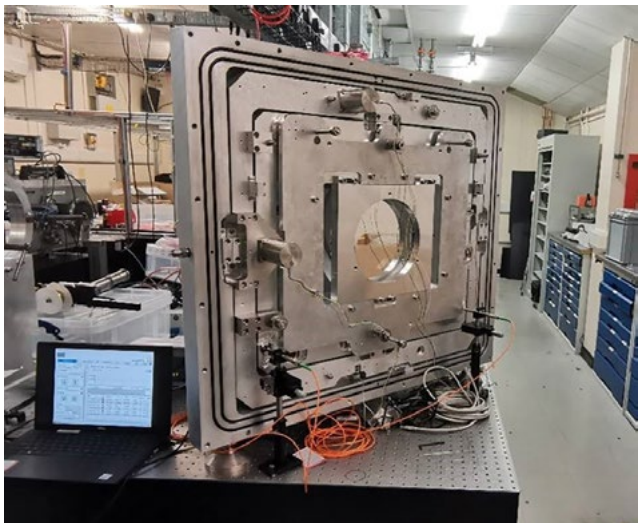

Contact: A. Stallwood (andrew.stallwood@stfc.ac.uk)

Deploying the SLAC liquid target at RAL

N. Bourgeois, P. Parsons, D. Symes *(Central Laser Facility, STFC Rutherford Appleton Laboratory, Harwell Campus, Didcot, UK)*

G.D. Glenn, C.B. Curry, F. Treffert, M. Gauthier, S.H. Glenzer *(SLAC National Accelerator Laboratory, High Energy Density Science (HEDS) Division, USA)*
C.A. Palmer, M. Streeter *(Centre for Plasma Physics, Queen's University Belfast, UK)*

A water-jet target developed at SLAC is capable of generating liquid sheets ranging in thickness from 100 nm to 100 microns. This device was successfully deployed in the ATA2 target area during a recent experiment, in which many thousands of laser shots were taken on the jet. High-purity water is forced through a thin nozzle to form the liquid jet, the thickness of which can be controlled by varying the pressure and flow rate. The water is collected in a catcher, which must be heated to prevent the water freezing before it can be pumped out of the chamber into a trap. To avoid exposing the compressor optics to water vapour, a thin silica window was placed in the beamline before the target chamber. An auxiliary vacuum pump was used instead of the turbo pumps normally used for pumping the target chamber, to prevent damage by water droplets.

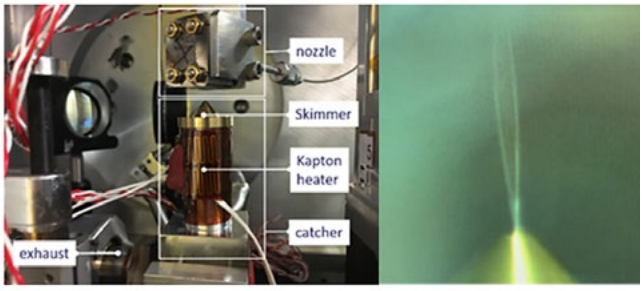

Ultra-thin liquid sheet generation. Picture of the nozzle and catcher in the vacuum chamber (left). A Kapton film heater is used to prevent the water freezing under vacuum. Image of the liquid sheet (right). The nozzle output is at the top, the liquid is flowing downwards.

Contact: N. Bourgeois (nicolas.bourgeois@stfc.ac.uk)

A Michelson interferometer for pulse-train generation on Gemini

C.J. Hooker *(Central Laser Facility, STFC Rutherford Appleton Laboratory, Harwell Campus, Didcot, UK)*

An experiment to investigate the effectiveness of multiple pulses for laser wakefield acceleration required a means of generating pulse trains from the Gemini laser facility. A compact Michelson interferometer was set up in the output of the south amplifier of Gemini, to modulate the spectrum of the beam and thereby produce a pulse train after the compressor. A small angle between the input and rejected beams prevented damage to the laser amplifier by back reflected energy. The compressor was de-tuned to give a pulse duration of approximately 1 ps, and with the modulated spectrum the output was a fully-modulated pulse containing ten sub-pulses with a duration and spacing of around 170 fs. The spacing and uniformity of the pulses could be remotely controlled by the experimenters. Although not part of the regular configuration of Gemini, the interferometer can be re-installed if required for future experiments.

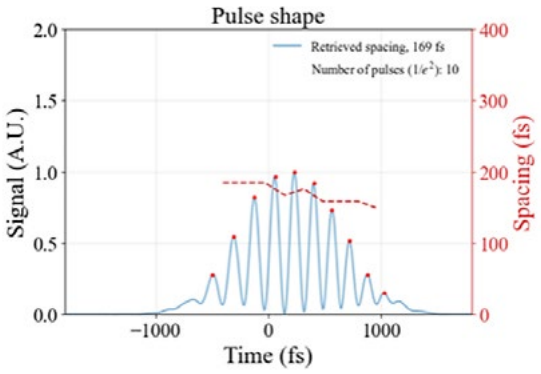

Pulse train generated after compression of the modulated pulse
NOTE: this figure was provided by the Oxford Plasma Physics group specifically for use in the Annual Report.

Contacts: C.J. Hooker (chris.hooker@stfc.ac.uk)
T. de Faria Pinto (tiago.pinto@stfc.ac.uk)

Software developments in Gemini

V.A. Marshall, S. Dann, O. Chekhlov *(Central Laser Facility, STFC Rutherford Appleton Laboratory, Harwell Campus, Didcot, UK)*

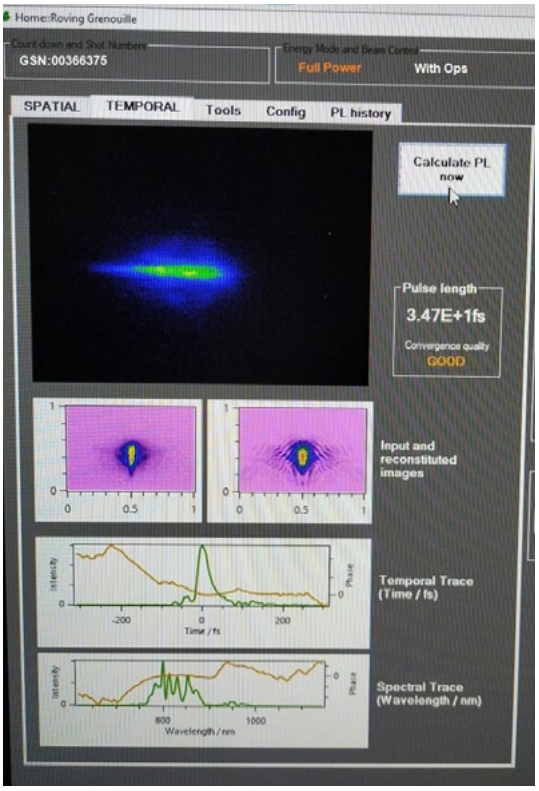

Over the last year there have been two significant updates to the Gemini diagnostics. Firstly, a new Grenouille analysis application, using EPICS PVs to streamline operations, and a reconstruction algorithm based on that described by Sidorenko *et al.* Secondly, a control and data acquisition application for the new D-TACQ ACQ2106 device, reading data from Rogowski coils to diagnose lamp failures in the two Quantel lasers.

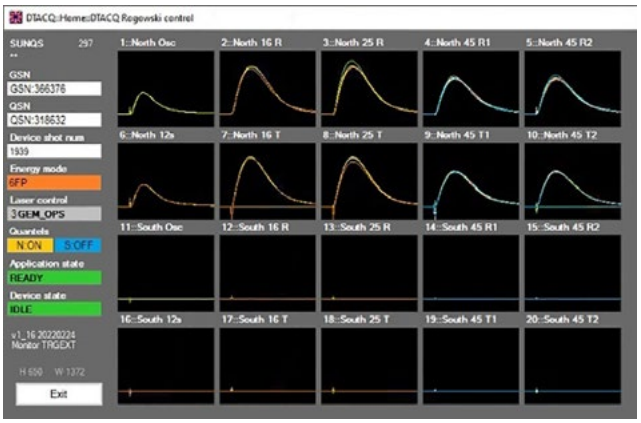

Left: Figure 1: Grenouille application "Temporal" image window showing a false-colour image of the beam, reconstructed images, analysis traces and best-convergence pulse length. The operator is poised to initiate an on-demand analysis.

Above: Figure 2: Typical Rogowski curves. Only the North Quantel is on, and it can be seen that a couple of the 16T and 45T2 lamps are failing.

Contact: V.A. Marshall (victoria.marshall@stfc.ac.uk)

New mounting for grating G1 of the Astra TA2 compressor

C.J. Hooker, B. Matthews *(Central Laser Facility, STFC Rutherford Appleton Laboratory, Harwell Campus, Didcot, UK)*

A new mount for the first grating of the Astra TA2 compressor has been installed in the compressor chamber. The goals of the design were to increase the accuracy of aligning the grating, eliminate instabilities that had previously caused the compressor to become misaligned, and make changing the grating simpler and less risky.

The new mount uses higher-quality bearings for the rotation axes, and vacuum-compatible picomotors for the pitch, yaw and groove rotation adjustments, giving angular sensitivities of less than 1 micro-radian per step. The grating is held in a cassette that locates easily onto the mount, and ensures that the groove face always lies in the same plane. Replacement gratings with different thickness and diameter can be accommodated by making custom-designed cassettes. The accuracy and stability of the new mount have been tested during several experiments, and it has significantly improved the ease and reliability of operations.

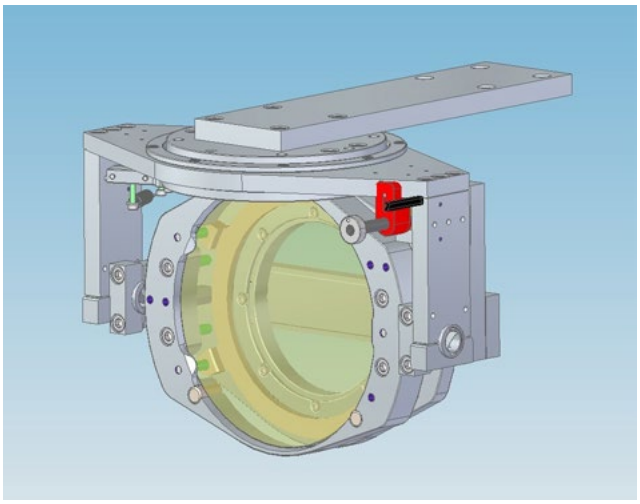

CAD drawing of the new grating mount. The mount is supported from a frame (not shown) inside the compressor chamber.

Contact: C.J. Hooker (chris.hooker@sftc.ac.uk)

mJ-level 5 Hz probe beam for Gemini target area

T. de Faria Pinto, N. Bourgeois, S. Hawkes *(Central Laser Facility, STFC Rutherford Appleton Laboratory, Didcot, UK)*

For a recent experiment on Gemini, the experimental team requested a mJ-level probe beam operating at 5 Hz, in order to build up a large number of probe shots before and after the main target shot. This probe beam was derived from a portion of the 5 Hz input to the Gemini area, taken in transmission through a mirror, and sent down the existing probe beam path. An optical delay line in the form of a cavity was built in the target area, to allow the probe and main pulses to be synchronised. After losses in the delay optics and the probe pulse compressor, the energy in the probe pulse was about 2.5 mJ, but there is potential for this to be improved for future experiments.

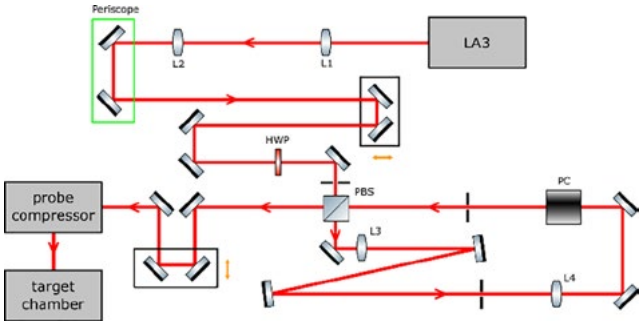

Diagram of the experimental setup. L1: f = 3 m; L2: f = 2 m; L3: f = 1 m; L4: f = 1 m; HWP: Half-wave plate; PBS: Polarising beamsplitter; PC: Pockels cell (Gooch & Housego TX 7595)

Contact: T. de Faria Pinto (tiago.pinto@stfc.ac.uk)

Microassembly of Buried Wire Targets for the European XFEL

P. Ariyathilaka, C. Spindloe, M. Tolley *(Target Fabrication Group, Central Laser Facility, STFC Rutherford Appleton Laboratory, Harwell Campus, Didcot, UK)*

M. Oliver *(Experimental Science Group, Central Laser Facility, RAL Space, STFC Rutherford Appleton Laboratory, Harwell Campus, Didcot, UK)*

Scitech Precision Ltd were tasked with fabricating buried wire targets for the European XFEL, to be used for experiments to study transport properties and hydrodynamics at a metal/plastic interface, as well as for detector testing. Four target arrays in total were fabricated, two with 4 µm tungsten wire and two with 10 µm tungsten wire, in each case with the wires coated with 50 µm (100 µm diameter) of Parylene C (PyC). The wires were fixed by hand to an additive manufactured jig on which they were coated. The coated wire was then attached to a micro-machined silicon mount with target assembly completed manually.

The targets were deployed successfully on experiments.

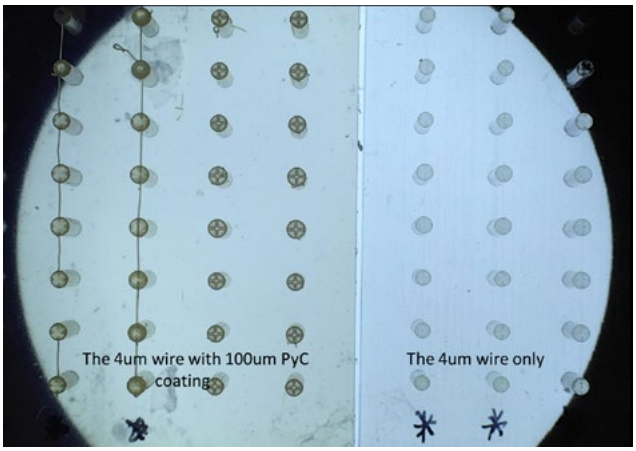

Figure 1: An optical image comparison of the 4 µm wire post and pre PyC coating. The lighter half (right) is before the coating, and the left shows the wire after the PyC coating.

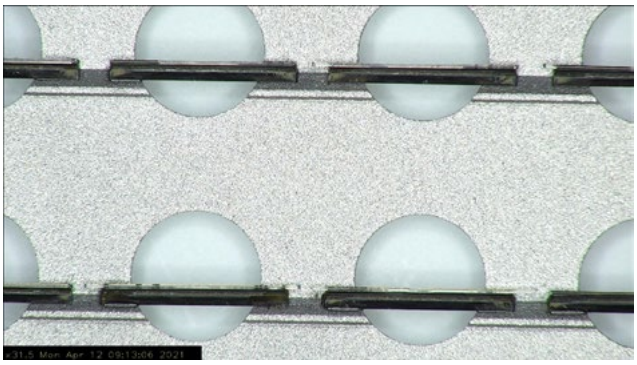

Figure 2: An optical image of the completed assembly mount showing the three parts of the completed target

Contact: P. Ariyathilaka (pawala.ariyathilaka@stfc.ac.uk)

Experimental Testing and Fielding of the CLF Precision Tape Drive in the Gemini Target Area

W. Robins, S. Astbury, C. Spindloe, M. Tolley *(Target Fabrication Group, Central Laser Facility, STFC Rutherford Appleton Laboratory, Harwell Campus, Didcot, UK)*
R. Sarasola, K. Rodgers *(Electrical and Control Group, Central Laser Facility, RAL Space, STFC Rutherford Appleton Laboratory, Harwell Campus, Didcot, UK)*
G. Hull, D. Symes *(Gemini Group, Central Laser Facility, STFC Rutherford Appleton Laboratory, Harwell Campus, Didcot, UK)*

As part of the ongoing development of the CLF high-precision tape drive for high repetition rate experiments access was given to Gemini. The deployment gave vital feedback under experimental conditions on robustness, EMP and debris. Initial runs highlighted issues which were difficult to diagnose. The Target Fabrication team were granted two additional days for testing of several modifications made to the set-up. A camera was installed pointing directly at the system which confirmed 400 shots with no non-recoverable faults. The system was deployed for a commercial run performing faultlessly on hundreds of 12 J (before compressor) shots and subjected to multiple electron beams.

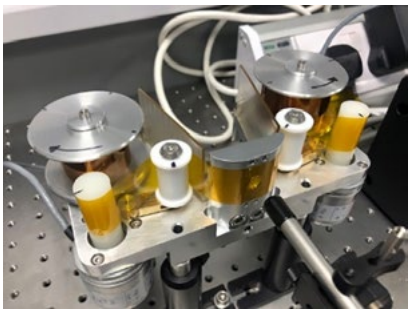

Figure 1: CLF High Precision Tape Drive

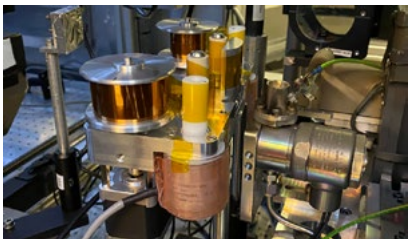

Figure 2: Tape Drive by the Gas Jet in GEMINI, CLF

Contact: W.Robins (wayne.robins@stfc.ac.uk)

A system engineering architecture for robotic microtarget production

P. Umesh, T. Neumann, S. Astbury, D. Haddock, C. Spindloe, M. Tolley *(Target Fabrication Group, Central Laser Facility, STFC Rutherford Appleton Laboratory, Harwell Campus, Didcot, UK)*

A robotic Target Array Assembly System (TAAS) is being developed by the Target Fabrication Group at the Central Laser Facility to automatically assemble microtarget arrays.

Currently all target arrays made by the Group are assembled by hand, but assembly of a single array (of 60 microtargets) can take at least two hours. However, the assembly process of target arrays includes many highly repetitive tasks that can be performed by robots.

This report outlines the main objective and requirements for the first TAAS prototype. From the design, integration, and testing of the prototype, a deeper understanding of the automated assembly process was gained enabling the specification of upgrades required to demonstrate the robotic assembly of high-precision (2D) microtargets.

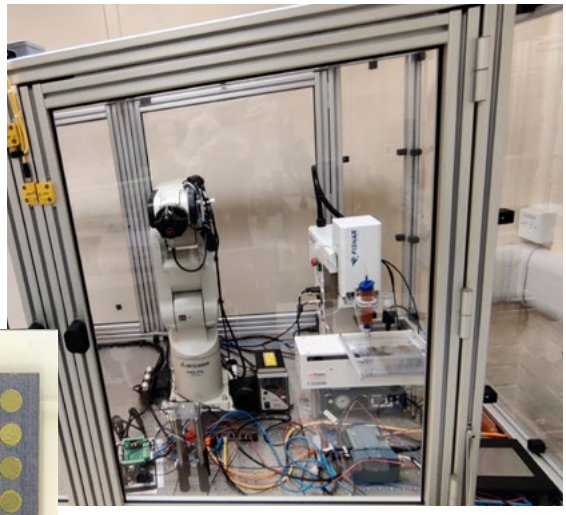

Figure 1: TAAS prototype

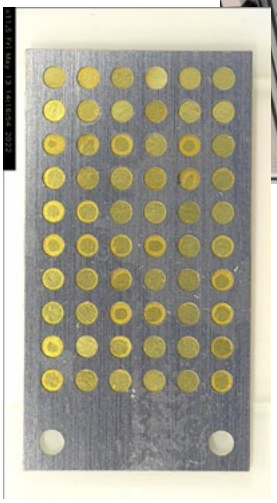

Figure 2: Laser-facing side of the Target Array with sixty 2.8 mm square gold foil targets that are 30 µm thick

Contacts: P. Umesh (pranavsumesh@gmail.com)
S. Astbury (sam.astbury@stfc.ac.uk)

Wavefront-tilt correction of laser pulses by dispersion management

S. Buck, M. Galimberti *(Central Laser Facility, STFC Rutherford Appleton Laboratory, Harwell Campus, Didcot, UK)*

A new diagnostic has been tested to visualise pulse-front-tilt in ultrashort laser pulses. Dispersive mediums (4° glass prisms) were rotationally controlled about the beam axis in accordance to the diagnostic, via an automated loop, to successfully minimise existing angular dispersion from a commercial oscillator output.

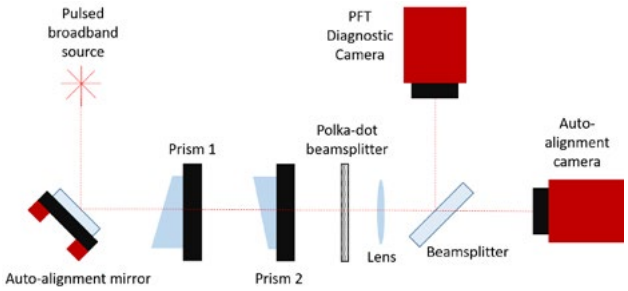

Figure 1: Schematic layout of the experimental setup: a broadband pulse from a commercial oscillator is directed by an automatic alignment loop through two 4° prisms, a polka-dot beamsplitter and a focusing lens

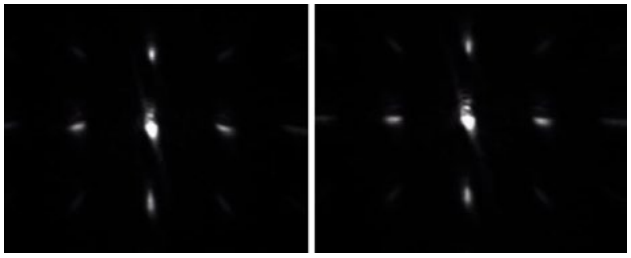

Figure 2: Angular dispersion (AD) diagnostic camera images of undeviated (left) and optimised (right) pulse

Contact: S. Buck (samuel.buck@stfc.ac.uk)

Compressor grating optimisation using the D scan technique

T. Murphy, P. Oliveira, A.C. Aiken, I.O. Musgrave *(Central Laser Facility, STFC Rutherford Appleton Laboratory, Harwell Campus, Didcot, UK*

In this contribution we report on our use of the D scan technique to optimise a grating compressor in the Front-End of the Vulcan Laser Facility. We present theoretical and experimental results, and demonstrate that this technique is ideal to tune both the incidence angle of the grating and the distance between the gratings. Optimal compression is achieved by eliminating any residual second and third order dispersion, resulting in a shorter compressed pulse.

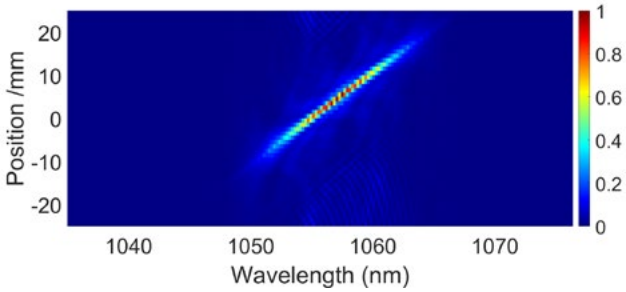

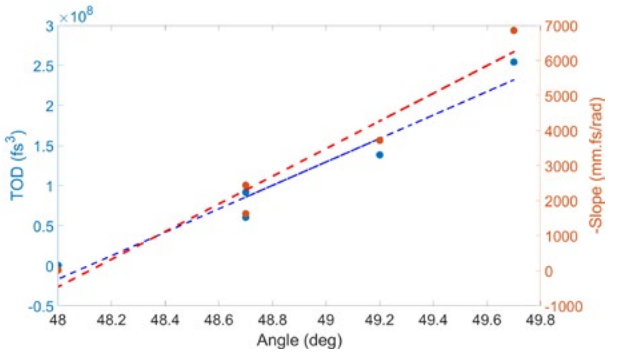

Top: Figure 1: Example of a D scan where the phase only contains third order dispersion

Bottom: Figure 2: Experimental results of TOD (blue) and slope (red) of the D scan trace as a function of the angle.

Contact: P. Oliveira (pedro.oliveira@stfc.ac.uk)

Design of high contrast OPA system for the Vulcan Laser System

T. Murphy, P. Oliveira, W.A. Carter, I.O. Musgrave *(Central Laser Facility, STFC Rutherford Appleton Laboratory, Harwell Campus, Didcot, UK)*

Temporal contrast is a key feature of any high intensity laser. One method of improving contrast is short pulse Optical Parametric Amplification (OPA). Here we present a new high contrast Optical Parametric Chirped Pulsed Amplifier (OPCPA), which is specifically designed for the unique Optical Parametric Oscillator of the Vulcan laser system. We review the current high contrast OPCPA system at the Vulcan laser facility, discuss the new architecture of picosecond pump laser, and present simulations of two different regenerative amplifiers, each with different crystals (Nd:YLF and Yb:SSO) used as the gain material in the Regenerative Amplifier. This is followed by simulations on the non-linear processes of second harmonic generation, OPA and the output pulse.

An investigation of the relationship of the pump-seed pulse duration and the overall efficiency of the system is carried out. This ratio is then determined to maximise the output efficiency of the system.

Finally, a scan of the input and output intensities of the pulse is carried out, to determine the input spectrum and intensity of the pulse for the most stable configuration of the system.

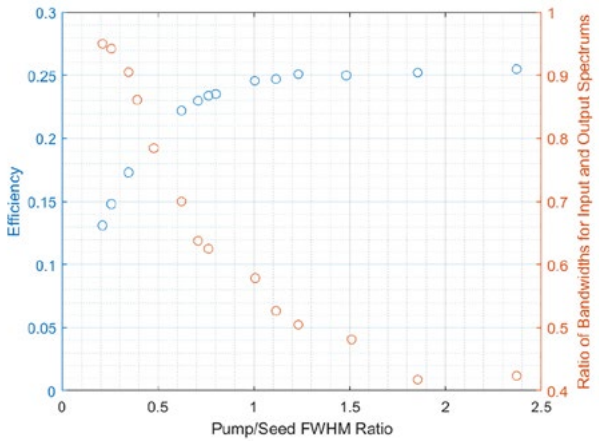

Figure 1: Relationship between pump/seed FWHM ratios, efficiency and bandwidth of the output seed of the OPA

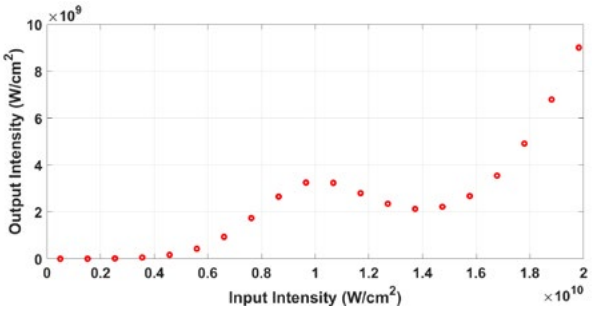

Figure 2: Intensity vs output intensity of OPA system

Contact: P. Oliveira (pedro.oliveira@stfc.ac.uk)

Plasma diagnostics

Deconvolution of multi-Boltzmann x-ray distribution from linear absorption spectrometer via analytical parameter reduction

C.D. Armstrong, D. Neely *(Central Laser Facility, STFC Rutherford Appleton Laboratory, Harwell Campus, Didcot, UK)*
D. Kumar *(Department of Radiation and Chemical Physics, Institute of Physics of the Czech Academy of Sciences, Prague, Czechia)*
P. McKenna, R.J. Gray *(SUPA Department of Physics, University of Strathclyde, Glasgow, UK)*
A.S. Pirozhkov *(Kansai Photon Science Institute, National Institutes for Quantum and Radiological Science and Technology, Kyoto, Japan)*

Accurate characterization of incident radiation is a fundamental challenge for diagnostic design. Herein, we present an efficient spectral analysis routine that is able to characterize multiple components within the spectral emission by analytically reducing the number of parameters. The technique is presented alongside the design of a hard x-ray linear absorption spectrometer using the example of multiple Boltzmann-like spectral distributions; however, it is generally applicable to all absorption based spectrometer designs and can be adapted to any incident spectral shape. This routine is demonstrated to be tolerable to experimental noise and suitable for real-time data processing at multi-Hz repetition rates.

Reprinted from C.D. Armstrong et al., Rev. Sci. Instrum. 92, 113102 (2021) under the terms of the Creative Commons 4.0 International License; doi: 10.1063/5.0057486

Contacts: C.D. Armstrong (chris.armstrong@stfc.ac.uk)
A.S. Pirozhkov (pirozhkov.alexander@qst.go.jp)

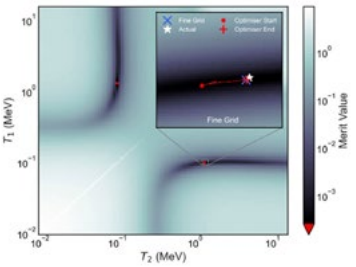

Figure 1: Example of second stage reconstruction. The inset shows the parameter space evaluated by the fine grid, and the red line shows the evaluation points for the Nelder-Mead routine—the color scale of the inset is the same as the primary figure.

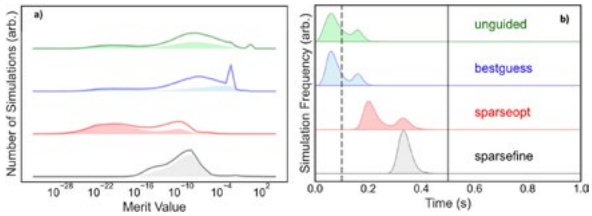

Figure 2: Averaged computation time for each methodology on a standard desktop machine. The vertical solid and dashed lines correspond to 2 and 10 Hz reconstructions, respectively

Deployment of active Thomson spectrometer at Vulcan petawatt

D. Bedilu, H. Ahmed, D.C. Carroll, R.J. Clarke *(Experimental Science Group, Central Laser Facility, STFC Rutherford Appleton Laboratory, Harwell Campus, Didcot, UK)*

Decaying emission of 511 keV annihilation X-rays from materials activated by >3 MeV photons can be used to diagnose laser-plasma interactions. Low-voltage operable silicon-photomultipliers (SiPM) coupled to scintillators are a favourable alternative to large, high voltage photomultiplier tube (PMT) detectors for measuring low photon numbers.

To optimise the design, the performance of scintillators of varying size is explored, and a simple model is presented which achieves good agreement with the spectra obtained from bismuth germanate (BGO) - SiPM detector combinations tested.

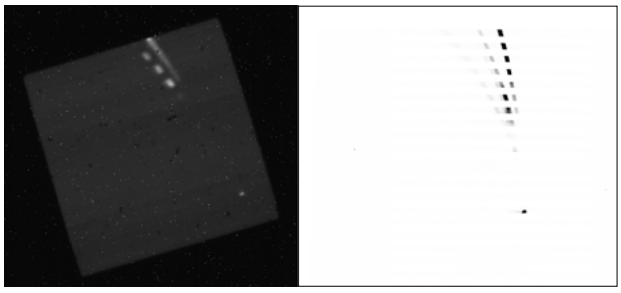

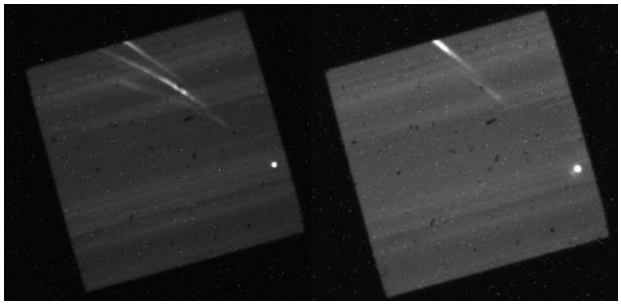

Top: Figure 1: Images from the slotted image plate (left) with ceramic Gadox (right) placed behind for cross-calibration

Bottom: Figure 2: Comparison between Gadox (left) and Lanex (right) scintillators

Contacts: D. Bedilu (daniel.bedilu@stfc.ac.uk)
H. Ahmed (hamad.ahmed@stfc.ac.uk)

Investigating the Working Distances of the Questar QM-1SZ Tele-Microscopes

J.J. Bush *(Physics Department, Loughborough University, UK)*

M.M. Notley, D. C. Carroll, R.J. Clarke *(Central Laser Facility, STFC Rutherford Appleton Laboratory, Harwell Campus, Didcot, UK)*

Tele-microscopes are an exciting new tool for the Central Laser Facility to use in the referencing of targets, helping to streamline the running of experiments. They are long range, high resolution imagers that allow for a wide or narrow field of view (FoV) from outside of the target chamber, for positional referencing of a target in 3D space.

This report is a continuation of *Investigating Contrast, Resolution and Field-of-View (FoV) of the Questar QM-1SZ Tele-Microscope* by J.A. Hodson et al. [1], which looked to measure the resolution, contrast and FoV of the tele-microscopes QM-41and QM-42 (serial numbers QM110541SZ and QM110542SZ) at distances of 65 cm and 1.4 m.

This later investigation looks into the working distance of these two tele-microscopes, as well as QM-40 and QM-43 (serial numbers QM110540SZ and QM110543SZ) that are advertised to have a much longer working distance at the cost of resolution. Measurements are taken of the resolution and FoV of the QM-40 and QM-41 at their nearest focus, 1.2 m, and at their farthest focus. The working distance stated in the specifications for the QM-41 and QM-42 was from 560 mm to 1520 mm, whereas the working distance for the QM-40 and QM-43 was from 914 mm (3 feet) to infinity. However, the effective working distance from the front plate of the tele-microscopes was found to be 621 mm to 1370 mm for the QM-41 and QM-42, while a value of 1036 mm to infinity was found for the QM-40 and QM-43. An analysis of the capabilities of a custom built adjust able stand for the tele-microscopes was also included, as well as an evaluation of the performance of these tele-microscopes as a referencing tool in the Dr G Scott experiment [2].

Contact: C.D. Armstrong (chris.armstrong@stfc.ac.uk)

[1] J.A. Hodson et al., Investigating Contrast, Resolution and Field-of-View of the Questar QM-1SZ Tele-Microscope. Tech. rep., Central Laser Facility Annual Report 2018/19. **https://www.clf.stfc.ac.uk/Gallery/45%20-%20Hodson.pdf**

[2] Dr G Scott. Direct Laser Acceleration of Electrons to Superponderomotive Energies. Experiment Proposal. 2020.

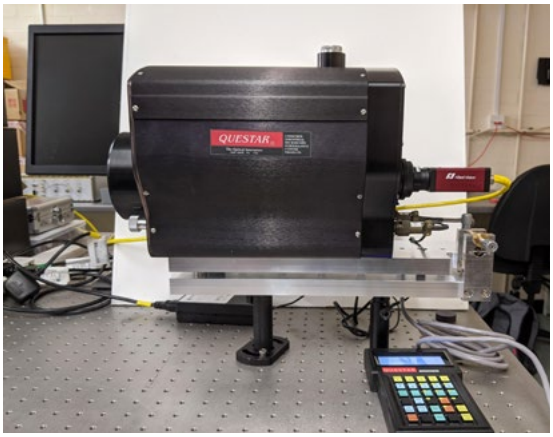

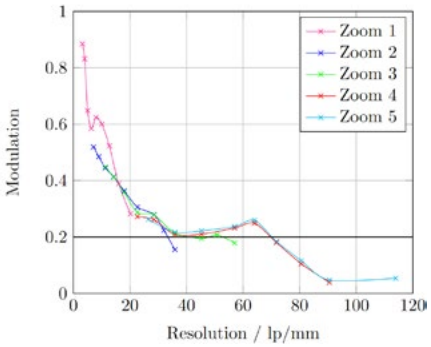

Above: Figure 1: Setup of QM-41 on custom stand

Left: Figure 2: QM-41 1.2 m Vertical Modulation

Modelling Tomographic Reconstruction using Scintillator Fibres for active proton imaging

A.R.L. Illoul *(School of Physics, University of Bristol, UK)*

C.D. Armstrong *(Central Laser Facility, STFC Rutherford Appleton Laboratory, Harwell Campus, Didcot, UK)*

High repetition rate laser facilities require active diagnostic systems in order to process data promptly. Current methods to image the spectral-spatial distribution of protons are incapable of this, and so novel diagnostic tools need to be developed. Here we present software as a proof-of-concept active proton imaging system, capable of measuring the spectral-spatial distribution of proton beams. This novel approach utilises tomographic reconstruction, with scintillating fibres as the medium of signal transport. We exhibit the reconstructed images as further projected angles are used, and demonstrate the necessity of correcting for light absorption within a scintillator fibre. We analytically present how the spectral resolution of such a diagnostic tool would vary as further projected angles are used.

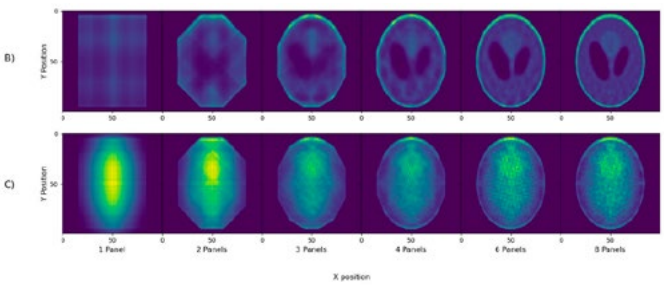

Demonstration of reconstruction of a Shepp-Logan phantom with increasing angles, with and without accounting for attenuation of the light emission

Contact: C.D. Armstrong (chris.armstrong@stfc.ac.uk)

Demonstrating Light Yield and Energy Resolution trends for different sized Scintillators using Monte Carlo Simulations

A.R.L. Illoul *(School of Physics, University of Bristol, UK)*

C.D. Armstrong *(Central Laser Facility, STFC Rutherford Appleton Laboratory, Harwell Campus, Didcot, UK)*

Light yield loss due to larger scintillator dimensions has been documented for a number of different scintillators, and was explained using the overlap between the characteristic emission and absorption spectrum of the scintillator – causing self-absorption, an effect which rises with respect to the average photon path length. Monte Carlo simulations were used to demonstrate that the in- crease in surface area of a diffusely-reflecting surface wrapped around the scintillator will produce a similar trend, independent of self-absorption. The aspect ratio of two sides of the scintillator was varied to observe its effect on the light yield measured, showing a gradual climb in yield as the ratio increased. There is indication that the detector planes surface area is not driving this increase independently. The energy resolution of scintillators of a given length were established, producing higher resolutions at smaller scintillator lengths. Increased resolution was also found for higher reflection coefficients of the reflective wrapping. A literature comparison is also shown to demonstrate the simulations consistency.

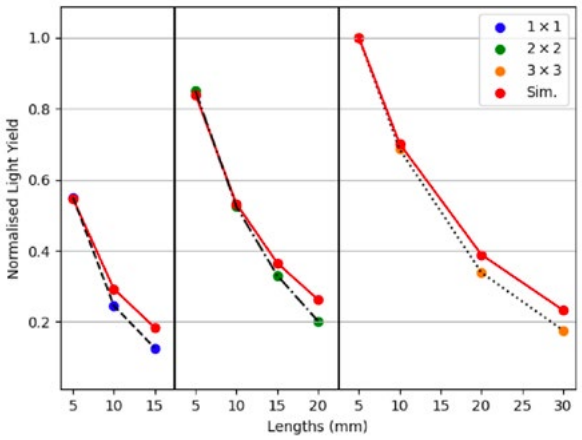

Light yield from a scintillator as a function of cross-section and aspect ratio, comparing the results from Cherry et al.[1] with the presented Monte Carlo simulation

[1] S R Cherry *et al.* Collection of scintillation light from small bgo crystals. IEEE Transactions on Nuclear Science, 42(4):1058-1063, 1995

Contact: C.D. Armstrong (chris.armstrong@stfc.ac.uk)

Scintillator Light Yield Variation due to the Reflective Wrapping

A.R.L. Illoul *(School of Physics, University of Bristol, UK)*

C.D. Armstrong *(Central Laser Facility, STFC Rutherford Appleton Laboratory, Harwell Campus, Didcot, UK)*

During calibration of an X-ray spectrometer composed of rails of scintillator blocks, Dasgupta *et. al.*[1] observed large discrepancies between each scintillator block's light yield when radiated by a Sodium-22 (Na-22) source. Forty individual scintillator blocks of the same shape and type collectively constituted the yield data set with a variation of 16.7%. We demonstrate, using Monte Carlo simulations of light transport in scintillators, that the cause of this high variance could be accounted for in variations of thickness of the reflective material on the scintillators' surface. Literature figures that related the number of layers of reflector tape to the reflectance coefficient were employed to then produce a distribution of reflectance coefficients, which fully justify variations in the reflectivity as the source of light yield variation.

[1] A. Dasgupta, C.D Armstrong, D.Neely, D.R. Rusby, G.G. Scott - Calibrating LYSO crystals part of a hard X-ray spectrometer CLF Annual Report 2019

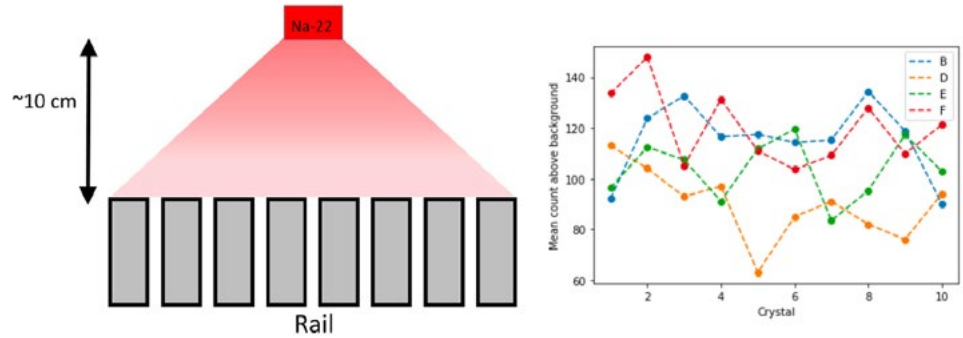

Rail calibration schematic (left) and results (right) demonstrating high variability in uniform set of crystals. Subtle variation in average reflective coefficient can explain the measured variation in yield.

Contact: C.D. Armstrong (chris.armstrong@stfc.ac.uk)

Facility upgrades for Artemis: new and upgraded XUV beamlines

The Artemis facility has recently moved into new labs in the Research Complex at Harwell and had a major upgrade of capability, with a new 100 kHz laser system and new beamlines. In 2020-21, we focused on developing the vacuum beamlines that allow us to generate ultrashort pulses in the extreme ultraviolet (XUV) through high harmonic generation (HHG), select the XUV wavelength, and re-focus them on target at the end-stations.

Artemis facility upgrade

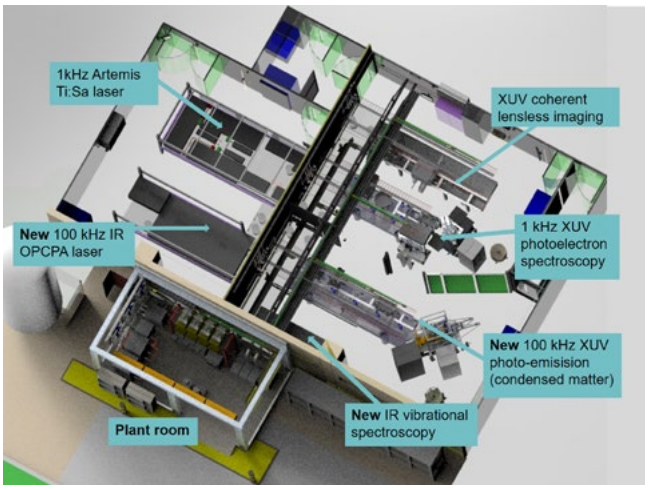

Figure 1: New Artemis labs in the Research Complex at Harwell

The new lab (Figure 1) contains four independent beamlines that support user experiments in time-resolved photoemission from the gas and solid states using HHG probes, XUV coherent imaging, and IR spectroscopy. The two laser systems are housed in a temperature- and humidity-controlled laser room, while the experimental stations are in the neighbouring room. A plant room segregates compressors and mechanical pumps from the lab, so as to reduce noise and vibrations in the measurement area.

Artemis has a new, 100 kHz laser system, based on optical parametric chirped pulse amplification of the output from a Yb:YAG thin-disc pump. The laser produces 50 fs pulses at 1750 nm wavelength with an average power of 20 W. It can also be tuned to produce 100 fs pulses across the wavelength regions from 1430-1850 nm and 2330-3680 nm. This laser currently serves our IR spectroscopy area and a new beamline that is being built for the material science program. This will ultimately support beam times for pump-probe photoemission spectroscopy with improved signal-to-noise characteristics, and will also be the basis for new capabilities in pump-probe transient absorption spectroscopy. The beamline will generate short pulses in the tens of fs regime, with photon energies of tens of eV through HHG.

The 1 kHz KLM Labs Red Dragon titanium-sapphire laser system that has served Artemis since 2008 has been refurbished with new Pockels cells, stretcher and compressor upgrades, and a third amplifier. This laser primarily serves beamlines for XUV coherent imaging, and for gas-phase time-resolved photoemission spectroscopy. The combination of laser upgrades and improvements to the XUV beamline has increased XUV flux on target by an order of magnitude.

New 100 kHz XUV beamline

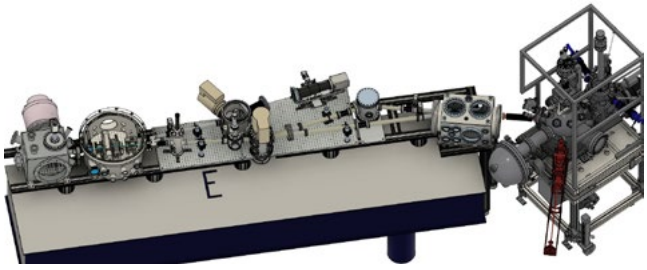

Figure 2: New 100 kHz XUV beamline for Artemis. The laser enters from the left and generates harmonics in the first chamber. This is followed by a time-preserving monochromator and focusing optics. The end-station for time-and-angle-resolved photoemission is shown on the right

As part of the upgrade and relocation of Artemis to the Research Complex at Harwell, we are installing a new beamline dedicated to materials science and transient absorption experiments with the tuneable 100 kHz laser (Figure 2). The beamline consists of a differentially pumped high harmonic generation (HHG) source for the production of extreme ultraviolet (XUV) radiation (optimised in the 20-50 eV photon energy range but with the potential capability to extend beyond the carbon K-edge); a time-preserving monochromator; flat-field XUV spectrometer; dual-magnification XUV relay imaging; and materials science end station.

The main objective for materials science at 100 kHz is to increase the data acquisition rate whilst maintaining the photon density per pulse, and thus maintaining the space-charge. The benefits of this are two-fold: (1) to reduce the data collection time and/or allow a wider parameter space to be studied; and (2) to enable a reduction of the XUV spot size to match the sample or domain sizes (down to the 10 µm level).

The objective for transient absorption spectroscopy is to allow high spectral resolution measurements to be performed at photon energies up to and potentially beyond the carbon K-edge. The higher repetition rate and stability of the laser should significantly improve the signal-to-noise and thus enable pump-probe measurements to be performed at these photon energies.

Table 1 below lists estimated expected parameters for initial materials science experiments on the beamline, based on modelling and benchmark experiments performed on our 1 kHz beamline.

Photon parameter	Expected performance of 100 kHz XUV beamline
Probe energy range	15 – 45 eV initially. Higher photon energies will be offered later.
Pump energy range	λ = 850 – 900 nm, 1700 – 1800 nm, and 2650 – 2950 nm initially.
Energy resolution (limited by short-pulse characteristics and by space charge)	~100 meV expected (Photon-energy and pulse-length dependent)
Time resolution (limited by pulse lengths of pump and probe)	~50 fs expected
Beam spot size at normal emission	<100 µm expected; smaller spot sizes to be pursued over the course of subsequent development
Probe flux	Expected: ~10^5 photons/pulse (~10^{10} photons/second) at about 25 eV
Pump fluence	Expected: several mJ/cm^2/pulse. Under development.
Probe polarization	Linear polarization, *s* or *p*
Pump polarization	Fully controllable

Table 1: Expected performance parameters of the 100 kHz XUV beamline

XUV radiation is produced via HHG in a purposely-designed differentially-pumped vacuum chamber. A gas cell/jet is inserted into a small conically shaped chamber, attached to a high-throughput pump and isolated from the main chamber using pinholes matched to the size of the optical beam. This should allow gas pressures in the generation region to reach above 1 bar whilst maintaining a vacuum level better than 10^{-4} mbar. The backing gas pressure can be controlled digitally. Three motorised stages allow the gas target to be positioned with micrometre accuracy, with a longitudinal travel of 50 mm. This should allow the optimal and repeatable phase matching conditions to be achieved reliably for the given optical source. A second pinhole is used to isolate the subsequent mono-chromator chamber.

After generation, a single harmonic can be selected using a time-preserving monochromator that uses gratings in conical diffraction geometry at grazing incidence to maximise throughput with minimal temporal and spatial aberration.[1] This has been specifically designed for the highly divergent beams expected from the required focusing geometry. It consists of three interchangeable gratings with maximum efficiency in the 20-45 eV and 60-100 eV photon energy ranges. The performance specification of the harmonics will depend on the grating and the mode of operation of the laser. The spectral resolution will be limited by the bandwidth of the harmonics (~1 eV in short pulse mode and >100 meV in long pulse mode), with a high temporal resolution (tens of femtoseconds in short pulse mode and hundreds of femtoseconds in long pulse mode). In addition, the monochromator can be by-passed to allow the HHG source to be relay imaged onto the exit slit of the monochromator, providing access to the full harmonic spectrum or the use of fixed transmission filters.

Two fully automated beam paths are available to relay-image the exit slit plane of the monochromator onto the sample in the end station. A single grazing incidence toroidal mirror will allow 1:1 imaging, yielding a spot size of ~100 µm and providing maximum flux on the sample.

Alternatively, a double toroid arrangement[2] specifically designed for this beamline can be used to give better than 3:1 demagnification, compensating the elongated beam from the monochromator, and giving a spot size on the order of 20 µm with monochromatisation and <10 µm using the grating by-pass (e.g. with fixed transmission filters). High precision six-axis stages allow spatial aberrations to be fully minimised and enable switching between the XUV beam paths without the need to realign the optical pump.

Upgrades to 1 kHz XUV beamline

Figure 3: Upgraded 1 kHz XUV beamline with monochromator.

The Artemis 1 kHz XUV beamline has also been overhauled and improved as part of the upgrade project (Figure 3). Improvements include a new, more compact chamber for high harmonic generation, similar to that on the new 100 kHz beamline, and upgrades to the differential pumping and positioning of the gas-jet. The geometry of the beamline has been changed, with the path lengths between the XUV focus and the first toroidal mirror in the monochromator, and from the second toroidal mirror to the grating exit slit, increased to 600 mm. This reduces the rate of damage to the optics, which always deteriorate over time due to the gas-jet being slightly ablated and metal being deposited on the mirrors. The toroidal mirrors in the beamline have been replaced, and this has increased the throughput of the beamline by about a factor of 10. The measured XUV flux after the monochromator is now ~2 x 10^{10} photons/sec at 30 eV. We are carefully monitoring the mirror surfaces and quality of the exit slit in order to maintain this performance. The flux can be increased further by generating harmonics of the second harmonic of the laser at 400 nm.

After the monochromator, the XUV pulses are refocused into the end-stations with a gold-coated mirror used at grazing incidence. The XUV can be recombined inside the end-station, with laser pulses at wavelengths from the ultraviolet to the far-infrared for pump-probe experiments. The high XUV flux and UV pump makes this beamline particularly well-suited for gas-phase chemistry.

Conclusions

Artemis is now installed in its new lab in the Research Complex at Harwell, and has carried out major upgrades to its capabilities. With a new laser, upgrades to the existing laser, new beamlines, and a new lab layout, users can expect major improvements in measurement capabilities and in the user experience. More details of the current status are posted on our website.[3]

References

1. *L. Poletto et al., "Time-delay compensated monochromator for the spectral selection of extreme-ultraviolet high-order laser harmonics," Rev. Sci. Instrum., vol. 80, no. 12, p. 123109, Dec. 2009. https://doi.org/10.1063/1.3273964*
2. *F. Frassetto et al., "High-throughput beamline for attosecond pulses based on toroidal mirrors with microfocusing capabilities," Rev. Sci. Instrum., vol. 85, no. 10, p. 103115, Oct. 2014. https://doi.org/10.1063/1.4898671*
3. *https://www.clf.stfc.uk/Pages/Artemis.aspx*

Contact: E. Springate (emma.springate@stfc.ac.uk)

Imaging and dynamics for physical and life sciences

Directly imaging the localisation and photosensitization properties of the pan-mTOR inhibitor, AZD2014, in living cancer cells

A.R. Ahmed *(Central Laser Facility, Research Complex at Harwell, STFC Rutherford Appleton Laboratory, Harwell Campus, Didcot, UK; Larch House, Woodlands Business Park, Breckland, Linford Wood, Milton Keynes MK14 6FG, UK)*
A. Candeo, S.R. Needham, S.W. Botchway, A.W. Parker *(Central Laser Facility, Research Complex at Harwell, STFC Rutherford Appleton Laboratory, Harwell Campus, Didcot, UK)*
S. D'Abrantes *(Central Laser Facility, Research Complex at Harwell, STFC Rutherford Appleton Laboratory, Harwell Campus, Didcot, UK; CRUK/MRC Oxford Institute for Radiation Oncology, University of Oxford, Gray Laboratories, UK)*
R.B. Yadav *(Evotec (UK) Ltd, Milton Park, Abingdon, UK)*

The range of cellular functions the mechanistic target of rapamycin (mTOR) protein performs makes it an attractive drug target for cancer therapy. However, the cellular localisation and mode of action of second generation inhibitors of mTOR is poorly understood despite the level of attention there is in targeting the mTOR protein. We have therefore studied the properties of the pan-mTOR inhibitor AZD2014, an ideal candidate to study because it is naturally fluorescent, characterising its photochemical properties in solution phase (DMSO, PBS and BSA) and within living cells, where it localises within both the nucleus and the cytoplasm but with different excited state lifetimes of 4.8 (+/- 0.5) and 3.9 (+/- 0.4) ns respectively. We measure the uptake of the inhibitor AZD2014 (7 μM) in monolayer HEK293 cells occurring with a half-life of 1 min but observe complex behaviour for 3D spheroids with the core of the spheroid showing a slower uptake and a slow biphasic behaviour at longer times. From a cellular perspective using fluorescence lifetime imaging microscopy AZD2014 was found to interact directly with GFP-tagged mTORC1 proteins including the downstream target, S6K1. We observe light sensitive behaviour of the cells containing AZD2014 which leads to cell death, in both monolayer and spheroids cells, demonstrating the potential of AZD2014 to act as a possible photodynamic drug under both single photon and multiphoton excitation and discuss its use as a photosensitizer. We also briefly characterise another panmTOR inhibitor, INK128.

Reproduced from Ahmed, Abdullah R., et al. "Directly imaging the localisation and photosensitization properties of the pan-mTOR inhibitor, AZD2014, in living cancer cells." Journal of Photochemistry and Photobiology B: Biology (2020): 112055, under the terms of the Creative Commons Attribution 4.0 International (CC BY 4.0) License. doi: 10.1016/j.jphotobiol.2020.112055

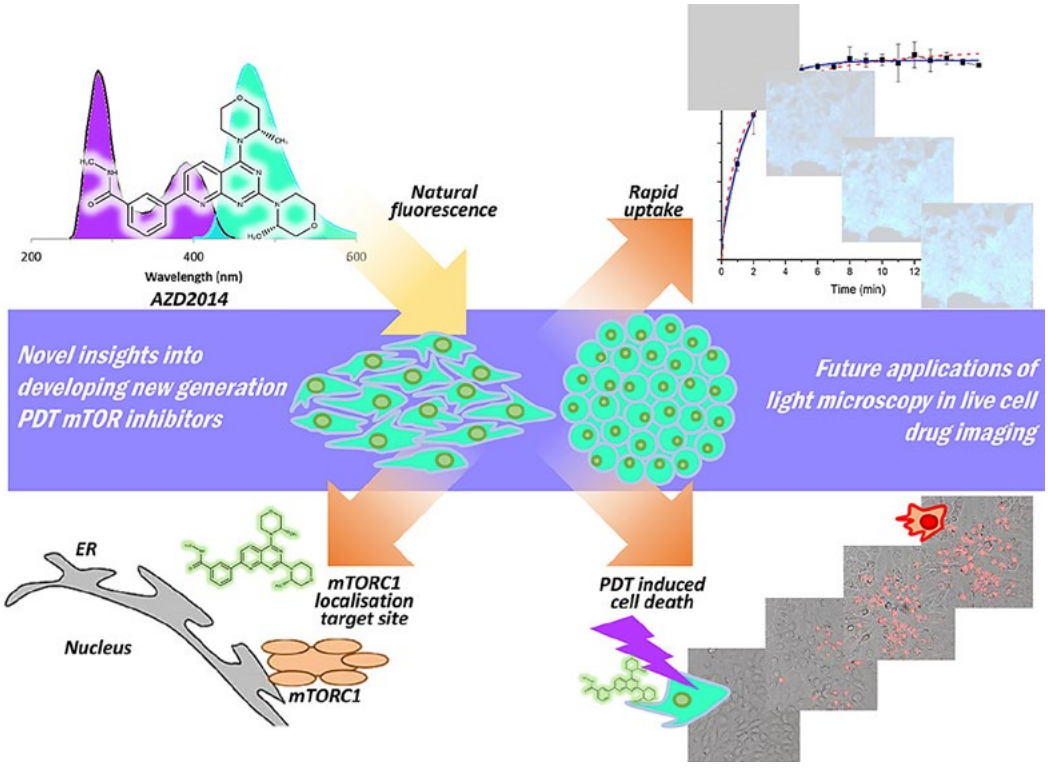

Contacts: S.W. Botchway (stan.botchway@stfc.ac.uk)
A.W. Parker (a.w.parker@stfc.ac.uk)

The smfBox is an open-source platform for single-molecule FRET

B. Ambrose, J.M. Baxter, J. Cully, M. Willmott, J. Shewring, M. Aaldering. T.D. Craggs *(Sheffield Institute for Nucleic Acids, Department of Chemistry, University of Sheffield, UK)*
E.M. Steele, A. Cadby *(Department of Physics, University of Sheffield, UK)*
B.C. Bateman, M. Martin-Fernandez *(Central Laser Facility, Research Complex at Harwell, STFC Rutherford Appleton Laboratory, Harwell Campus, Didcot, UK)*

Single-molecule Förster Resonance Energy Transfer (smFRET) is a powerful technique capable of resolving both relative and absolute distances within and between structurally dynamic biomolecules. High instrument costs, and a lack of open-source hardware and acquisition software have limited smFRET's broad application by non-specialists. Here, we present the smfBox, a cost-effective confocal smFRET platform, providing detailed build instructions, open-source acquisition software, and full validation, thereby democratising smFRET for the wider scientific community.

Reproduced from Ambrose, B., Baxter, J.M., Cully, J. et al. The smfBox is an open-source platform for single-molecule FRET. Nat Commun 11, 5641 (2020), published by Springer Nature, under the terms of a Creative Commons Attribution 4.0 International License. doi: 10.1038/s41467-020-19468-4

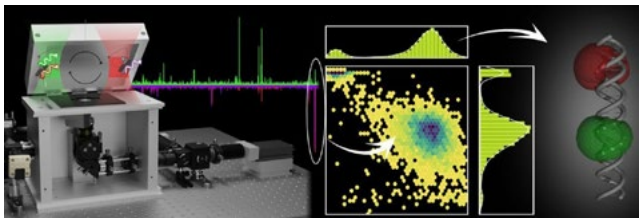

The smfBox (left) is a robust, affordable instrument for single-molecule FRET experiments, built from machined aluminium and off-the-shelf components. Molecules diffuse through a confocal volume and are alternately excited by a green and red lasers (left top), generating FRET and stoichiometry values, which are plotted on a 2D histogram (centre). The FRET efficiencies can be related to the structure of the biomolecule under investigation (right).

Contact: T.D. Craggs (t.craggs@sheffield.ac.uk)

Preparation of polymer gold nanoparticle composites with tunable plasmon coupling and their application as SERS substrates

S.A. Belhout, F.R. Baptista, S.J. Devereux, S.J. Quinn *(School of Chemistry, University College Dublin, Republic of Ireland)*
A.W. Parker, A.D. Ward *(Central Laser Facility, Research Complex at Harwell, STFC Rutherford Appleton Laboratory, Harwell Campus, Didcot, UK)*

The controlled surface functionalisation of polystyrene beads (200 nm) with a lipoic acid derivative is used to assemble composites with between 4 to 20% loadings of citrate stabilised gold nanoparticles (13 nm–30 nm), which exhibit variable optical properties arising from interactions of the nanoparticle surface plasmon resonance (SPR). The decrease in average interparticle distance at higher loadings results in a red-shift in the SPR wavelength, which is well described by a universal ruler equation. The composite particles are shown to act as good SERS substrates for the standard analyte 4-mercaptophenol. The direct assessment of the SERS activity for individual composite particles solution is achieved by Raman optical tweezer measurements on 5.3 µm composite particles. These measurements show an increase in performance with increasing AuNP size. Importantly, the SERS activity of the individual particles compares well with the bulk measurements of samples deposited on a surface, indicating that the SERS activity arises primarily from the composite and not due to composite–composite interactions. In both studies the optimum SERS response is obtained with 30 nm AuNPs.

Reproduced from S. A. Belhout, F. R. Baptista, S. J. Devereux, A. W. Parker, A. D. Ward and S. J. Quinn, Preparation of polymer gold nanoparticle composites with tunable plasmon coupling and their application as SERS substrates. Nanoscale, 2019, 11, 19884-19894. DOI: 10.1039/C9NR05014K with permission from the Royal Society of Chemistry.

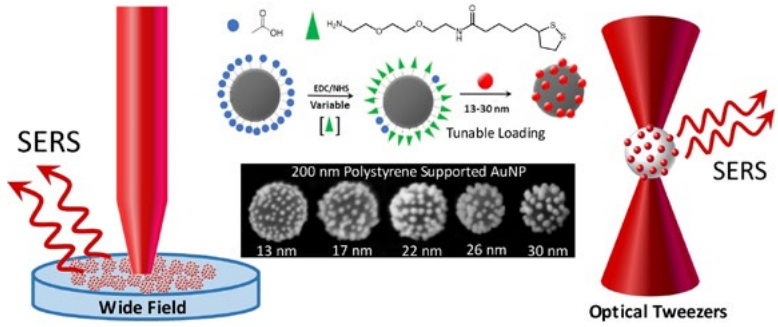

Contact: S.J. Quinn (susan.quinn@ucd.ie)

Adaptive lipid immiscibility and membrane remodeling are active functional determinants of primary ciliogenesis

M. Bernabé-Rubio *(Department of Cell Biology and Immunology, Centro de Biología Molecular Severo Ochoa, Consejo Superior de Investigaciones Científicas and Universidad Autónoma de Madrid, Spain; King's College London Centre for Stem Cells and Regenerative Medicine, Guy's Campus, London, UK)*
M. Bosch-Fortea *(Department of Cell Biology and Immunology, Centro de Biología Molecular Severo Ochoa, Consejo Superior de Investigaciones Científicas and Universidad Autónoma de Madrid, Spain; Institute of Bioengineering and School of Engineering and Materials Science, Queen Mary University of London, UK)*
M.A. Alonso *(Department of Cell Biology and Immunology, Centro de Biología Molecular Severo Ochoa, Consejo Superior de Investigaciones Científicas and Universidad Autónoma de Madrid, Spain)*
E. García *(Central Laser Facility, Research Complex at Harwell, STFC Rutherford Appleton Laboratory, Harwell Campus, Didcot, UK; CR-UK Beatson Institute, Glasgow, UK)*
J. Bernadino de la Serna *(Central Laser Facility, Research Complex at Harwell, STFC Rutherford Appleton Laboratory, Harwell Campus, Didcot, UK; National Heart and Lung Institute, Imperial College London, UK; NIHR Imperial Biomedical Research Centre, London, UK)*

Lipid liquid–liquid immiscibility and its consequent lateral heterogeneity have been observed under thermodynamic equilibrium in model and native membranes. However, cholesterol-rich membrane domains, sometimes referred to as lipid rafts, are difficult to observe spatiotemporally in live cells. Despite their importance in many biological processes, robust evidence for their existence remains elusive. This is mainly due to the difficulty in simultaneously determining their chemical composition and physicochemical nature, whilst spatiotemporally resolving their nanodomain lifetime and molecular dynamics. In this study, a bespoke method based on super-resolution stimulated emission depletion (STED) microscopy and raster imaging correlation spectroscopy (RICS) is used to overcome this issue. This methodology, laser interleaved confocal RICS and STED-RICS (LICSR), enables simultaneous tracking of lipid lateral packing and dynamics at the nanoscale. Previous work indicated that, in polarized epithelial cells, the midbody remnant licenses primary cilium formation through an unidentified mechanism. LICSR shows that lipid immiscibility and its adaptive collective nanoscale self-assembly are crucial for the midbody remnant to supply condensed membranes to the centrosome for the biogenesis of the ciliary membrane. Hence, this work poses a breakthrough in the field of lipid biology by providing compelling evidence of a functional role for liquid ordered-like membranes in primary ciliogenesis.

Reproduced from Bernabé-Rubio, M., Bosch-Fortea, M., García, E., Bernardino de la, J., Alonso, M. A., Adaptive Lipid Immiscibility and Membrane Remodeling Are Active Functional Determinants of Primary Ciliogenesis. Small Methods 2021, 5, 2000711, published by Wiley-VCH GmbH, under the terms of the Creative Commons Attribution-NonCommercial-NoDerivs License. doi: 10.1002/smtd.202000711

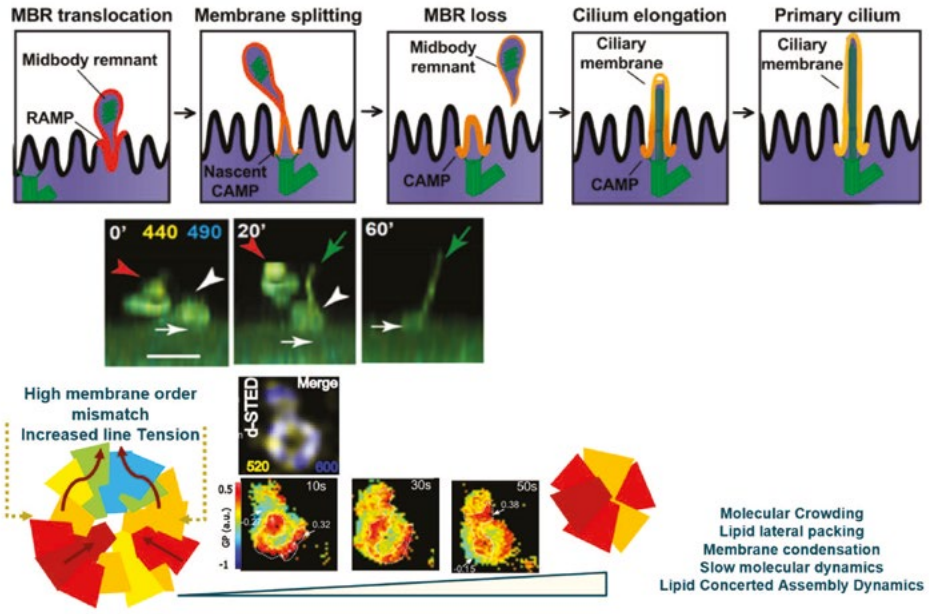

Contact: M.A. Alonso (maalonso@cbm.csic.es)

Combining Multicolor FISH with Fluorescence Lifetime Imaging for Chromosomal Identification and Chromosomal Sub Structure Investigation

A. Bhartiya *(London Centre for Nanotechnology, University College London, UK; Research Complex at Harwell, STFC Rutherford Appleton Laboratory, Harwell Campus, Didcot, UK)*
I. Robinson *(London Centre for Nanotechnology, University College London, UK; Condensed Matter Physics and Materials Science Division, Brookhaven National Lab, Upton, NY, USA)*
M. Yusuf *(London Centre for Nanotechnology, University College London, UK; Research Complex at Harwell, STFC Rutherford Appleton Laboratory, Harwell Campus, Didcot, UK; Centre for Regenerative Medicine and Stem Cell Research, Aga Khan University, Karachi, Pakistan)*
S.W. Botchway *(Central Laser Facility, Research Complex at Harwell, STFC Rutherford Appleton Laboratory, Harwell Campus, Didcot, UK)*

Understanding the structure of chromatin in chromosomes during normal and diseased state of cells is still one of the key challenges in structural biology. Using DAPI staining alone together with Fluorescence lifetime imaging (FLIM), the environment of chromatin in chromosomes can be explored. Fluorescence lifetime can be used to probe the environment of a fluorophore such as energy transfer, pH and viscosity. Multicolor FISH (M-FISH) is a technique that allows individual chromosome identification, classification as well as assessment of the entire genome. Here we describe a combined approach using DAPI as a DNA environment sensor together with FLIM and M-FISH to understand the nanometer structure of all 46 chromosomes in the nucleus covering the entire human genome at the single cell level. Upon DAPI binding to DNA minor groove followed by fluorescence lifetime measurement and imaging by multiphoton excitation, structural differences in the chromosomes can be studied and observed. This manuscript provides a blow by blow account of the protocol required to perform M-FISH-FLIM of whole chromosomes.

Reproduced from Bhartiya A, Robinson I, Yusuf M and Botchway SW (2021) Combining Multicolor FISH with Fluorescence Lifetime Imaging for Chromosomal Identification and Chromosomal Sub Structure Investigation. Front. Mol. Biosci. 8:631774, under the terms of the Creative Commons Attribution License (CC BY). doi: 10.3389/fmolb.2021.631774

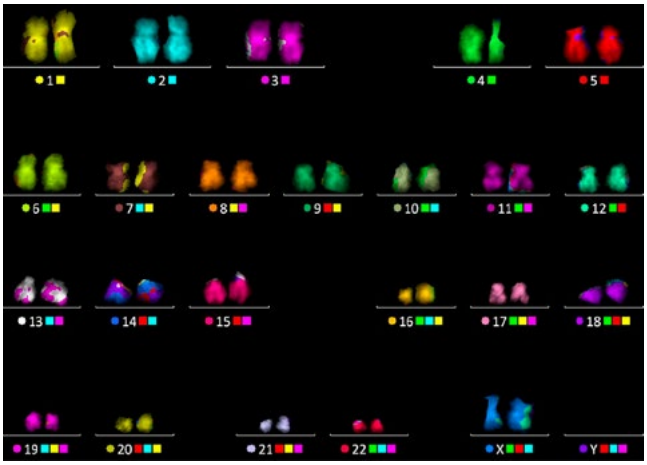

Multicolor FISH performed on the chromosome spread, after FLIM imaging, followed by karyotype as shown in image.

Contacts: M. Yusuf (yusuf.mohammed@ucl.ac.uk)
S.W. Botchway (stan.botchway@stfc.ac.uk)

Porous Carbon Microparticles as Vehicles for the Intracellular Delivery of Molecules

L.M. Magno, D.T. Hinds, S.J. Quinn *(School of Chemistry, University College Dublin, Ireland)*
P. Duffy, P.E. Colavita *(School of Chemistry, Trinity College Dublin, Ireland)*
A.D. Ward, S.W. Botchway, R.B. Yadav *(Central Laser Facility, Research Complex at Harwell, STFC Rutherford Appleton Laboratory, Harwell Campus, Didcot, UK)*

In this study the application of porous carbon microparticles for the transport of a sparingly soluble material into cells is demonstrated. Carbon offers an intrinsically sustainable platform material that can meet the multiple and complex requirements imposed by applications in biology and medicine. Porous carbon microparticles are attractive as they are easy to handle and manipulate and combine the chemical versatility and biocompatibility of carbon with a high surface area due to their highly porous structure. The uptake of fluorescently labelled microparticles by cancer (HeLa) and normal human embryonic Kidney (HEK293) cells was monitored by confocal fluorescence microscopy. In this way the influence of particle size, surface functionalization and the presence of transfection agent on cellular uptake were studied. In the presence of transfection agent both large (690 nm) and small microparticles (250 nm) were readily internalized by both cell lines. However, in absence of the transfection agent the uptake was influenced by particle size and surface PEGylation with the smaller nanoparticle size being delivered. The ability of microparticles to deliver a fluorescein dye model cargo was also demonstrated in normal (HEK293) cell line. Taken together, these results indicate the potential use of these materials as candidates for biological applications.

Reproduced from Magno LM, Hinds DT, Duffy P, Yadav RB, Ward AD, Botchway SW, Colavita PE and Quinn SJ (2020) Porous Carbon Microparticles as Vehicles for the Intracellular Delivery of Molecules. Front. Chem. 8:576175, under the terms of the Creative Commons Attribution (CC BY) License. DOI: 10.3389/fchem.2020.576175

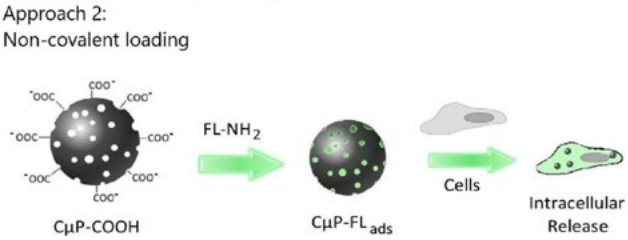

Negatively charged CμP-COOH particles were non-covalently loaded with a highly fluorescent amino-fluorescein dye to prepare CμP-FLads. The ability of these particles to deliver their model cargo to cells was then investigated.

Contact: S.J. Quinn (susan.quinn@ucd.ie)

A small molecule inhibitor of HER3: a proof-of-concept study

A. Colomba, J. Claus *(Protein Phosphorylation Laboratory, The Francis Crick Institute, London, UK)*
M. Fitzek *(Hit Discovery, Discovery Sciences, R&D, AstraZeneca, Macclesfield, UK)*
R. George, S. Kjaer *(Structural Biology Science Technology Platform, The Francis Crick Institute, London, UK)*
G. Weitsman, T. Ng *(Richard Dimbleby Department of Cancer Research, School of Cancer and Pharmaceutical Sciences, King's College London, Guy's Campus, London, UK)*
S. Roberts, L. Zanetti-Domingues, M. Hirsch, D.J. Rolfe, M. Martin-Fernandez *(Central Laser Facility, Research Complex at Harwell, STFC Rutherford Appleton Laboratory, Harwell Campus, Didcot, UK)*
S. Mehmood, A.P. Snijders *(Protein Analysis and Proteomics Science Technology Platform, The Francis Crick Institute, London, UK)*
A. Madin *(Hit Discovery, Discovery Sciences, R&D, AstraZeneca, Cambridge, UK)*
D.M. Smith *(Emerging Innovations Unit, Discovery Sciences, R&D, AstraZeneca, Cambridge, UK)*
P.J. Parker *(Protein Phosphorylation Laboratory, The Francis Crick Institute, London, UK; CRUK KHP Centre, School of Cancer and Pharmaceutical Sciences, King's College London, Guy's Campus, London, UK)*

Despite being catalytically defective, pseudokinases are typically essential players of cellular signalling, acting as allosteric regulators of their active counterparts. Deregulation of a growing number of pseudokinases has been linked to human diseases, making pseudokinases therapeutic targets of interest. Pseudokinases can be dynamic, adopting specific conformations critical for their allosteric function. Interfering with their allosteric role, with small molecules that would lock pseudokinases in a conformation preventing their productive partner interactions, is an attractive therapeutic strategy to explore. As a well-known allosteric activator of epidermal growth factor receptor family members, and playing a major part in cancer progression, the pseudokinase HER3 is a relevant context in which to address the potential of pseudokinases as drug targets for the development of allosteric inhibitors. In this proof-of-concept study, we developed a multiplex, medium-throughput thermal shift assay screening strategy to assess over 100,000 compounds and identify selective small molecule inhibitors that would trap HER3 in a conformation which is unfavourable for the formation of an active HER2–HER3 heterodimer. As a proof-of-concept compound, AC3573 bound with some specificity to HER3 and abrogated HER2–HER3 complex formation and downstream signalling in cells. Our study highlights the opportunity to identify new molecular mechanisms of action interfering with the biological function of pseudokinases.

Reproduced from A. Colomba et al., Biochem J (2020) 477 (17): 3329–3347, published by Portland Press Limited on behalf of the Biochemical Society and distributed under the Creative Commons Attribution License 4.0 (CC BY). doi: 10.1042/BCJ20200496

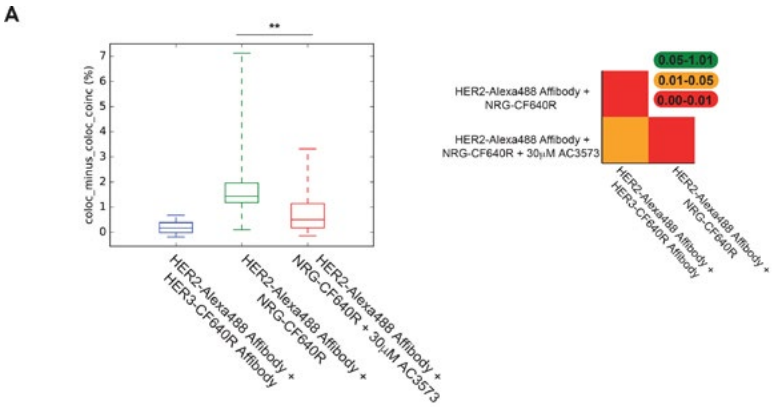

Left: AC3573 compound abrogates the formation of the active HER2–HER3 heterodimer.

(A) Left: the percentage of tracks where HER2 and HER3 molecules spent at least five 50 ms frames together within <1 pixel (pairwise particle colocalisation fraction) in CHO cells with and without treatment with AC3573. (B) Heat map of the probability of the distance of nearest HER2 neighbour of HER3. Cluster measurements from STORM data taken from SK-BR-3 cells labelled with HER2-Alexa488 Affibody and HER3-CF640R SE Affibody (HER2–HER3) or NRG-CF640R SE (HER2-NRG) ± 1 μM lapatinib or 30 μM AC3573 compound.

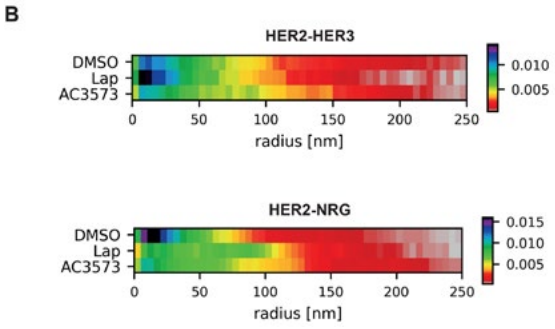

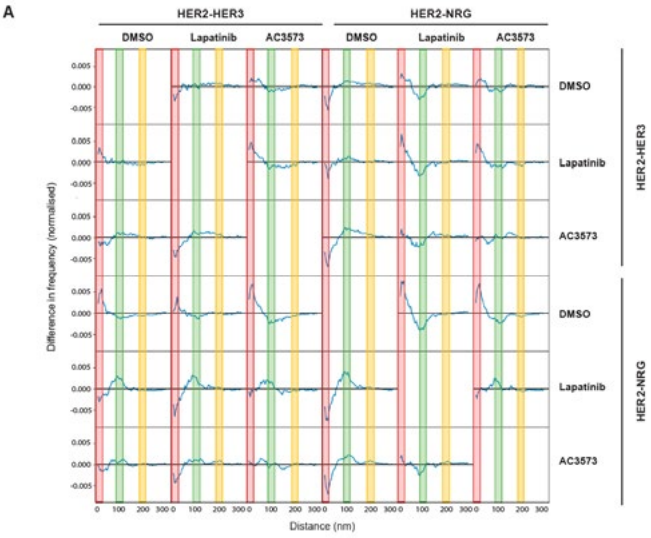

Right: AC3573 compound disrupts HER2-HER3 heterodimers but does not induce HER3 homodimers.

A) Differences in probability of HER2-HER3 nearest neighbour distances. Cluster measurements from STORM data taken from SK-BR-3 cells labelled with HER2-Alexa488 Affibody and HER3-CF640R SE Affibody (HER2-HER3) or NRG-CF640R SE (HER2-NRG) ± 1μM lapatinib or 30μM AC3573 compound. Graphs show near neighbour distribution of HER2 and HER3 molecules as Y condition (right-hand side) – X condition (top). A positive difference indicates that it is more likely to find a HER2 at the corresponding distance from a HER3 under Y condition than under X condition.

Contact: P.J. Parker (peter.parker@crick.ac.uk)

Super-Resolution Fluorescence Microscopy Reveals Clustering Behaviour of *Chlamydia pneumoniae's* Major Outer Membrane Protein

A. E. Danson *(School of Biological Sciences, University of Reading, UK; Diamond Light Source, Harwell Science and Innovation Campus, Didcot, UK; Research Complex at Harwell, STFC Rutherford Appleton Laboratory, Harwell Campus, Didcot, UK)*
A. McStea, L. Wang, M. L. Martin-Fernandez *(Central Laser Facility, Research Complex at Harwell, Science and Technology Facilities Council, Rutherford Appleton Laboratory, Harwell, Didcot, Oxford OX11 0QX, UK)*
A. Y. Pollitt, K. Watson, S. MacIntyre *(School of Biological Sciences, University of Reading, Berkshire RG6 6AS, UK)*
M. A. Walsh *(Diamond Light Source, Harwell Science and Innovation Campus, Oxfordshire OX11 0DE, UK; Research Complex at Harwell, Harwell Science and Innovation Campus, Oxfordshire OX11 0FA, UK)*
I. Moraes *(Research Complex at Harwell, Harwell Science and Innovation Campus, Oxfordshire OX11 0FA, UK; National Physical Laboratory, Teddington TW11 0LW, UK)*

Chlamydia pneumoniae is a Gram-negative bacterium responsible for a number of human respiratory diseases and linked to some chronic inflammatory diseases. The major outer membrane protein (MOMP) of *Chlamydia* is a conserved immunologically dominant protein located in the outer membrane, which, together with its surface exposure and abundance, has led to MOMP being the main focus for vaccine and antimicrobial studies in recent decades. MOMP has a major role in the chlamydial outer membrane complex through the formation of intermolecular disulphide bonds, although the exact interactions formed are currently unknown. Here, it is proposed that due to the large number of cysteines available for disulphide bonding, interactions occur between cysteine-rich pockets as opposed to individual residues. Such pockets were identified using a MOMP homology model with a supporting low-resolution (~4 Å) crystal structure. The localisation of MOMP in the *E. coli* membrane was assessed using direct stochastic optical reconstruction microscopy (dSTORM), which showed a decrease in membrane clustering with cysteine-rich regions containing two mutations. These results indicate that disulphide bond formation was not disrupted by single mutants located in the cysteine-dense regions and was instead compensated by neighbouring cysteines within the pocket in support of this cysteine-rich pocket hypothesis.

Reproduced from Danson AE, McStea A, Wang L, Pollitt AY, Martin-Fernandez ML, Moraes I, Walsh MA, MacIntyre S, Watson KA. Super-Resolution Fluorescence Microscopy Reveals Clustering Behaviour of Chlamydia pneumoniae's Major Outer Membrane Protein. Biology. 2020; 9(10):344. under the Creative Commons Attribution License 4.0 (CC BY) doi: 10.1042/BCJ20200496

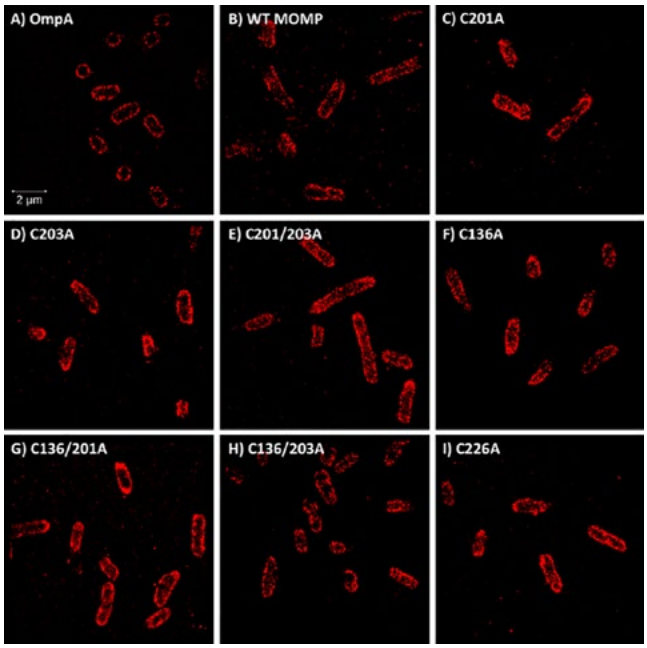

High-resolution dSTORM images reveal wild-type MOMP to be highly clustered. Double mutants C201/203A and C136/201A reduce the clustering of MOMP most significantly, suggesting that within cysteine-rich regions, a compensatory mechanism is occurring whereby neighbouring cysteine residues can continue to form intermolecular disulphide bonds in the absence of the most important cysteine residue and effectively form the protective cysteine rich chlamydial outer membrane complex.

Contact: K.A. Watson (k.a.watson@reading.ac.uk)

A Targeted and Tuneable DNA Damage Tool Using CRISPR/Cas9

I. Emmanouilidis, Y. Hari-Gupta, P.J.I. Ellis *(School of Biosciences, University of Kent, Canterbury, UK)*
N. Fili, A.W. Cook, Á. Dos Santos. C.P. Toseland *(Department of Oncology and Metabolism, University of Sheffield, UK)*
L. Wang, M. Martin-Fernandez *(Central Laser Facility, Research Complex at Harwell, STFC Rutherford Appleton Laboratory, Harwell Campus, Didcot, UK)*

Mammalian cells are constantly subjected to a variety of DNA damaging events that lead to the activation of DNA repair pathways. Understanding the molecular mechanisms of the DNA damage response allows the development of therapeutics which target elements of these pathways. Double-strand breaks (DSB) are particularly deleterious to cell viability and genome stability. Typically, DSB repair is studied using DNA damaging agents such as ionising irradiation or genotoxic drugs. These induce random lesions at non-predictive genome sites, where damage dosage is difficult to control. Such interventions are unsuitable for studying how different DNA damage recognition and repair pathways are invoked at specific DSB sites in relation to the local chromatin state. The RNA-guided Cas9 (CRISPR-associated protein 9) endonuclease enzyme is a powerful tool to mediate targeted genome alterations. Cas9-based genomic intervention is attained through DSB formation in the genomic area of interest. Here, we have harnessed the power to induce DSBs at defined quantities and locations across the human genome, using custom-designed promiscuous guide RNAs, based on in silico predictions. This was achieved using electroporation of recombinant Cas9-guide complex, which provides a generic, low-cost and rapid methodology for inducing controlled DNA damage in cell culture models.

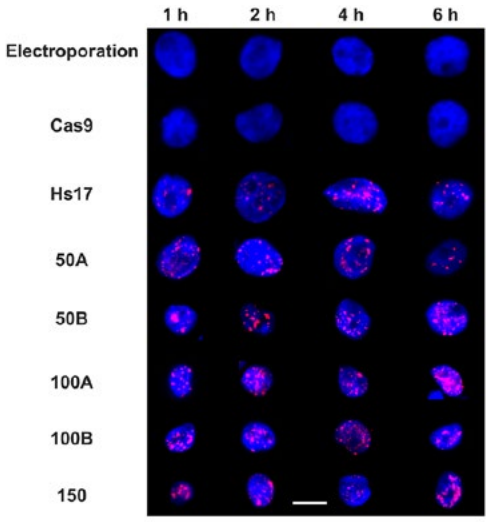

Time course of Cas9-induced DNA damage. Example widefield images of MCF10a cells stained for DNA with Hoechst (blue) and γH2AX (red). Electroporation is a control for background signals. Cas9 refers to electroporation of Cas9 alone. HS17 is the crRNA predicted to cut the genome at 17 locations [16], while 50A/B, 100A/B and 150 are our designed promiscuous crRNA which cut at 50, 100 and 150 predicted sites, respectively. 'A' versions are GC-selective sequences while 'B' versions are AT-selective. The timing is measured from electroporation onwards. Scale bar is 10 um.

Contacts: P.J.I. Ellis (p.j.i.ellis@kent.ac.uk) C. Toseland (c.toseland@sheffield.ac.uk)

Using Mie scattering to determine the wavelength-dependent refractive index of polystyrene beads with changing temperature

M.R. McGrory *(Central Laser Facility, Research Complex at Harwell, STFC Rutherford Appleton Laboratory, Harwell Campus, Didcot, UK; Department of Earth Sciences, Royal Holloway University of London, Egham, UK)*
A.D. Ward *(Central Laser Facility, Research Complex at Harwell, STFC Rutherford Appleton Laboratory, Harwell Campus, Didcot, UK)*
M.D. King *(Department of Earth Sciences, Royal Holloway University of London, Egham, UK*

Polystyrene beads are often used as test particles in aerosol science. Here, a contact-less technique is reported for determining the refractive index of a solid aerosol particle as a function of wavelength and temperature (20–234°C) simultaneously. Polystyrene beads with a diameter of 2 µm were optically trapped in air in the central orifice of a ceramic heating element, and Mie spectroscopy was used to determine the radius and refractive index (to precisions of 0.8 nm and 0.0014) of eight beads as a function of heating and cooling. Refractive index, n, as a function of wavelength, λ (0.480–0.650 µm), and temperature, T, in centigrade, was found to be $n = 1.5753 - (1.7336 \times 10^{-4})T + (9.733 \times 10^{-3})\lambda^{-2}$ in the temperature range $20 < T < 100$°C and $n = 1.5877 - (2.9739 \times 10^{-4})T + (9.733 \times 10^{-3})\lambda^{-2}$ in the temperature range $100 < T < 234$°C. The technique represents a step change in measuring the refractive index of materials across an extended range of temperature and wavelength in an absolute manner and with high precision.

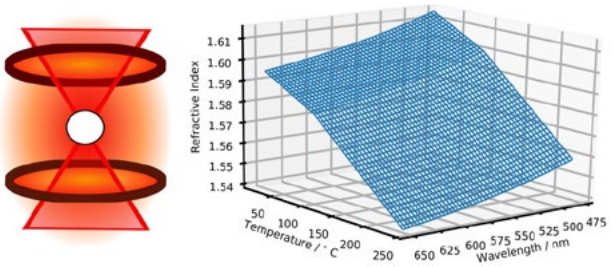

Contact: A.D. Ward (andy.ward@stfc.ac.uk)

Mononuclear ruthenium(II) theranostic complexes that function as broad-spectrum antimicrobials in therapeutically resistant pathogens through interaction with DNA

K.L. Smitten *(Department of Chemistry, University of Sheffield, UK; Department of Molecular Biology and Biotechnology, University of Sheffield, UK)*
E.J. Thick, J.A. Thomas *(Department of Chemistry, University of Sheffield, UK)*
H.M. Southam, S.J. Foster (Department of Molecular Biology and Biotechnology, University of Sheffield, UK)
J. Bernadino de la Serna *(National Heart and Lung Institute, Faculty of Medicine, Imperial College London, UK; Central Laser Facility, Research Complex at Harwell, STFC Rutherford Appleton Laboratory, Harwell Campus, Didcot, UK)*

Six luminescent, mononuclear ruthenium(II) complexes based on the tetrapyridophenazine (tpphz) and dipyridophenazine (dppz) ligands are reported. The therapeutic activities of the complexes against Gram-negative bacteria (*E. coli, A. baumannii, P. aeruginosa*) and Gram-positive bacteria (*E. faecalis and S. aureus*) including pathogenic multi- and pan-drug resistant strains were assessed. Estimated minimum inhibitory and bactericidal concentrations show the activity of the lead compound is comparable to ampicillin and oxacillin in therapeutically sensitive strains and this activity was retained in resistant strains. Unlike related dinuclear analogues the lead compound does not damage bacterial membranes but is still rapidly taken up by both Gram-positive and Gram-negative bacteria in a glucose independent manner. Direct imaging of the complexes through super-resolution nanoscopy and transmission electron microscopy reveals that once internalized the complexes' intracellular target for both Gram-negative and Gram-positive strains is bacterial DNA. Model toxicity screens showed the compound is non-toxic to *Galleria mellonella* even at exposure concentrations that are orders of magnitude higher than the bacterial MIC.

Contact: J.A. Thomas (james.thomas@sheffield.ac.uk)

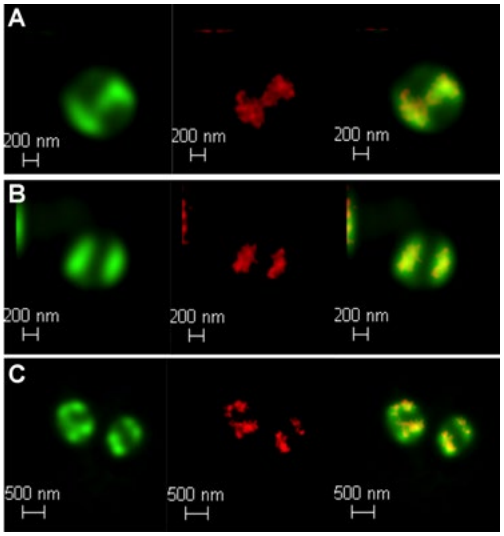

Localization of 4^{2+} in S. aureus SH1000 cells visualized through laser scanning confocal microscopy, d-LCSM, (green, left) and stimulated emission depletion nanoscopy, STED, (red, middle) and overlay image (right) at; (A) 20 min, (B) 60 min and (C)120 min. Cells imaged using the emission of 4^{2+} on excitation at 470 nm with a white light laser and a 470 nm notch filter. STED effect was obtained by employing a 770 nm depletion laser, and a 780 nm vortex phase plate. Both d-LCSM and d-STED images were processed using Hyugens software (SVI).

Serial cryoFIB/SEM Reveals Cytoarchitectural Disruptions in Leigh Syndrome Patient Cells

Y. Zhu *(Division of Structural Biology, Wellcome Trust Centre for Human Genetics, University of Oxford, UK)*
P. Zhang *(Division of Structural Biology, Wellcome Trust Centre for Human Genetics, University of Oxford, UK; Department of Structural Biology, University of Pittsburgh School of Medicine, USA; Electron Bio-Imaging Centre, Diamond Light Source, Harwell Science and Innovation Campus, Didcot, UK)*
D. Sun, J. Ning, X. Fu *(Department of Structural Biology, University of Pittsburgh School of Medicine, USA)*
A. Schertel *(Carl Zeiss Microscopy GmbH, Zeiss Customer Center Europe, Oberkochen, Germany)*
P.P. Gwo *(Department of Psychiatry, University of Pittsburgh, USA)*
A.M. Watson *(Department of Cell Biology, University of Pittsburgh, USA)*
L.C. Zanetti-Domingues, M.L. Martin-Fernandez *(Central Laser Facility, Research Complex at Harwell, STFC Rutherford Appleton Laboratory, Harwell Campus, Didcot, UK)*
Z. Freyberg *(Department of Psychiatry, University of Pittsburgh, USA; Department of Cell Biology, University of Pittsburgh, USA)*

The advancement of serial cryoFIB/SEM offers an opportunity to study large volumes of near-native, fully hydrated frozen cells and tissues at voxel sizes of 10 nm and below. We explored this capability for pathologic characterization of vitrified human patient cells by developing and optimizing a serial cryoFIB/SEM volume imaging workflow. We demonstrate profound disruption of subcellular architecture in primary fibroblasts from a Leigh syndrome patient harboring a disease-causing mutation in USMG5 protein responsible for impaired mitochondrial energy production.

Contact: P. Zhang (peijun@strubi.ox.ac.uk)

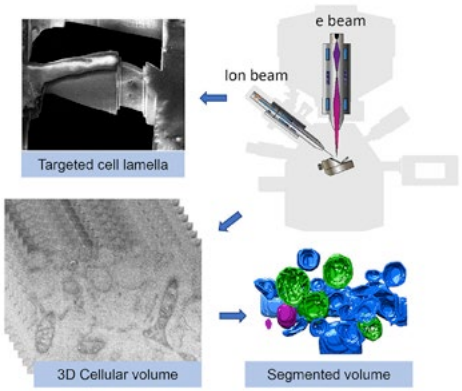

Operando Kerr gated Raman spectroscopy of lithium insertion into graphite enables high state of charge diagnostics

L.J. Hardwick, A.R. Neale, D.C. Milan, F. Braga *(Stephenson Institute for Renewable Energy, Department of Chemistry, University of Liverpool, UK)*

I.V. Sazanovich *(Central Laser Facility, Research Complex at Harwell, STFC Rutherford Appleton Laboratory, Harwell Campus, Didcot, UK)*

Operando electrochemical Kerr gated Raman spectroscopy measurements are reported for the first time to track the lithium insertion/extraction processes in a graphite-based negative electrode for Li-ion batteries. At high depths of lithiation from $Li_{0.5}C_6$ to LiC_6, large fluorescence/emission signals swamp the weaker Raman scattering effect in conventional Raman spectroscopy, making it difficult to track material changes at high states of charge. The efficacy of the Kerr gate in suppressing strong fluorescence/emission signals, combined with the dedicated design of the *operando* spectroelectrochemical cell (Figure 1), facilitated continued detection of the changing graphitic Raman bands even at high depths of lithiation to fully intercalated LiC_6 (Figure 2). This creates the opportunity to interrogate high states of charge in graphitic negative electrodes for Li-ion batteries.

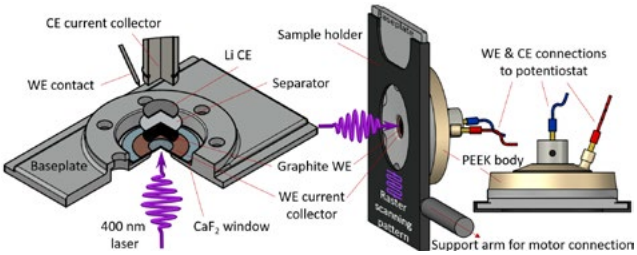

Figure 1: A schematic of the operando Raman cell assembly. The cell (left), and WE and CE connections, were sealed using PEEK body of the ECC-Opto cell (EL-Cell) and the Kerr gate Raman sample holder system (right) attached to the motor system (not shown) that provides the raster scanning motion during spectra collection.

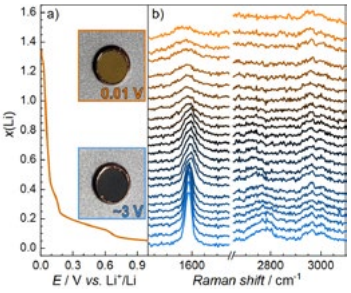

Figure 2: (a) Voltage profile of the graphite electrode and (b) the operando Kerr gated Raman spectra (stacked as a function of x(Li)) collected at 2 ps delay times showing the primary G and 2D graphite bands at 1580 and 2780 cm^{-1}, respectively (electrolyte bands at ca. 2980 cm^{-1}). Spectra are stacked as a function of the depth of lithiation (x(Li)). Inset images in a-i) show images of the electrode via the optical window before and after full lithiation to LiC_6.

Contact: L.J. Hardwick (hardwick@liverpool.ac.uk)

Temperature-Jump Time Resolved 2D-IR Spectroscopy of DNA Hairpin Unfolding

C.P. Howe, B. Procacci, D.J. Shaw, N.T. Hunt *(Department of Chemistry, University of York, UK)*

G.M. Greetham, M. Towrie, A.W. Parker *(Central Laser Facility, STFC Rutherford Appleton Laboratory, Harwell Campus, Didcot, UK)*

The ULTRA T-jump-infrared spectroscopy instrument has been extended to include the use of two-dimensional infrared (2D-IR) spectroscopy, to probe the melting dynamics of DNA hairpins in real time.

Dynamic changes in nucleic acid macromolecular structures are central to biological function, and the hairpin studied features a tetraloop motif commonly found in RNA-based ribozymes and synthetic nucleic acid aptamer molecules.

We demonstrate that T-jump-2D-IR spectroscopy on the ULTRA spectrometer has sufficient sensitivity, as well as scale and duration of the temperature jump, to enable detection of hairpin melting. This experiment establishes proof of concept for more detailed studies of the hairpin melting process, that will lead to enhanced understanding of nucleic acid structure and dynamics in solution.

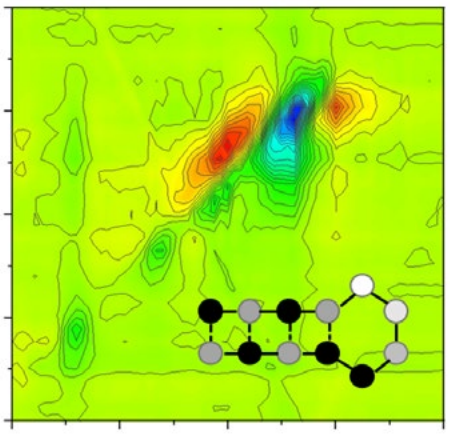

T-jump-2D-IR difference spectrum showing effects of DNA hairpin melting

Contact: N.T. Hunt (neil.hunt@york.ac.uk)

Manganese-Mediated C–H Bond Activation of Fluorinated Aromatics and the ortho-Fluorine Effect: Kinetic Analysis by *In Situ* Infrared Spectroscopic Analysis and Time-Resolved Methods

J.M Lynam, I.J.S. Fairlamb, L.A. Hammarback, A.L. Bishop, C. Jordan, G. Athavan, J.B. Eastwood, T.J. Burden, J.T.W. Bray, F. Clarke, A. Whitwood *(Department of Chemistry, University of York, UK)*

A. Robinson, J-P. Krieger *(Sygenta Crop Protection AG, Münchwilen, Switzerland)*
I.P. Clark, M. Towrie *(Central Laser Facility, STFC Rutherford Appleton Laboratory, Harwell Campus, Didcot, UK)*

Insights into the factors controlling the site selectivity of transition metal-catalyzed C–H bond functionalization reactions are vital to their successful implementation in the synthesis of complex target molecules. The introduction of fluorine atoms into substrates has the potential to deliver this selectivity. In this study, we employ spectroscopic and computational methods to demonstrate how the "*ortho*-fluorine effect" influences the kinetic and thermodynamic control of C–H bond activation in manganese(I)-mediated reactions. The C–H bond activation of fluorinated *N,N*-dimethylbenzylamines and fluorinated 2-phenylpyridines by benzyl manganese(I) pentacarbonyl $BnMn(CO)_5$ leads to the formation of cyclomanganated tetracarbonyl complexes (**2a–b** and **4a–e**), which all exhibit C–H bond activation *ortho*-to-fluorine. Corroboration of the experimental findings with density functional theory methods confirms that a kinetically controlled irreversible σ-complex-assisted metathesis mechanism is operative in these reactions. The addition of benzoic acid results in a mechanistic switch, so that cyclomanganation proceeds through a reversible AMLA-6 mechanism (kinetically and thermodynamically controlled). These stoichiometric findings are critical to catalysis, particularly subsequent insertion of a suitable acceptor substrate into the C–Mn bond of the regioisomeric cyclomanganated tetracarbonyl complex intermediates. The employment of time-resolved infrared spectroscopic analysis allowed for correlation of the rates of terminal acetylene insertion into the C–Mn bond with the relative thermodynamic stability of the regioisomeric complexes. Thus, more stable manganacycles, imparted by an *ortho*-fluorine substituent, exhibit a slower rate of terminal acetylene insertion, whereas a *para*-fluorine atom accelerates this step. A critical factor in governing C–H bond site selectivity under catalytic conditions is the generation of the regioisomeric cyclomanganated intermediates, rather than their subsequent reactivity toward alkyne insertion.

Reproduced with permission from ACS Catal. 2022, 12, 2, 1532–1544. Copyright © 2022 American Chemical Society. doi: 10.1021/acscatal.1c05477

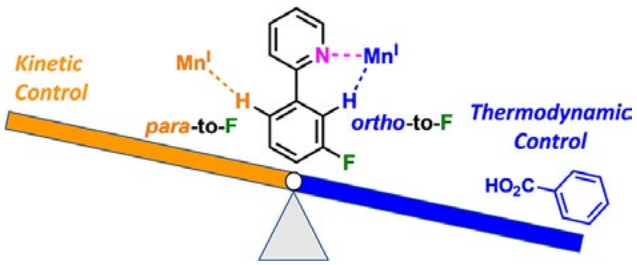

Contacts: J.M. Lynam (jason.lynam@york.ac.uk)
I.J.S. Fairlamb (ian.fairlamb@york.ac.uk)

Dynamics around a hydrogen bond – The dynamics of UV excited acetic acid dimers

E. Plackett, R.S. Minns *(School of Chemistry, University of Southampton, UK)*
H. McGhee, R. Ingle *(Department of Chemistry, University College London, UK)*
G.M. Greetham, G. Karras, I.V. Sazanovich *(Central Laser Facility, Research Complex at Harwell, STFC Rutherford Appleton Laboratory, Harwell Campus, Didcot, UK)*

C. Robertson, A. De Matos Loja, M. Patterson *(Institute of Chemical Sciences, School of Engineering and Physical Sciences, Heriot-Watt University, Edinburgh, UK)*

We measure the transient infrared absorption spectrum of UV excited acetic acid dimers. The measurements cover vibrational modes related to the ring structure of the dimer and highlight the stabilising effects of the hydrogen bonds and their effect on the excited state dynamics.

The results suggest that absorption at 200 nm leads to population of the S_2 state and dynamics that change the hydrogen bonded region that stabilises the molecule against dissociation. In the excited state, the dimer initially skews and then undergoes internal conversion to S_1 and buckles from the originally planar ring structure, to form a new stable configuration in the S_1 excited state. The buckled structure then relaxes back to the electronic ground state, reforming the planar ground state dimer structure.

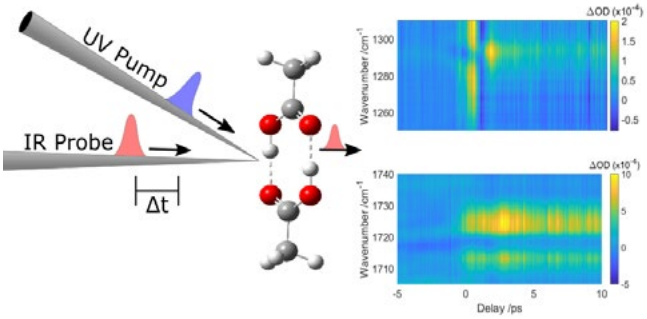

Left: Schematic representation of the experiment, where a pump pulse electronically excites the acetic acid dimer. The resulting dynamics are probed via changes in the infrared absorption spectrum as a function of pump-probe delay.

Right: Representative spectra around the carbonyl stretch (1720 cm^{-1}) and the ring wag (1290 cm^{-1}) vibrations.

Contact: R.S. Minns (r.s.minns@soton.ac.uk)

Femtosecond to microsecond tracking of the complete mechanism of a radical reaction cycle

L. Lewis-Borrell, M. Sneha, V. Fasano, A. Noble, V.K. Aggarwal, A.J. Orr-Ewing *(School of Chemistry, University of Bristol, Bristol, UK)*

Chemical reactions driven by light are increasingly being used in synthetic chemistry, because they can efficiently access new chemical structures, but the reaction pathways are often difficult to understand. The absorption of ultraviolet or visible light produces short-lived reactive intermediates which drive the chemistry. Time-resolved infrared (TRIR) spectroscopy can observe these transient intermediates directly, track the timescales for their formation and loss, and hence unravel complicated reaction mechanisms.

The wide range of timescales for different reaction steps presents a challenge, with the initial radical formation occurring on femtosecond to picosecond timescales, but subsequent reaction steps extending out to microseconds or milliseconds. The extraordinary capability of the LIFEtime Facility to record TRIR spectra at intervals spanning ten orders of magnitude of time now makes this type of investigation possible. For the first time, complete mechanisms of a multi-step reaction can be tracked and understood.

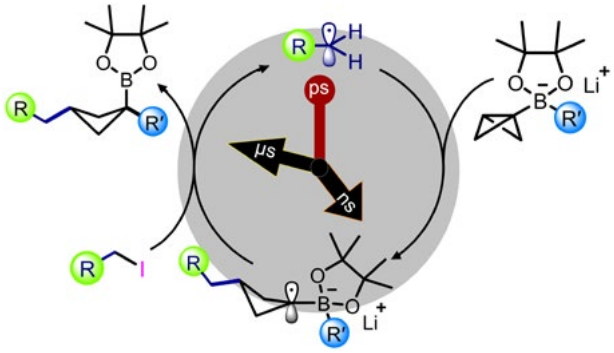

Schematic representation of the timescales over which the studied chemical reactions occur

Contact: A.J. Orr-Ewing (a.orr-ewing@bristol.ac.uk)

COVID research on Octopus during the pandemic

Early in the pandemic it was recognised that the CLF, and in particular Octopus, had the potential to assist with research into SARS-CoV-2 and COVID-19. Having shut down normal operations, the facility was able to issue a rapid call for research proposals relevant to COVID-19. This call was open to researchers worldwide, from both academia and industry. Given the urgency of the situation, a light touch review process was used, with a brief scientific case for support being assessed by two members of the usual Facility Access Panel. A number of successful proposals were received, and the research was done by members of the Octopus team, working under stringent COVID control measures and in close contact with the researchers. Brief descriptions of the projects are below.

These projects demonstrate how the CLF is able to respond quickly to new challenges, and show the potential of Octopus for research into infection and immunity, an extremely important area for society. We believe this will be a growth area for the facility in years to come.

Cryo "slice and view" scanning electron microscopy to look at the location of SARS-CoV-2 virus in cells

eBIC/Diamond – Oxford – Cambridge – Pittsburgh – CLF (Benji Bateman, Marisa Martin-Fernandez, Laura Zanetti Domingues)

The objective of this project was to obtain a high resolution 3D map of the location of the virus within the cells of patients, to discover more about infection mechanisms and possibly give clues as to how the infection could be treated. Using cryogenically-preserved rather than chemically-fixed samples meant we were closer to the native state of the cells.

3D data sets were obtained which, after a significant amount of intensive manual data processing, revealed the location of the virus particles in the cells. The data were correlated with cryo-electron tomography data from eBIC to provide a detailed structural and ultrastructural picture of the virus's replication cycle, for example showing extensive membrane tunnels formed for the virus to exit, and lesions near the exit region of the cell. The work was subsequently published in *Nature Communications* (Mendonça, L., Howe, A., Gilchrist, J.B. *et al*. Correlative multi-scale cryo-imaging unveils SARS-CoV-2 assembly and egress. *Nat Commun* **12**, 4629 (2021). https://doi.org/10.1038/s41467-021-24887-y).

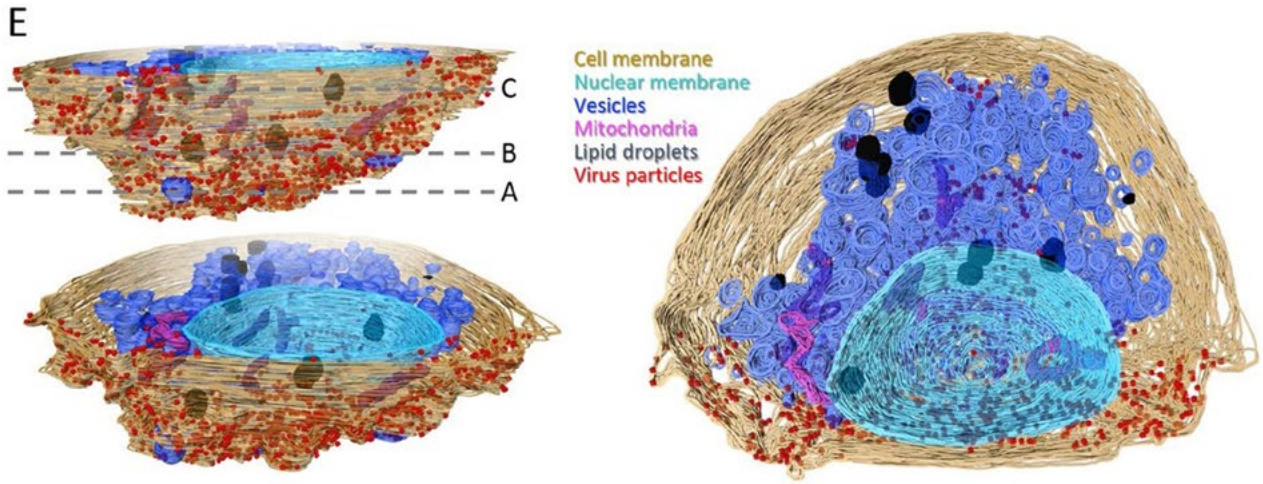

Surface rendering of the segmented volume of a SARS-CoV-2-infected cell. Segmented organelles and virus particles are labelled with the colours indicated (Howe et al., Nature Communication 2021).

Investigating the action of drugs designed to modulate the immune response

Metamorph Therapeutics – CLF (Stan Botchway)

Acute Respiratory Distress Syndrome (ARDS) is a form of inflammation that results from an over-reaction of the immune system, and is a common cause of serious illness and death in COVID-19. This project used super-resolution microscopy to investigate the effects of a drug candidate molecule designed to "turn down" the immune system and reduce inflammation.

Sample preparation for this project was challenging, and was a good example of the difficulties that occur with remote working, which makes the regular interaction between user and CLF link scientists more difficult.

After a number of iterations of sample preparation, good images were obtained that show the reduced expression of inflammatory markers in response to the treatment.

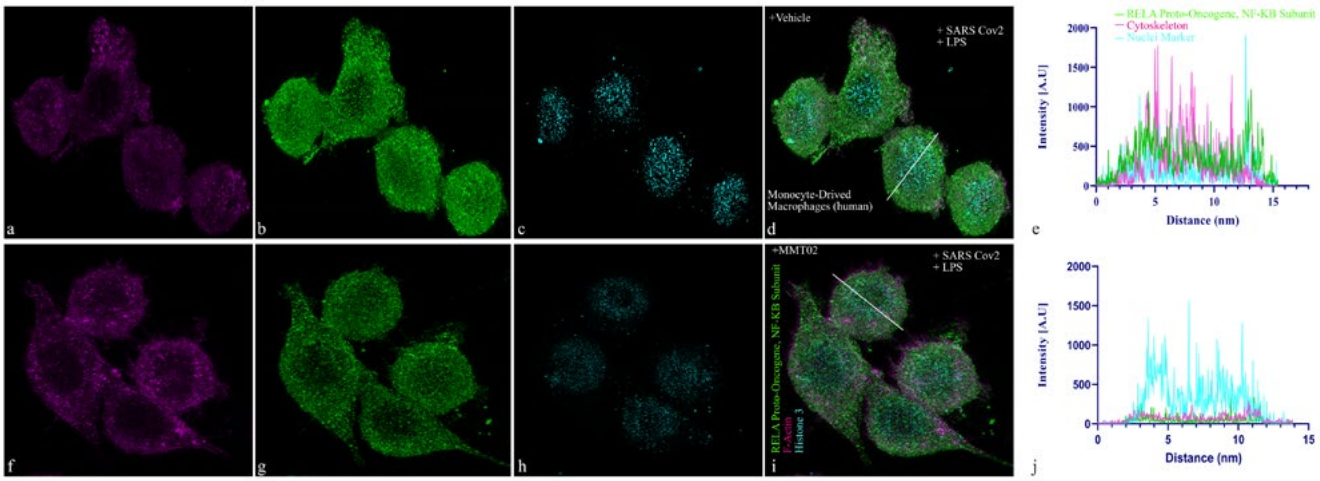

STED nanoscopy results showing reduced number localization of RELA with MMT02 treatment compared to a vehicle control in macrophages challenged with LPS and the novel Coronavirus SARS Cov2

Looking at systems to deliver antiviral drugs to the brain

Biocyto – CLF (Benji Bateman, Laura Zanetti Domingues)

Doctors have recorded a number of life-threatening brain related symptoms of COVID-19 infection, such as stroke and inflammation that have been recorded in about 30 – 40% of cases. Recent studies have found the novel coronavirus in the brains of fatal cases of COVID-19 and it is plausible that this is causing neurological disorders by directly infecting the brain, or as a result of the strong activation of the immune system. Neural and immune cells can serve as reservoirs of latent coronavirus. The blood-brain barrier makes it difficult to deliver drugs to the brain, and Biocyto have developed nanoparticle drug delivery platforms to overcome this problem. They used high-resolution SEM at Octopus to characterise the nanoparticles for size and uniformity. Large numbers of particles were screened, with an example image shown.

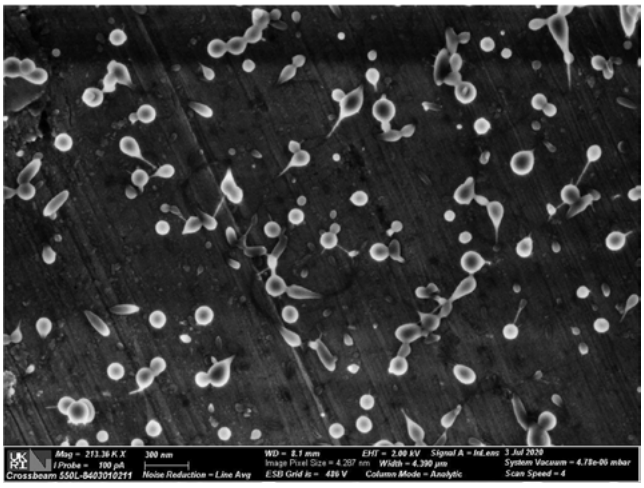

Studying the interaction between SARS-CoV-2 spike protein and its target receptor

Biocyto – CLF (Benji Bateman, Laura Zanetti Domingues)

The SARS-CoV-2 virus infects cells through binding of the spike protein on its coat to the ACE2 receptor molecule on cells (left). This project used a technique called Förster Resonance Energy Transfer (FRET) with Fluorescence Lifetime Imaging (FLIM) to study the interaction between the spike protein and its target.

FRET-FLIM is able to show the level and location of molecular interactions in the cell. In the image (right), short fluorescence lifetimes, which show interactions between ACE2 and the spike protein, appear orange.

The method was used to image cells treated with drugs: Losartan, which is known to block interactions of the receptor; and CBD, a drug that modifies membranes. FRET-FLIM allowed us to measure whether these drugs interfere with binding of the virus to its target.

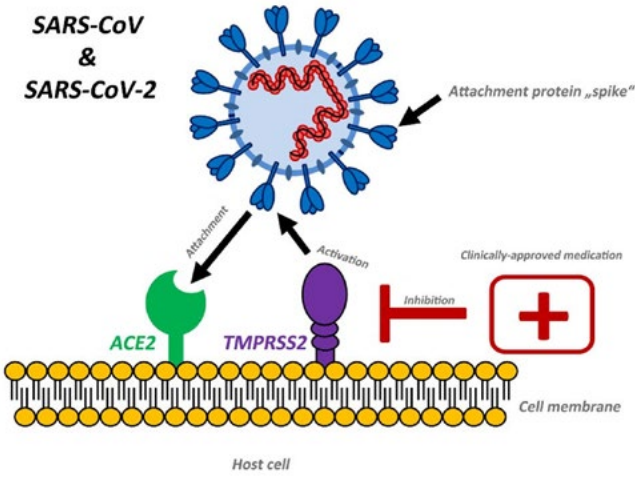

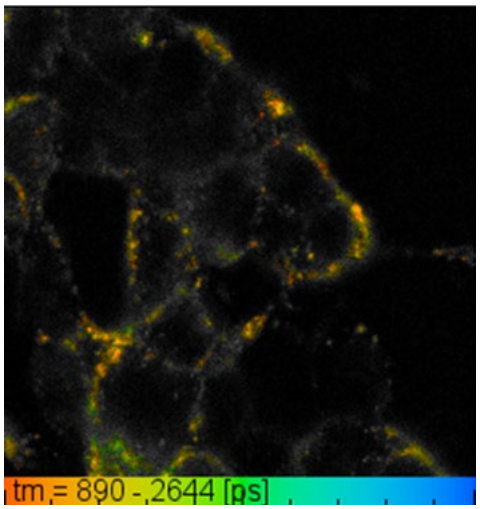

Contact: D.T. Clarke (dave.clarke@stfc.ac.uk)

Artemis operational report and statistics

R.T. Chapman and E. Springate *(Central Laser Facility, Research Complex at Harwell, STFC Rutherford Appleton Laboratory, Harwell Campus, Didcot, UK)*

Introduction

This was the final year of the Artemis upgrade project, which saw Artemis move into the Research Complex at Harwell, adding a new 100 kHz laser system and a third XUV beamline to its capability. Only one external experiment was scheduled, with the remainder of the time dedicated to engineering and commissioning tasks, or lost due to lockdowns.

Activities

During the shutdown period, the Artemis team carried out data acquisition projects on a new detector for the angle-resolved photoemission end-station, and for a new small chamber for measurements of the magneto-optical Kerr effect (MOKE). The team also numerically modelled the optical design of the 100 kHz XUV beamline, to allow both small spot sizes (for inhomogeneous samples and devices) and larger spot sizes (for lower space charge) to be used.

Once staff were allowed back in the lab, substantial staff effort went in to bringing the 1 kHz Ti:Sa system back into operation, as this 12-year old system had been brought across the lab and reconfigured just before shutdown. The laser interlock system was commissioned and the installation of the two 1 kHz beamlines and their vacuum control systems was completed. The beamline with monochromator was redesigned and refurbished as part of the project. Following re-commissioning, we measure ten times higher XUV flux.

The first experiment in the new labs took place in October 2020 (Figure 1). This was an all-optical experiment using the 1 kHz laser system and the new MOKE chamber, with users participating remotely from Paris.

We found problems with the pump laser for the new 100 kHz laser system just before lockdown. This laser was sent back to the manufacturer for complete refurbishment, and re-installed in December 2020. Commissioning of the full 100 kHz laser system (an infrared OPCPA) started in January 2021, with remote support from service engineers in France and Germany. Simulations, design and procurement for the optical parametric amplifiers that will be pumped by the new laser were completed during this period.

Finally, mechanical design, manufacturing and procurement of the 100 kHz beamline was completed in this year, with all major components delivered and ready for assembly by the end of the financial year.

Figure 1: First user experiment in the new Artemis labs, October 2020

w/b	Activity
30/03/2020	COVID lockdown #1: beamline design and software upgrades
06/04/2020	
13/04/2020	
20/04/2020	
27/04/2020	
04/05/2020	
11/05/2020	
18/05/2020	
25/05/2020	
01/06/2020	
08/06/2020	Engineering and restart of 1 kHz laser
15/06/2020	
22/06/2020	
29/06/2020	
06/07/2020	
13/07/2020	
20/07/2020	
27/07/2020	
03/08/2020	
10/08/2020	
17/08/2020	
24/08/2020	
31/08/2020	
07/09/2020	
14/09/2020	
21/09/2020	
28/09/2020	
05/10/2020	Hricovini 17120011 (set-up)
12/10/2020	Hricovini 17120011
19/10/2020	
26/10/2020	Engineering and a/c work
02/11/2020	Hricovini 17120011
09/11/2020	
16/11/2020	Laser maintenance
23/11/2020	Hricovini 17120011 (2 days)
30/11/2020	Engineering and 100 kHz laser installation
07/12/2020	
14/12/2020	
21/12/2020	
28/12/2020	Christmas
04/01/2021	100 kHz laser commissioning and beamline alignment
11/01/2021	
18/01/2021	
25/01/2021	
01/02/2021	
08/02/2021	
15/02/2021	
22/02/2021	
01/03/2021	
08/03/2021	
15/03/2021	
22/03/2021	
29/03/2021	

Table 1: Artemis operations by week in 2020/21

Contact: R. Chapman (richard.chapman@stfc.ac.uk)

Gemini operational statistics

S. Hawkes *(Central Laser Facility, STFC Rutherford Appleton Laboratory, Harwell Campus, Didcot, UK)*

During the reporting year, April 20 – April 21, a total of two complete experiments were delivered in the Astra-Gemini Target Area and one experiment in TA2. In total of 21 high power laser experimental weeks were delivered the Gemini Target Area and four weeks to TA2. The delivered schedule is presented in Figure 2.

The availability of the Gemini laser system (delivery to the Gemini Target Area) was 78% during normal working hours, rising to 124% with time made up from running out of normal working hours. The reliability of the Gemini laser was 85%. An individual breakdown of the availability and reliability for the experiments conducted is presented in Figure 1.

TA2 availability was 95% during normal working hours, rising to 139% with time made up from running out of normal working hours. The reliability of the laser delivery to TA2 was 97%.

The high levels of total availability were made possible by the continued unique operational model employed on Gemini, which involves running the laser late into the evening. In addition, frequent weekend operational days were made available.

During the reporting year, the COVID-19 pandemic had a significant impact on facility operations. The laboratory was shut down for the first four months, and difficulties in arranging laser servicing from overseas companies severely impacted the Kettle campaign.

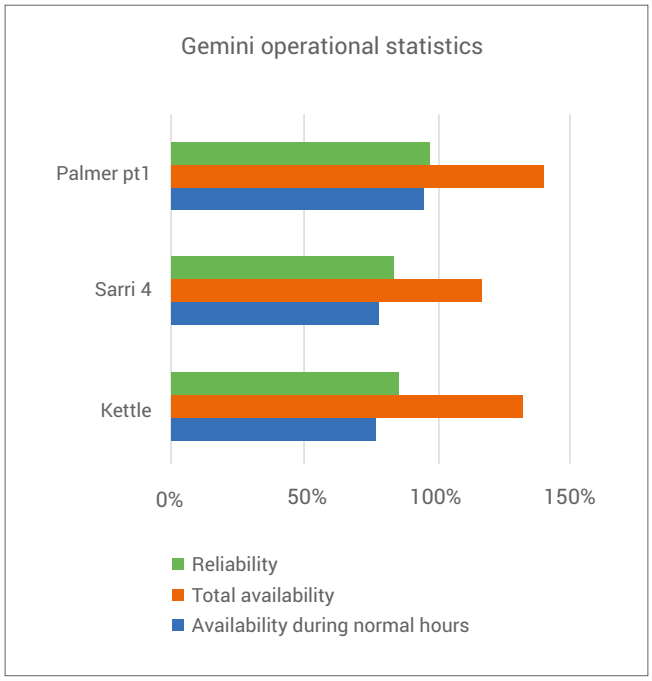

Figure 1: 2020/21 Gemini/TA2 operational statistics

w/b	Gemini	TA2
06/04/2020	Shutdown and preparations for operational restart	
13/04/2020		
20/04/2020		
27/04/2020		
04/05/2020		
11/05/2020		
18/05/2020		
25/05/2020		
01/06/2020		
08/06/2020		
15/06/2020		
22/06/2020		
29/06/2020		
06/07/2020		
13/07/2020		
20/07/2020		
27/07/2020		
03/08/2020	LWFA optimisation	
10/08/2020		
17/08/2020		
24/08/2020	Kettle **19210012**	
31/08/2020		
07/09/2020		Compressor work
14/09/2020		
21/09/2020		
28/09/2020	Extension	
05/10/2020		
12/10/2020	Laser maintenance and repair	
19/10/2020		
26/10/2020		
02/11/2020		System access Source development
09/11/2020		
16/11/2020	Extension	
23/11/2020		
30/11/2020		
07/12/2020		
14/12/2020		Target Fab Plant Servicing
21/12/2020	Shutdown	
28/12/2020		
04/01/2021		
11/01/2021	Ops Shutdown	
18/01/2021		
25/01/2021		
01/02/2021	Sarri **19210006**	System Access
08/02/2021		
15/02/2021		
22/02/2021		
01/03/2021		
08/03/2021		Palmer (part 1) **20110001**
15/03/2021		
22/03/2021		
29/03/2021	3 days	

Figure 2: 2020/21 Gemini experimental schedule

Contact: S. Hawkes (steve.hawkes@stfc.ac.uk)

Octopus and Ultra operational statistics

B.C. Bateman, M. Szynkiewicz, E. Gozzard, I.P. Clark, D.T. Clarke *(Central Laser Facility, Research Complex at Harwell. STFC Rutherford Appleton Laboratory, Harwell Campus, Didcot, UK)*

Octopus facility

In the reporting period (April 2020 to March 2021), 23 unique User groups submitted a total of 26 proposals bidding for time at the Octopus facility. 14 experiments comprising 43 weeks of access time were awarded to the UK User community throughout the year. A full breakdown of number of weeks applied for versus number of weeks scheduled is shown in Figure 1, indicating an oversubscription ratio of 1.81:1. Figure 3 shows that Biology and Bio-materials formed the majority of applications.

A total of 25 formal reviewed publications were recorded throughout the year.

Ultra facility

In the reporting period (April 2020 to March 2021), 15 unique User groups submitted a total of 15 proposals bidding for time at the Ultra facility. 12 experiments comprising 30 weeks of access time were awarded to the UK User community. A full breakdown of number of weeks applied for versus number of weeks scheduled is shown in Figure 2, indicating an oversubscription ratio of 1.27:1. Figure 4 shows that Chemistry formed the majority of applications. Ultra also facilitated one week of industrial access.

A total of 18 formal reviewed publications were recorded throughout the year.

Octopus and Ultra availability and user satisfaction feedback

A total of 49 hours downtime was reported over the combined 61 weeks of delivered access during this reporting period. Eight weeks of user access was not delivered due to the COVID-19 pandemic. Figure 5 shows an average user satisfaction rating of 91.8% over the five surveyed categories.

Figure 1: Octopus experiments by subject

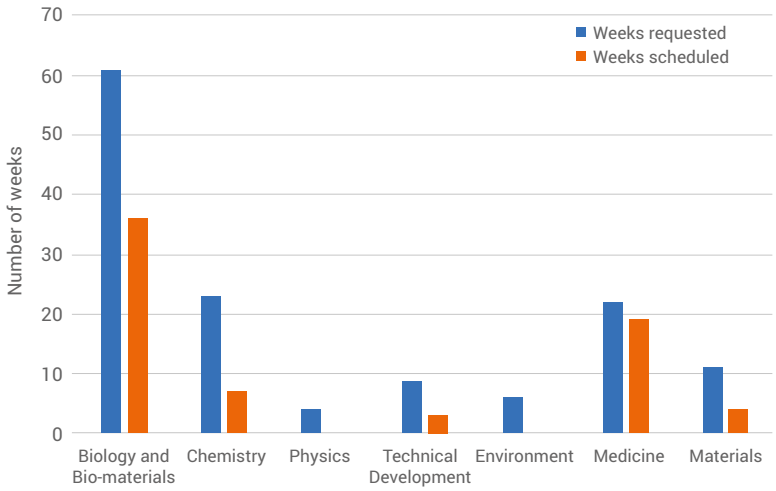

Figure 2: Ultra experiments by subject

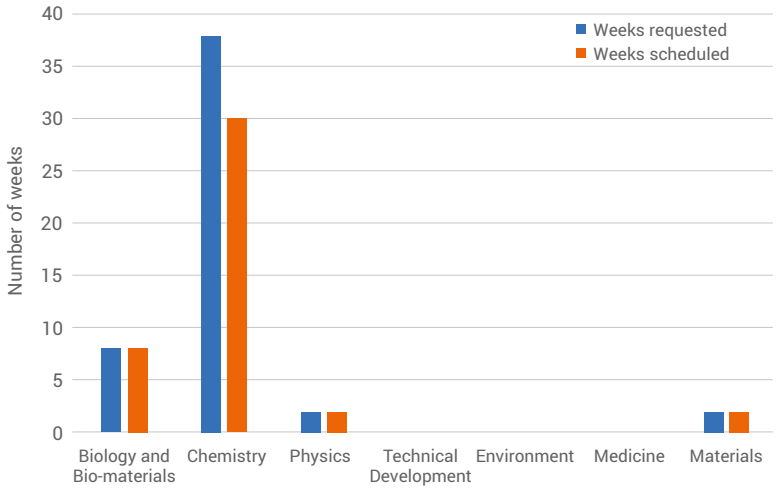

Figure 3: Octopus experiment bids by subject group

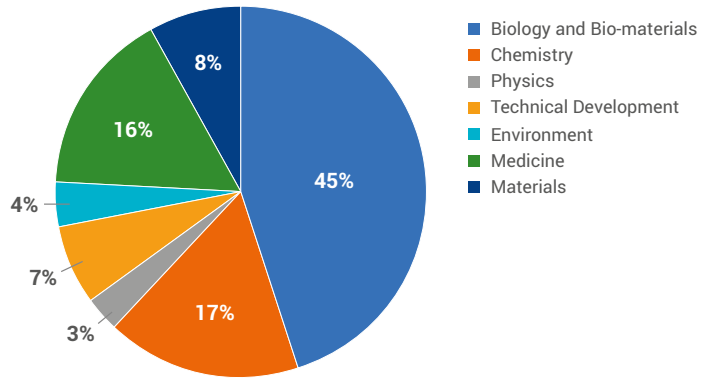

Figure 4: Ultra experiment bids by subject group

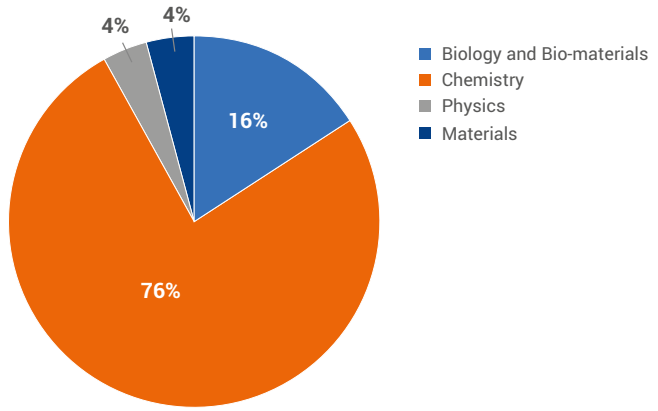

Figure 5: Average user satisfaction

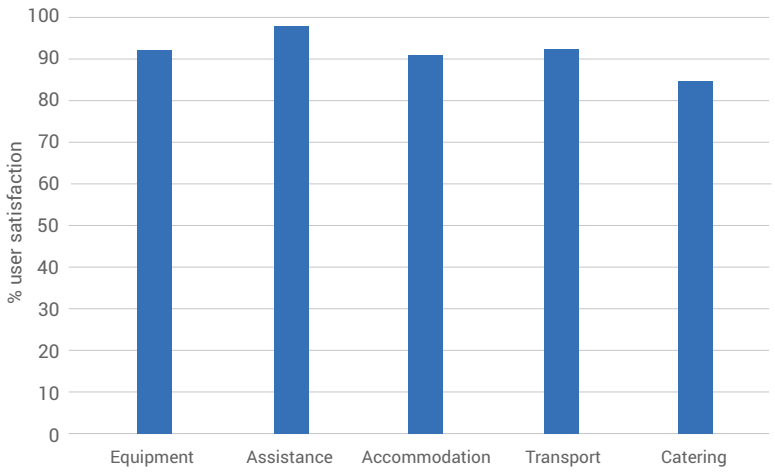

Contact: D.T. Clarke (dave.clarke@stfc.ac.uk)

Target Fabrication operational statistics

S. Astbury, D. Haddock, C. Spindloe & M. K. Tolley *(Target Fabrication Group, Central Laser Facility, STFC Rutherford Appleton Laboratory, Harwell Campus, Didcot, UK)*

Introduction

This report documents the experimental support offered by the Target Fabrication Group to the high power laser user community from January 2020 to April 2021. The Vulcan TAP and TAW target areas, as well as those in Gemini TA2 and TA3, are covered. Support to external facilities is also detailed. Experimental operations were hindered due to the COVID-19 pandemic, resulting in a postponement of experiments between 23rd March and 10th August 2020. This is reflected in the lower number of experimental support weeks compared with earlier years: the Target Fabrication Group provided 50 weeks of experimental support in the 2019-20 reporting period compared to 38 weeks offered in 2020-21.

The reporting period saw a total of three supported experiments in the Vulcan areas, and three experiments in Gemini. The Target Fabrication Group also provided numerous diagnostic elements, such as filter packs and fiducial arrays, as well as lens assemblies for cryo-fluorescence microscopy for other experiments across the CLF, which are not documented as part of these statistics. For example, the Target Fabrication Group provided non-targetry support for the 0321 TA2 Palmer Liquid Targetry experiment (proposal 20110001), as detailed in Bourgeois *et al.* "*Deploying the SLAC liquid target at RAL.*"[1]

Supported Experiments

Table 1 details the experiments supported over the reporting period and their duration, including extension weeks.

Proposal Number	Date/Area/PI	Supported Weeks
19210013	0120 TA3 Higginbotham	5
19210012	0320 TA3 Kettle	7
19210006	0221 TA3 Sarri	8
20110009	0620 TAP Kar	6
19210011	0320 TAW Palmer	6
19210003	0221 TAW Scott	6
	Total	**38**

Table 1: Experiments supported by the Target Fabrication Group through the 2020-21 reporting period

Due to the difference in energy and repetition rate of the lasers and the area of physics that they are tailored to investigate, target types often differ from area to area and experiment to experiment. On Vulcan experiments, the predominant target type is that of a single target on a stalk, or a cluster of components in an assembly, often multi-layered or complex in nature, that is ideally suited to lower repetition rate experiments. Targets for the Gemini target area are primarily simple foils held on an array mount, with tens of targets on a single mount, and up to ten mounts loaded onto a target wheel. Over the last two to three years, Gemini experiments are seeing an increase in targets manufactured on a tape substrate, following the design and fielding of a tape-drive targetry system designed by the Target Fabrication Group[2][3] another technology the Group have made available to the HPL community.[4]

The varying target types are categorised as Class 1, 2 and 3 targets, which provides a method of classifying the complexity and research/planning necessary for experimental delivery. These definitions are somewhat subjective in nature but are typically classified as follows:

- **Class 1 targets** require fewer specialist resources to manufacture. Materials are typically procured 'off-the-shelf' and minimal specialist equipment is required for assembly. Typical targets include micron-thick foils or alignment wires glued to posts.
- **Class 2 targets** require the use of specialist manufacturing equipment and knowledge, and would be a very involved process for a non-Target Fabrication entity to replicate. Examples include nanometres-thick thin-film and multilayer coatings. Tape Targets that have been previously produced and are not R&D projects fall into this category.
- **Class 3 targets** require long-term R&D projects to establish and perfect, and are often referred to as "high-specification targets". Such targets include complex 3D assemblies, MEMS produced components, low-density materials such as aerogels and foams, and processed (coated or etched) tape targets that are novel and require R&D.

Classifying each target type provides a metric of how the Target Fabrication Group's resources are used throughout the year, and is shown in Figure 1. It can also prove useful to distinguish the distribution of shots that require a high number of low complexity target types, compared to those that require fewer, higher complexity targets (Table 2).

Target Supply

The 2020-21 reporting period saw a total of 2,959 targets supplied across the six experiments supported in the CLF, with 83% being provided to Gemini experiments and the remaining 17% to Vulcan.

Gemini	Total Targets	Class 1	Class 2	Class 3
0120 TA3 Higginbotham	621	619	2	0
0820 TA3 Kettle	1,134	12	1122	0
0221 TA3 Sarri	696	696	0	0
Total	**2,451**			

Vulcan	Total Targets	Class 1	Class 2	Class 3
0221 TAW Scott	169	15	0	154
0320 TAW Palmer	154	91	4	59
1020 TAP Kar	185	19	0	166
Total	**508**			

Table 2: Breakdown of targets supplied to a) Gemini experiments and b) Vulcan experiments over the 2020-2021 reporting period

The disparity in target complexity is highlighted in Figure 1, which shows that Vulcan experiments had a large proportion of complex targets (65%), whereas Gemini had none over the year. The majority of Vulcan targets were complex 3D micro-structures, which require a combination of specialist skills, high accuracy characterisation, and thin-film coating to assemble. The vast majority of Class 2 Gemini targets were thin-film coated and laser-etched tape driven targets, the production process for which had previously been established for the 0218 TA3 Kettle campaign in February 2018. While they are still very complex targets to produce, due to the specialism and expertise required in the manufacturing steps, their fabrication has formed a research project within the Target Fabrication Group over the last three years; therefore, because it is an established process, they are categorised as Class 2 targets.

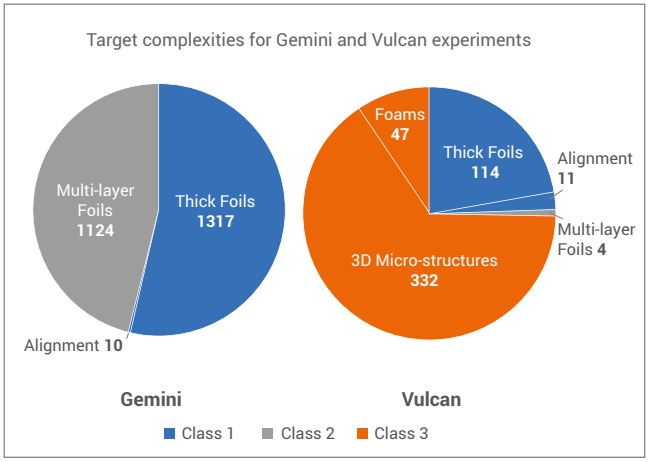

Figure 1: A breakdown of the complexity of targets requested by Gemini and Vulcan target areas over the 2020-2021 period.

Historical target supply

The supply of solid targets is having to evolve, due to the driver technologies increasing in repetition rate. Consequently, over the last few years the Target Fabrication Group have established numerous R&D projects to address the anticipated increase in production requirements.

Gemini experiments have been somewhat of a testbed for the aforementioned increased repetition rate experiments since 2018, with three tape target experiments having greatly contributed to the increase in targets produced. It is worth noting that there were twice the number of experiments in 2017-18 compared with 2018-19, 2019-20 and 2020-21, showing a definite upward trend in target supply per experiment. Figure 2 shows the total targets supplied over the yearly reporting periods since 2011-12.

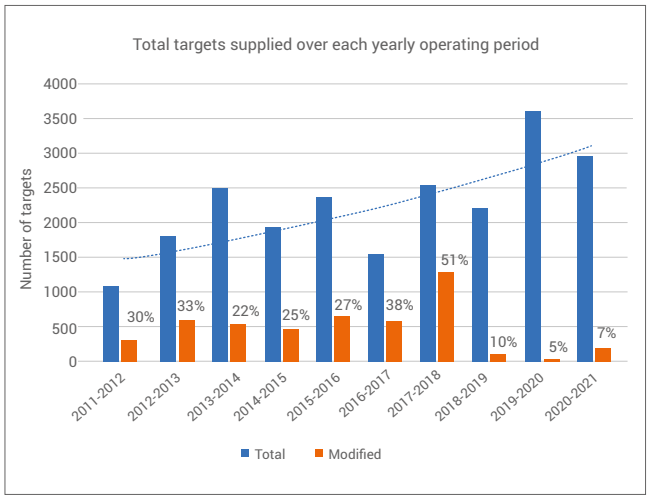

Figure 2: Total targets supplied to CLF solid target experiments throughout each reporting period [5-14]

With EPAC coming online in 2023 target supply is expected to increase exponentially over the next three to four years, which is reflected in the trendline on Figure 2.

Adapting to Demand
One of the major strengths of the CLF is direct access to state-of-the-art fabrication and characterisation equipment, and to expertise within the department. Having a dedicated Target Fabrication Laboratory allows the CLF to adapt to the demand of its users mid-experiment, which can and does often lead to the success of an experimental campaign.

Target Fabrication support offers the ability to thin-film coat a multitude of materials to a very fine thickness tolerance, laser machine components to high levels of precision, and be able to characterise material thicknesses, composition and densities.

The benefit of these capabilities is shown by the yellow bars on Figure 2, which detail the total number of modified targets, i.e. the quantity of targets issued over the operating period that were not initially requested in the planning processes. These modified targets require additional effort during the experimental runs, but maximise the science output from the limited shots available. Although the total percentage of modified targets seems to have significantly dropped in the last few years, this is due to the large contribution of tape driven targets since 2018, which a) required a significant planning process to fabricate and were not modifiable mid-experiment and b) were planned many weeks prior to beam-time.

Of the 2,451 targets delivered on Gemini experiments, only nine (0.4%) were modified from the original target list (due to the reasons mentioned above). For example the 0820 TA3 Kettle experiment was attempting to obtain as much data as possible using only two germanium target thicknesses whilst having flexibility within their specified parameters.

By contrast, on Vulcan, 198 of the 508 total targets delivered (i.e. 39%) were modified targets. The majority of these targets were thick foils or multi-layer foils on single target stalks, or complex 3D assemblies. The main benefit of these targets is that users can home in on specific materials and thicknesses, and to a lesser extent geometries, to achieve their scientific aims. The targets for such experiments are typically categorised as being more complex in design and as having a lower output (as shown in Figure 1), demonstrating why on-site Target Fabrication support is crucial for the success of such experiments and is a key capability of the CLF.

Production Economy and Waste Management
One of the challenges for Target Fabrication is striking a balance between pre-production of targets and just-in-time production during the run. Being able to deliver the requested targets, but not over supply in the event that targets are not required for science reasons, allows staff effort and resources to be allocated to other experiments as needed.

It is often the case that targets are not returned until some considerable time after the end of the experiment, making this a difficult metric to track. For experiments operating on a shot-by-shot basis, as is often the case on Vulcan, return percentages are typically considerably higher. Figure 3 shows the trend for returned vs total target supply over the last ten reporting periods, with 40 total returned targets for the 2020-21 year, all from Vulcan experiments.

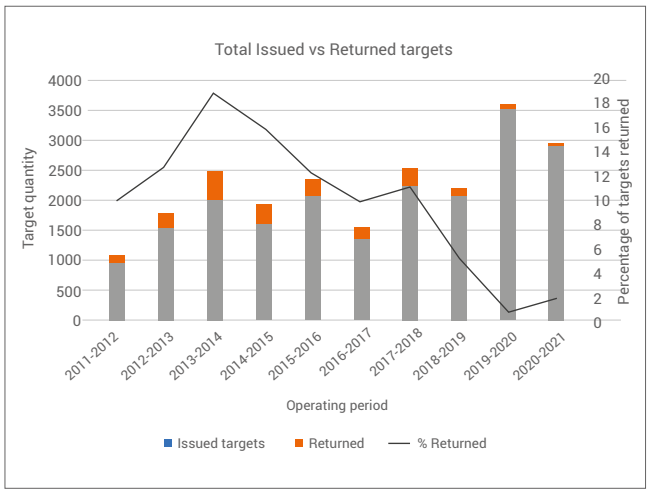

Figure 3: Returned targets vs total targets supplied over the last ten operating periods

Where possible, unused targets are stored for potential use in future experiments or recycled for components.

A further explanation for the reduction in returned target numbers is the addition of an additive manufacturing capability within the Target Fabrication Group. Target stalks, which were historically machined from metal at significant expense, are now primarily 3D printed (at a cost reduction factor of ~50) and not typically re-used or returned post-experiment. Consequently un-shot targets are typically kept (or discarded) by the users, which therefore leads to a reduction in target returns.

External Contracts
In the reporting period 2020-21 the operations of Scitech Precision Ltd (SPL), Target Fabrication Group's commercial spinout company, were heavily hit by the COVID-19 pandemic. The reduction of operations at many of its core customers subsequently led to a reduction in orders and turnover. A total of 21 institutions engaged with SPL for 63 individual contracts, generating a turnover of £182k. During the reporting period SPL moved to a new, dedicated laser-machining laboratory on the Rutherford Appleton Laboratory site, offering improved infrastructure. SPL also engaged in a programme of upgrades to its lasers, with the addition of a femto-second laser machining system and upgraded control systems and stages, to allow it to carry out more processes at a higher level of accuracy.

Summary
Over the 2020-21 reporting period, the Target Fabrication Group have delivered a total of 2,959 high power laser targets across six experimental campaigns within the CLF, over 38 experimental weeks. This includes set-up weeks and laser delays, as well as a significant impact to operations caused by the COVID-19 pandemic which paused experiments between March and August 2020.

The majority of the 2451 laser targets delivered on Gemini campaigns were in the form of tape-driven targets – a technology which the Target Fabrication Group have been researching over the last two years in preparation for EPAC. Such targets were mainly 'Class 2' targets.

The remaining 508 targets were issued for Vulcan experiments and were generally more complex to produce and characterise, comprising foams and 3D micro-structures, and are categorised as 'Class 3' targets. There were no ultra-thin foils requested for experimental campaigns during the operational period.

Total target production is continuing in an upward trajectory, even accounting for the significant drop in total HPL access weeks, and is expected to rise considerably over the next reporting period, dependent on pandemic recovery, particularly across Gemini experiments.

References

1. *N. Bourgeois et al, "Deploying the SLAC liquid target at RAL", CLF Annual Report 2020-2021*
2. *S. Astbury, W. Robins, C. Spindloe & M. Tolley, "Progression of a tape-drive targetry solution for high rep-rate HPL experiments within the CLF", CLF Annual Report 2018-2019*
3. *W. Robins, S. Astbury, C. Spindloe & M. Tolley, "Experimental Testing and Fielding of the CLF Precision Tape Drive in the Gemini Target Area", CLF Annual Report 2020-2021*
4. *S. Astbury, C. Spindloe & M. Tolley, "Development of patterned tape-drive targets for high rep-rate HPL experiments", CLF Annual Report 2017-2018*
5. *D. Haddock, C. Spindloe & M. Tolley, "Target Fabrication Operational Statistics", CLF Annual Report 2019-2020*
6. *D. Haddock, C. Spindloe & M. Tolley, "Target Fabrication Operational Statistics", CLF Annual Report 2018-2019*
7. *D. Haddock, C. Spindloe & M. Tolley, "Target Fabrication Operational Statistics", CLF Annual Report 2017-2018, p45-48*
8. *D. Haddock, C. Spindloe & M. Tolley, "Target Fabrication Operational Statistics", CLF Annual Report 2016-2017, p48-50*
9. *D. Haddock, C. Spindloe & M. Tolley, "Target Fabrication Operational Statistics", CLF Annual Report 2015-2016, p49-51*
10. *D. Haddock, C. Spindloe & M. Tolley, "Target Fabrication Operational Statistics", CLF Annual Report 2014-2015, p58-60*
11. *D. Haddock, C. Spindloe & M. Tolley, "Target Fabrication Operational Statistics", CLF Annual Report 2013-2014, p68-70*
12. *D. Haddock, C. Spindloe & M. Tolley, "Target Fabrication Operational Statistics", CLF Annual Report 2012-2013, p74-75*
13. *D. Haddock, C. Spindloe & M. Tolley, "Target Fabrication Operational Statistics", CLF Annual Report 2011-2012, p71-72*
14. *H. F. Lowe, C. Spindloe & M. Tolley, "Target Fabrication Operational Statistics", CLF Annual Report 2010-2011, p76-77*

Contact: D. Haddock (david.haddock@stfc.ac.uk)

Vulcan operational statistics

A.K. Kidd *(Central Laser Facility, STFC Rutherford Appleton Laboratory, Harwell Campus, Didcot, UK)*

Introduction

Vulcan has completed an active experimental year, with 27 full experimental weeks allocated to target areas TAW and TAP between April 2020 and March 2021; the schedule was interrupted from March 2020 due to COVID-19. Table 1 shows the operational schedule for the year, and reports the shot rate statistics for each experiment.

PERIOD	TAW	TAP
	2020	
02 Mar – 22 Nov	C Palmer *Laboratory investigation of dust charging and destruction in shocked plasma* (Shots 104, Failed 36, Reliability 65.4%) (Availability 74.0%, w extra hours 168.8%) (5 weeks + extra 7 weeks) 19210011	
02 Mar – 02 Dec		D Carroll *Investigation of EMP emissions for understanding the source mechanisms and the rules for tuning and employing them in high power lasers* (Shots 119, Failed 7, Reliability 94.1%) (Availability 67.4, w extra hours 88.9%) (5 weeks + extra 1 week 3 days) 19210019
	2021	
15 Feb – 13 Apr	G Scott *Direct laser acceleration of electrons to superponderomotive energies* (Shots 102, Failed 21, Reliability 79.4%) (Availability 72.0%, w extra hours 114.6%) (5 weeks + extra 3 weeks 2 days) 19210003	

Table 1: Experimental schedule for the period April 2020 – March 2021

(Total shots fired, failed shots, reliability)
(Availability normal, additional hours)

Numbers in parentheses indicate the total number of full energy laser shots delivered to target, followed by the number of these that failed, and the percentage of successful shots. The second set of numbers shows the availability of the laser to target areas during normal operating hours, along with outside hours operations.

The total number of full disc amplifier shots that have been fired to target this year is 325. Table 2 shows how this figure compares with that for the four previous years. 64 shots failed to meet user requirements. The overall shot success rate to target for the year is 80%, compared to 90%, 86%, 81% and 84% in the previous four years. Figure 1 shows the reliability of the Vulcan laser to all target areas over the past five years.

Year	No of shots	Failed shots	Reliability
16 – 17	948	93	90%
17 – 18	934	132	86%
18 – 19	607	113	81%
19 – 20	653	102	84%
20 – 21	325	64	80%

Table 2: Shot totals and proportion of failed shots for the past five years

The shot reliability to TAW is 72%, down 10% from the previous year. The shot reliability to TAP is 94%, up from 84% in 2019-20.

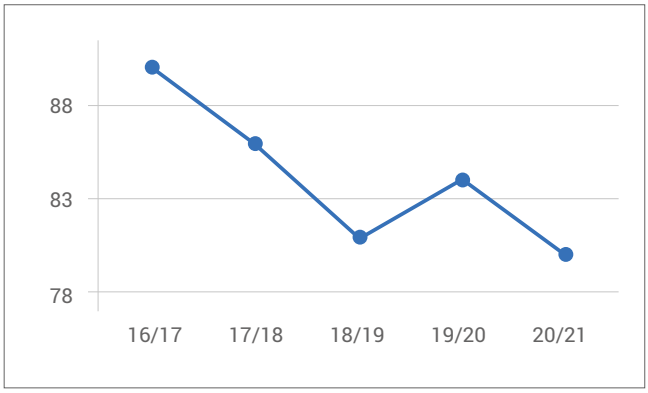

Figure 1: All areas shot reliability for each year 2016-17 to 2020-21

Analysis of the failure modes reveals that the overriding causes of failed shots are beam alignment, front-end related issues, and triggering. The first two causes are manifested in low or high energy output of the rod amplifier chain (outside of +/-20% of the requested energy). Instability in the pulse energy is introduced during propagation from the front-end room to the laser area. Novel methods of beam stabilisation are being investigated to improve this fault mode.

There is a requirement that was originally instigated for the EPSRC FAA that the laser system be available, during the five-week periods of experimental data collection, from 09:00 to 17:00 hours, Monday to Thursday, and from 09:00 to 16:00 hours on Fridays (a total of 195 hours over the five-week experimental period). The laser has not always met the start-up target of 09:00, but it has been common practice to operate the laser well beyond the standard contracted finish time on several days during the week. In addition, the introduction of early start times on some experiments continues to lead to improvements in availability.

On average, Vulcan has been available for each experiment to target areas for 71.2% of the time during contracted hours, compared with 86.7% for the previous year. The overall availability to all target areas has increased to 124.1% compared with 112.6% in 2019-20. The time that the laser is unavailable to users is primarily the time taken for beam alignment at the start of the day.

Contacts: A.K. Kidd (andy.kidd@stfc.ac.uk)
P. Oliveira (pedro.oliveira@stfc.ac.uk)

Publications

Journal Papers

ARTEMIS

EM Warne, AD Smith, DA Horke, E Springate, AJH Jones, C Cacho, RT Chapman, RS Minns
Time resolved detection of the S(1D) product of the UV induced dissociation of CS2
THE JOURNAL OF CHEMICAL PHYSICS, 154, 34302 (2021)

D Biswas, AJH Jones, P Majchrzak, BK Choi, T Lee, K Volckaert, J Feng, I Marković, F Andreatta, C Kang, HJ Kim, IH Lee, C Jozwiak, E Rotenberg, A Bostwick, CE Sanders, Y Zhang, G Karras, RT Chapman, AS Wyatt, E Springate, JA Miwa, P Hofmann, PDC King, YJ Chang, N Lanatà, S Ulstrup
Ultrafast Triggering of Insulator-Metal Transition in Two-Dimensional VSe2
NANO LETTERS, 21, 1968-1975 (2021)

JWL Lee, H Köckert, D Heathcote, D Popat, RT Chapman, G Karras, P Majchrzak, E Springate, C Vallance
Three-dimensional covariance-map imaging of molecular structure and dynamics on the ultrafast timescale
COMMUNICATIONS CHEMISTRY, 3, 72 (2020)

H Ganjitabar, DP Singh, R Chapman, A Gardner, RS Minns, I Powis, KL Reid, A Vredenborg
The role of the intermediate state in angle-resolved photoelectron studies using resonance-enhanced multiphoton ionization of the chiral terpenes, α-pinene and 3-carene
MOLECULAR PHYSICS, 119, e1808907 (2020)

EM Warne, B Downes-Ward, J Woodhouse, MA Parkes, E Springate, PAJ Pearcy, Y Zhang, G Karras, AS Wyatt, RT Chapman, RS Minns
Photodissociation dynamics of methyl iodide probed using femtosecond extreme ultraviolet photoelectron spectroscopy
PHYSICAL CHEMISTRY CHEMICAL PHYSICS, 22, 25695-25703 (2020)

PD Baksh, M Ostrčil, M Miszczak, C Pooley, RT Chapman, AS Wyatt, E Springate, JE Chad, K Deinhardt, JG Frey, WS Brocklesby
Quantitative and correlative extreme ultraviolet coherent imaging of mouse hippocampal neurons at high resolution
SCIENCE ADVANCES, 6, eaaz3025 (2020)

CALTA

M De Vido, PD Mason, M Fitton, RW Eardley, G Quinn, D Clarke, K Ertel, TJ Butcher, P Jonathan Phillips, S Banerjee, J Smith, J Spear, C Edwards, JL Collier
Modelling and measurement of thermal stress-induced depolarisation in high energy, high repetition rate diode-pumped Yb:YAG lasers
OPTICS EXPRESS, 29, 5607-5623 (2021)

JP Phillips, S Banerjee, P Mason, J Smith, J Spear, M De Vido, K Ertel, T Butcher, G Quinn, D Clarke, C Edwards, C Hernandez-Gomez, J Collier
Second and third harmonic conversion of a kilowatt average power, 100-J-level diode pumped Yb:YAG laser in large aperture LBO
OPTICS LETTERS, 46, 1808-1811 (2021)

S Banerjee, P Mason, J Phillips, J Smith, T Butcher, J Spear, M De Vido, G Quinn, D Clarke, K Ertel, C Hernandez-Gomez, C Edwards, J Collier
Pushing the boundaries of diode-pumped solid-state lasers for high-energy applications
HIGH POWER LASER SCIENCE AND ENGINEERING, 8, e20 (2020)

F Albert, M Couprie, AD Debus, M Downer, J Faure, A Flacco, LA Gizzi, TE Grismayer, A Huebl, C Joshi, M Labat, WP Leemans, A Maier, S Mangles, P Mason, F Mathieu, P Muggli, M Nishiuchi, J Osterhoff, PP Rajeev, U Schramm, J Schreiber, AGR Thomas, J Vay, M Vranic, K Zeil
2020 Roadmap on Plasma Accelerators
NEW JOURNAL OF PHYSICS, 23, 31101 (2020)

JP Phillips, S Banerjee, K Ertel, P Mason, J Smith, T Butcher, M De Vido, C Edwards, C Hernandez-Gomez, J Collier
Stable high-energy, high-repetition-rate, frequency doubling in a large aperture temperature-controlled LBO at 515 nm
OPTICS LETTERS, 45, 2946-2949 (2020)

GEMINI

RJ Shalloo, SJD Dann, J Gruse, CID Underwood, AF Antoine, C Arran, M Backhouse, CD Baird, MD Balcazar, N Bourgeois, JA Cardarelli, P Hatfield, J Kang, K Krushelnick, SPD Mangles, CD Murphy, N Lu, J Osterhoff, K Põder, PP Rajeev, CP Ridgers, S Rozario, MP Selwood, AJ Shahani, DR Symes, AGR Thomas, C Thornton, Z Najmudin, MJV Streeter
Automation and control of laser wakefield accelerators using Bayesian optimization
NATURE COMMUNICATIONS, 11, 6355 (2020)

J Gruse, M Streeter, C Thornton, C Armstrong, C Baird, N Bourgeois, S Cipiccia, O Finlay, C Gregory, Y Katzir, N Lopes, S Mangles, Z Najmudin, D Neely, L Pickard, K Potter, P Rajeev, D Rusby, C Underwood, J Warnett, M Williams, J Wood, C Murphy, C Brenner, D Symes
Application of compact laser-driven accelerator X-ray sources for industrial imaging
NUCLEAR INSTRUMENTS AND METHODS IN PHYSICS RESEARCH SECTION A ACCELERATORS SPECTROMETERS DETECTORS AND ASSOCIATED EQUIPMENT, 983, 164369 (2020)

M Bloom, M Streeter, S Kneip, R Bendoyro, O Cheklov, J Cole, A Döpp, C Hooker, J Holloway, J Jiang, N Lopes, H Nakamura, P Norreys, P Rajeev, D Symes, J Schreiber, J Wood, M Wing, Z Najmudin, S Mangles
Bright x-ray radiation from plasma bubbles in an evolving laser wakefield accelerator
PHYSICAL REVIEW ACCELERATORS AND BEAMS, 23, 61301 (2020)

R Scott, C Thornton, N Bourgeois, J Cowley, W Rittershofer, T Kleinwächter, J Osterhoff, D Symes, C Hooker, S Hooker
Electron trapping and reinjection in prepulse-shaped gas targets for laser-plasma accelerators
PHYSICAL REVIEW ACCELERATORS AND BEAMS, 23, 111301 (2020)

A Picksley, A Alejo, J Cowley, N Bourgeois, L Corner, L Feder, J Holloway, H Jones, J Jonnerby, H Milchberg, L Reid, A Ross, R Walczak, S Hooker
Guiding of high-intensity laser pulses in 100-mm-long hydrodynamic optical-field-ionized plasma channels
PHYSICAL REVIEW ACCELERATORS AND BEAMS, 23, 81303 (2020)

S Williamson, R Wilson, M King, M Duff, B Gonzalez-Izquierdo, Z Davidson, A Higginson, N Booth, S Hawkes, D Neely, R Gray, P McKenna
Self-referencing spectral interferometric probing of the onset time of relativistic transparency in intense laser-foil interactions
PHYSICAL REVIEW APPLIED, 14, 34018 (2020)

A Picksley, A Alejo, RJ Shalloo, C Arran, A von Boetticher, L Corner, JA Holloway, J Jonnerby, O Jakobsson, C Thornton, R Walczak, SM Hooker
Meter-scale conditioned hydrodynamic optical-field-ionized plasma channels
PHYSICAL REVIEW E, 102, 53201 (2020)

R Aboushelbaya, K Glize, AF Savin, M Mayr, B Spiers, R Wang, N Bourgeois, C Spindloe, R Bingham, PA Norreys
Measuring the orbital angular momentum of high-power laser pulses
PHYSICS OF PLASMAS, 27, 53107 (2020)

CID Underwood, CD Baird, C Murphy, C Armstrong, C Thornton, O Finlay, MJV Streeter, MP Selwood, N Brierley, S Cipiccia, J Gruse, P McKenna, Z Najmudin, D Neely, D Rusby, D Symes, CM Brenner
Development of control mechanisms for a laser wakefield accelerator-driven bremsstrahlung X-ray source for advanced radiographic imaging
PLASMA PHYSICS AND CONTROLLED FUSION, 62, 124002 (2020)

LASER DEVELOPMENTS

M Galletti, P Oliveira, M Galimberti, M Ahmad, G Archipovaite, N Booth, E Dilworth, A Frackiewicz, T Winstone, I Musgrave, C Hernandez-Gomez
Ultra-broadband all-OPCPA petawatt facility fully based on LBO
HIGH POWER LASER SCIENCE AND ENGINEERING, 8, e31 (2020)

A Aiken, P Oliveira, L Bradley, E Dilworth, M Galletti, B Parry, M Galimberti, I Musgrave
Development of a single-shot third-order cross-correlator for picosecond laser systems
OPTICS COMMUNICATIONS, 483, 126672 (2021)

G Archipovaite, M Galletti, P Oliveira, M Galimberti, A Frackiewicz, I Musgrave, C Hernandez-Gomez
880 nm, 22 fs, 1 mJ pulses at 100 Hz as an OPCPA front end for Vulcan laser facility
OPTICS COMMUNICATIONS, 474, 126072 (2020)

PLASMA PHYSICS

K Weichman, M Murakami, APL Robinson, AV Arefiev
Sign reversal in magnetic field amplification by relativistic laser-driven microtube implosions
APPLIED PHYSICS LETTERS, 117, 244101 (2020)

LE Chen, AFA Bott, P Tzeferacos, A Rigby, A Bell, R Bingham, C Graziani, J Katz, M Koenig, CK Li, R Petrasso, H Park, JS Ross, D Ryu, TG White, B Reville, J Matthews, J Meinecke, F Miniati, EG Zweibel, S Sarkar, AA Schekochihin, DQ Lamb, DH Froula, G Gregori
Transport of High-energy Charged Particles through Spatially Intermittent Turbulent Magnetic Fields
ASTROPHYSICAL JOURNAL, 892, 114 (2020)

P Hatfield, S Rose, R Scott, I Almosallam, S Roberts, M Jarvis
Using Sparse Gaussian Processes for Predicting Robust Inertial Confinement Fusion Implosion Yields
IEEE TRANSACTIONS ON PLASMA SCIENCE, 48, 14-21 (2020)

B Ramakrishna, S Krishnamurthy, M Tayyab, S Bagchi, K Makur, R Trines, R Scott, A Robinson, JA Chakera
Ion source perturbation and control in intense laser plasma interaction
MATTER AND RADIATION AT EXTREMES, 5, 45402 (2020)

K Weichman, APL Robinson, M Murakami, AV Arefiev
Strong surface magnetic field generation in relativistic short pulse laser-plasma interaction with an applied seed magnetic field
NEW JOURNAL OF PHYSICS, 22, 113009 (2020)

E Boella, R Bingham, RA Cairns, P Norreys, R Trines, R Scott, M Vranic, N Shukla, LO Silva
Collisionless shock acceleration in the corona of an inertial confinement fusion pellet with possible application to ion fast ignition
PHILOSOPHICAL TRANSACTIONS OF THE ROYAL SOCIETY A: MATHEMATICAL PHYSICAL AND ENGINEERING SCIENCES, 379, 20200039 (2020)

SJ Rose, PW Hatfield, RHH Scott
Modelling burning thermonuclear plasma
PHILOSOPHICAL TRANSACTIONS OF THE ROYAL SOCIETY A: MATHEMATICAL PHYSICAL AND ENGINEERING SCIENCES, 378, 20200014 (2020)

RW Paddock, H Martin, RT Ruskov, RHH Scott, W Garbett, BM Haines, AB Zylstra, R Aboushelbaya, MW Mayr, BT Spiers, RHW Wang, PA Norreys
One-dimensional hydrodynamic simulations of low convergence ratio direct-drive inertial confinement fusion implosions
PHILOSOPHICAL TRANSACTIONS OF THE ROYAL SOCIETY A: MATHEMATICAL PHYSICAL AND ENGINEERING SCIENCES, 379, 20200224 (2020)

PA Norreys, C Ridgers, K Lancaster, M Koepke, G Tynan
Prospects for high gain inertial fusion energy: an introduction to the first special edition
PHILOSOPHICAL TRANSACTIONS OF THE ROYAL SOCIETY A: MATHEMATICAL PHYSICAL AND ENGINEERING SCIENCES, 378, 20200006 (2020)

S Bagchi, M Tayyab, J Pasley, APL Robinson, M Nayak, JA Chakera
Quasi mono-energetic heavy ion acceleration from layered targets
PHYSICS OF PLASMAS, 28, 23108 (2021)

AFA Bott, P Tzeferacos, L Chen, CAJ Palmer, A Rigby, AR Bell, R Bingham, A Birkel, C Graziani, DH Froula, J Katz, M Koenig, MW Kunz, C Li, J Meinecke, F Miniati, R Petrasso, H Park, BA Remington, B Reville, JS Ross, D Ryu, D Ryutov, FH Séguin, TG White, AA Schekochihin, DQ Lamb, G Gregori
Time-resolved turbulent dynamo in a laser plasma
PROCEEDINGS OF THE NATIONAL ACADEMY OF SCIENCES USA, 118, e2015729118 (2021)

A Arefiev, Z Gong, APL Robinson
Energy gain by laser-accelerated electrons in a strong magnetic field
PHYSICAL REVIEW E, 101, 43201 (2020)

N Rathee, A Mukherjee, RMGM Trines, S Sengupta
Wavebreaking amplitudes in warm, inhomogeneous plasmas revisited
PHYSICS OF PLASMAS, 28, 12105 (2021)

APL Robinson, J Pasley
Core electrons and specific heat capacity in the fast electron heating of solids
PHYSICS OF PLASMAS, 27, 72701 (2020)

M Shaikh, K Jana, AD Lad, I Dey, SL Roy, D Sarkar, YM Ved, APL Robinson, J Pasley, G Ravindra Kumar
Erratum: Tracking ultrafast dynamics of intense shock generation and breakout at target rear
PHYSICS OF PLASMAS, 27, 49901 (2020)

JLH East, EJ Hume, KL Lancaster, APL Robinson, J Pasley
Hydrodynamic motion of guiding elements within a magnetic switchyard in fast ignition conditions
PHYSICS OF PLASMAS, 27, 62701 (2020)

JG Lee, APL Robinson, J Pasley
Ignition criteria for x-ray fast ignition inertial confinement fusion
PHYSICS OF PLASMAS, 27, 42711 (2020)

RAB Alraddadi, APL Robinson, NC Woolsey
Improved fast electron transport through the use of foam guides
PHYSICS OF PLASMAS, 27, 92701 (2020)

T Peterken, APL Robinson, RMGM Trines, RJ Clarke
Increased hot electron production from the addition of a gas cell in sub-picosecond laser-foil interactions
PHYSICS OF PLASMAS, 27, 123101 (2020)

MJ Rosenberg, AA Solodov, W Seka, RK Follett, JF Myatt, AV Maximov, C Ren, S Cao, P Michel, M Hohenberger, JP Palastro, C Goyon, T Chapman, JE Ralph, JD Moody, RHH Scott, K Glize, SP Regan
Stimulated Raman scattering mechanisms and scaling behavior in planar direct-drive experiments at the National Ignition Facility
PHYSICS OF PLASMAS, 27, 42705 (2020)

H Schmitz, R Trines, R Bingham
Transverse beam envelope structures in strongly coupled stimulated Brillouin scattering
PHYSICS OF PLASMAS, 27, 102707 (2020)

AR Bell, RJ Kingham, HC Watkins, JH Matthews
Instability in a magnetised collisional plasma driven by a heat flow or a current
PLASMA PHYSICS AND CONTROLLED FUSION, 62, 95026 (2020)

RMGM Trines, EP Alves, E Webb, J Vieira, F Fiúza, RA Fonseca, LO Silva, RA Cairns, R Bingham
New criteria for efficient Raman and Brillouin amplification of laser beams in plasma
SCIENTIFIC REPORTS, 10, 19875 (2020)

VULCAN

SR Mirfayzi, H Ahmed, D Doria, A Alejo, S Ansell, RJ Clarke, B Gonzalez-Izquierdo, P Hadjisolomou, R Heathcote, T Hodge, P Martin, D Raspino, E Schooneveld, P McKenna, NJ Rhodes, D Neely, M Borghesi, S Kar
A miniature thermal neutron source using high power lasers
APPLIED PHYSICS LETTERS, 116, 174102 (2020)

F Consoli, VT Tikhonchuk, M Bardon, P Bradford, DC Carroll, J Cikhardt, M Cipriani, RJ Clarke, TE Cowan, CN Danson, R De Angelis, M De Marco, J Dubois, B Etchessahar, AL Garcia, DI Hillier, A Honsa, W Jiang, V Kmetik, J Krása, Y Li, F Lubrano, P McKenna, J Metzkes-Ng, A Poyé, I Prencipe, P Rączka, RA Smith, R Vrana, NC Woolsey, E Zemaityte, Y Zhang, Z Zhang, B Zielbauer, D Neely
Laser produced electromagnetic pulses: generation, detection and mitigation
HIGH POWER LASER SCIENCE AND ENGINEERING, 8, e22 (2020)

P Bradford, MP Read, M Ehret, L Antonelli, M Khan, N Booth, K Glize, D Carroll, R Clarke, R Heathcote, S Ryazantsev, S Pikuz, C Spindloe, JD Moody, BB Pollock, VT Tikhonchuk, CP Ridgers, JJ Santos, NC Woolsey
Proton deflectometry of a capacitor coil target along two axes
HIGH POWER LASER SCIENCE AND ENGINEERING, 8, e11 (2020)

V Scuderi, G Milluzzo, D Doria, A Alejo, A Amico, N Booth, G Cuttone, J Green, S Kar, G Korn, G Larosa, R Leanza, P Martin, P McKenna, H Padda, G Petringa, J Pipek, L Romagnani, F Romano, A Russo, F Schillaci, G Cirrone, D Margarone, M Borghesi
TOF diagnosis of laser accelerated, high-energy protons
NUCLEAR INSTRUMENTS AND METHODS IN PHYSICS RESEARCH SECTION A ACCELERATORS SPECTROMETERS DETECTORS AND ASSOCIATED EQUIPMENT, 978, 164364 (2020)

AS Martynenko, SA Pikuz, IY Skobelev, SN Ryazantsev, C Baird, N Booth, L Doehl, P Durey, AY Faenov, D Farley, R Kodama, K Lancaster, P McKenna, CD Murphy, C Spindloe, TA Pikuz, N Woolsey
Effect of plastic coating on the density of plasma formed in Si foil targets irradiated by ultra-high-contrast relativistic laser pulses
PHYSICAL REVIEW E, 101, 43208 (2020)

T Ebert, NW Neumann, LNK Döhl, J Jarrett, C Baird, R Heathcote, M Hesse, A Hughes, P McKenna, D Neely, D Rusby, G Schaumann, C Spindloe, A Tebartz, N Woolsey, M Roth
Enhanced brightness of a laser-driven x-ray and particle source by microstructured surfaces of silicon targets
PHYSICS OF PLASMAS, 27, 43106 (2020)

A Martynenko, I Skobelev, S Pikuz, S Ryazantsev, C Baird, N Booth, L Doehl, P Durey, D Farley, R Kodama, K Lancaster, P McKenna, C Murphy, C Spindloe, T Pikuz, N Woolsey
Determining the short laser pulse contrast based on X-Ray emission spectroscopy
HIGH ENERGY DENSITY PHYSICS, 38, 100924 (2021)

H Ahmed, P Hadjisolomou, K Naughton, A Alejo, S Brauckmann, G Cantono, S Ferguson, M Cerchez, D Doria, J Green, D Gwynne, T Hodge, D Kumar, A Macchi, R Prasad, O Willi, M Borghesi, S Kar
High energy implementation of coil-target scheme for guided re-acceleration of laser-driven protons
SCIENTIFIC REPORTS, 11, 699 (2021)

MP Selwood, CID Underwood, R Heathcote, CD Murphy
Coded apertures with scatter and partial attenuation for high-energy high-resolution imaging
MATTER AND RADIATION AT EXTREMES, 6, 14405 (2021)

F Romano, A Subiel, M McManus, ND Lee, H Palmans, R Thomas, S McCallum, G Milluzzo, M Borghesi, A McIlvenny, H Ahmed, W Farabolini, A Gilardi, A Schüller
Challenges in dosimetry of particle beams with ultra-high pulse dose rates
PLASMA PHYSICS AND CONTROLLED FUSION, 62, 74002 (2020)

ULTRA

JN Iuliano, JT Collado, AA Gil, PT Ravindran, A Lukacs, S Shin, HA Woroniecka, K Adamczyk, JM Aramini, UR Edupuganti, CR Hall, GM Greetham, IV Sazanovich, IP Clark, T Daryaee, JE Toettcher, JB French, KH Gardner, CL Simmerling, SR Meech, PJ Tonge
Unraveling the Mechanism of a LOV Domain Optogenetic Sensor: A Glutamine Lever Induces Unfolding of the Jα Helix
ACS CHEMICAL BIOLOGY, 15, 2752-2765 (2020)

R Fritzsch, S Hume, L Minnes, MJ Baker, GA Burley, NT Hunt
Two-dimensional infrared spectroscopy: an emerging analytical tool?
ANALYST, 145, 2014-2024 (2020)

SH Rutherford, GM Greetham, PM Donaldson, M Towrie, AW Parker, MJ Baker, NT Hunt
Detection of Glycine as a Model Protein in Blood Serum Using 2D-IR Spectroscopy
ANALYTICAL CHEMISTRY, 93, 920-927 (2020)

G Toupalas, J Karlsson, FA Black, A Masip-Sánchez, X López, Y Ben M'Barek, S Blanchard, A Proust, S Alves, P Chabera, IP Clark, T Pullerits, JM Poblet, EA Gibson, G Izzet
Tuning Photoinduced Electron Transfer in POM-bodipy Hybrids by Controlling the Environment, Experiment and Theory.
ANGEWANDTE CHEMIE INTERNATIONAL EDITION, 770, 6518-6525 (2020)

SJO Hardman, DJ Heyes, IV Sazanovich, NS Scrutton
Photocycle of Cyanobacteriochrome TePixJ
BIOCHEMISTRY, 59, 2909-2915 (2020)

A Lukacs, J Tolentino, J Iuliano, K Pirisi, PJ Tonge, G Greetham, M Towrie, SR Meech
Radical Formation in the Photoactivated Adenylate Cyclase OaPAC Revealed by Ultrafast Spectroscopy
BIOPHYSICAL JOURNAL, 118, 608A- (2020)

FR Baptista, SJ Devereux, SP Gurung, JP Hall, IV Sazanovich, M Towrie, DJ Cardin, J Brazier, JM Kelly, SJ Quinn
The influence of loops on the binding of the [Ru2dppz]2+ Light-Switch Compound to i motif DNA Structures revealed by Time-resolved Spectroscopy
CHEMICAL COMMUNICATIONS, 56, 9703-9706 (2020)

L Lewis-Borrell, M Sneha, A Bhattacherjee, IP Clark, AJ Orr-Ewing
Mapping the multi-step mechanism of a photoredox catalyzed atom-transfer radical polymerization reaction by direct observation of the reactive intermediates
CHEMICAL SCIENCE, 11, 4475-4481 (2020)

PM Keane, K O'Sullivan, FE Poynton, BC Poulsen, IV Sazanovich, M Towrie, CJ Cardin, X Sun, MW George, T Gunnlaugsson, SJ Quinn, JM Kelly
Understanding the factors controlling the photo-oxidation of natural DNA by enantiomerically pure intercalating ruthenium polypyridyl complexes through TA/TRIR studies with polydeoxynucleotides and mixed sequence oligodeoxynucleotides
CHEMICAL SCIENCE, 11, 8600-8609 (2020)

SJ Devereux, FE Poynton, FR Baptista, T Gunnlaugsson, CJ Cardin, IV Sazanovich, M Towrie, JM Kelly, SJ Quinn
Caught in the Loop: Binding of the [Ru] Light-Switch Compound to Quadruplex DNA in Solution Informed by Time-Resolved Infrared Spectroscopy
CHEMISTRY: A EUROPEAN JOURNAL, 26, 17103-17109 (2020)

I Fairlamb, JD Firth, LA Hammarback, TJ Burden, JB Eastwood, JR Donald, CS Horbaczewskyj, MT McRobie, A Tramaseur, IP Clark, M Towrie, A Robinson, J Krieger, JM Lynam
Light- and manganese-initiated borylation of aryl diazonium salts: mechanistic insight on the ultrafast time-scale revealed by time-resolved spectroscopic analysis
CHEMISTRY: A EUROPEAN JOURNAL, 27, 3979-3985 (2020)

JB Eastwood, LA Hammarback, MT McRobie, IP Clark, M Towrie, IJS Fairlamb, JM Lynam
Time-resolved infra-red spectroscopy reveals competitive water and dinitrogen coordination to a manganese carbonyl complex
DALTON TRANSACTIONS, 49, 5463-5470 (2020)

AA Cullen, K Heintz, L O'Reilly, C Long, A Heise, R Murphy, J Karlsson, E Gibson, GM Greetham, M Towrie, MT Pryce
A Time-Resolved Spectroscopic Investigation of a Novel BODIPY Copolymer and Its Potential Use as a Photosensitiser for Hydrogen Evolution
FRONTIERS IN CHEMISTRY, 8, 584060 (2020)

SJO Hardman, AI Iorgu, DJ Heyes, NS Scrutton, IV Sazanovich, S Hay
Ultrafast Vibrational Energy Transfer between Protein and Cofactor in a Flavoenzyme
JOURNAL OF PHYSICAL CHEMISTRY B, 124, 5163-5168 (2020)

A Artesani, S Mosca, MV Dozzi, G Valentini, D Comelli
Determination of crystal phases in mixed TiO2 paint films by non-invasive optical spectroscopies
MICROCHEMICAL JOURNAL, 155, 104739 (2020)

M Agote-Arán, AB Kroner, DS Wragg, WA Sławiński, M Briceno, HU Islam, IV Sazanovich, ME Rivas, AWJ Smith, P Collier, I Lezcano-González, AM Beale
Understanding the Deactivation Phenomena of Small-Pore Mo/H-SSZ-13 during Methane Dehydroaromatisation
MOLECULES, 25, 5048 (2020)

I Lezcano-Gonzalez, E Campbell, AEJ Hoffman, M Bocus, IV Sazanovich, M Towrie, M Agote-Aran, EK Gibson, A Greenaway, K De Wispelaere, V Van Speybroeck, AM Beale
Insight into the effects of confined hydrocarbon species on the lifetime of methanol conversion catalysts
NATURE MATERIALS, 19, 1081-1087 (2020)

B Procacci, SH Rutherford, GM Greetham, M Towrie, AW Parker, CV Robinson, CR Howle, NT Hunt
Differentiation of bacterial spores via 2D-IR spectroscopy
SPECTROCHIMICA ACTA PART A: MOLECULAR AND BIOMOLECULAR SPECTROSCOPY, 249, 119319 (2021)

LA Hammarback, BJ Aucott, JTW Bray, IP Clark, M Towrie, A Robinson, IJS Fairlamb, JM Lynam
Direct Observation of the Microscopic Reverse of the Ubiquitous Concerted Metalation Deprotonation Step in C-H Bond Activation Catalysis
JOURNAL OF THE AMERICAN CHEMICAL SOCIETY, 143, 1356-1364 (2021)

AA Cullen, A Rajagopal, K Heintz, A Heise, R Murphy, IV Sazanovich, GM Greetham, M Towrie, C Long, D Fitzgerald-Hughes, MT Pryce
Exploiting a Neutral BODIPY Copolymer as an Effective Agent for Photodynamic Antimicrobial Inactivation
JOURNAL OF PHYSICAL CHEMISTRY B, 125, 1550-1557 (2021)

K Pirisi, L Nag, Z Fekete, JN Iuliano, J Tolentino Collado, IP Clark, I Pécsi, P Sournia, U Liebl, GM Greetham, PJ Tonge, SR Meech, MH Vos, A Lukacs
Identification of the vibrational marker of tyrosine cation radical using ultrafast transient infrared spectroscopy of flavoprotein systems
PHOTOCHEMICAL AND PHOTOBIOLOGICAL SCIENCES, 20, 369-378 (2021)

A Bhattacherjee, M Sneha, L Lewis-Borrell, G Amoruso, TA Oliver, J Tyler, IP Clark, AJ Orr-Ewing
Singlet and Triplet Contributions to the Excited-State Activities of Dihydrophenazine, Phenoxazine, and Phenothiazine Organocatalysts Used in Atom Transfer Radical Polymerization
JOURNAL OF THE AMERICAN CHEMICAL SOCIETY, 143, 3613-3627 (2021)

OCTOPUS

A Milsom, AM Squires, B Woden, NJ Terrill, AD Ward, C Pfrang
The persistence of a proxy for cooking emissions in megacities: a kinetic study of the ozonolysis of self-assembled films by simultaneous Small & Wide Angle X-ray Scattering and Raman microscopy.
FARADAY DISCUSSIONS, 226, 364-381 (2020)

JKG Karlsson, A Atahan, A Harriman, NV Tkachenko, AD Ward, FA Schaberle, C Serpa, LG Arnaut
Singlet Exciton Fission and Associated Enthalpy Changes with a Covalently Linked Bichromophore Comprising TIPS-Pentacenes Held in an Open Conformation
JOURNAL OF PHYSICAL CHEMISTRY A, 125, 1184-1197 (2021)

FA Schaberle, C Serpa, LG Arnaut, AD Ward, JKG Karlsson, A Atahan, A Harriman
The Photophysical Properties of Triisopropylsilyl-ethynylpentacene—A Molecule with an Unusually Large Singlet-Triplet Energy Gap—In Solution and Solid Phases
CHEMISTRY, 2, 545-564 (2020)

MR McGrory, MD King, AD Ward
Using Mie Scattering to Determine the Wavelength-Dependent Refractive Index of Polystyrene Beads with Changing Temperature
JOURNAL OF PHYSICAL CHEMISTRY A, 124, 9617-9625 (2020)

A Colomba, M Fitzek, R George, G Weitsman, S Roberts, L Zanetti-Domingues, M Hirsch, DJ Rolfe, S Mehmood, A Madin, J Claus, S Kjaer, AP Snijders, T Ng, M Martin-Fernandez, DM Smith, PJ Parker
A small molecule inhibitor of HER3: a proof-of-concept study
BIOCHEMICAL JOURNAL, 477, 3329-3347 (2020)

AE Danson, A McStea, L Wang, AY Pollitt, ML Martin-Fernandez, I Moraes, MA Walsh, S MacIntyre, KA Watson
Super-Resolution Fluorescence Microscopy Reveals Clustering Behaviour of Chlamydia pneumoniae's Major Outer Membrane Protein
BIOLOGY, 9, 344 (2020)

LC Zanetti-Domingues, SE Bonner, RS Iyer, ML Martin-Fernandez, V Huber
Cooperation and Interplay between EGFR Signalling and Extracellular Vesicle Biogenesis in Cancer
CELLS, 9, 2639 (2020)

LC Zanetti-Domingues, SE Bonner, ML Martin-Fernandez, V Huber
Mechanisms of Action of EGFR Tyrosine Kinase Receptor Incorporated in Extracellular Vesicles
CELLS, 9, 2505 (2020)

KL Smitten, EJ Thick, HM Southam, J Bernardino de la Serna, SJ Foster, JA Thomas
Mononuclear ruthenium theranostic complexes that function as broad-spectrum antimicrobials in therapeutically resistant pathogens through interaction with DNA
CHEMICAL SCIENCE, 11, 8828-8838 (2020)

RR White, C Lin, I Leaves, IG Castro, J Metz, BC Bateman, SW Botchway, AD Ward, P Ashwin, I Sparkes
Miro2 tethers the ER to mitochondria to promote mitochondrial fusion in tobacco leaf epidermal cells
COMMUNICATIONS BIOLOGY, 3, 161 (2020)

L Fusaro, M Calvo Catoira, M Ramella, F Sacco Botto, M Talmon, LG Fresu, A Hidalgo-Bastida, F Boccafoschi
Polylysine Enriched Matrices: A Promising Approach for Vascular Grafts
FRONTIERS IN BIOENGINEERING AND BIOTECHNOLOGY, 8, 281 (2020)

LM Magno, DT Hinds, P Duffy, RB Yadav, AD Ward, SW Botchway, PE Colavita, SJ Quinn
Porous Carbon Microparticles as Vehicles for the Intracellular Delivery of Molecules
FRONTIERS IN CHEMISTRY, 8, 576175 (2020)

AVW Nunn, GW Guy, W Brysch, SW Botchway, W Frasch, EJ Calabrese, JD Bell
SARS-CoV-2 and mitochondrial health: implications of lifestyle and ageing
IMMUNITY & AGEING, 17, 33 (2020)

A Bello-Gamboa, M Velasco, S Moreno, G Herranz, R Ilie, S Huetos, S Dávila, A Sánchez, J Bernardino De La Serna, V Calvo, M Izquierdo
Actin reorganization at the centrosomal area and the immune synapse regulates polarized secretory traffic of multivesicular bodies in T lymphocytes
JOURNAL OF EXTRACELLULAR VESICLES, 9, 1759926 (2020)

L Masin, M Claes, S Bergmans, L Cools, L Andries, BM Davis, L Moons, L De Groef
A novel retinal ganglion cell quantification tool based on deep learning
SCIENTIFIC REPORTS, 11, 702 (2021)

ML Martin-Fernandez
A brief history of the octopus imaging facility to celebrate its 10th anniversary
JOURNAL OF MICROSCOPY, 281, 3-15 (2020)

I Emmanouilidis, N Fili, AW Cook, Y Hari-Gupta, Ã dos Santos, L Wang, ML Martin-Fernandez, PJI Ellis, CP Toseland
A Targeted and Tuneable DNA Damage Tool Using CRISPR/Cas9
BIOMOLECULES, 11, 288 (2021)

AR Ahmed, A Candeo, S D'Abrantes, SR Needham, RB Yadav, SW Botchway, AW Parker
Directly imaging the localisation and photosensitization properties of the pan-mTOR inhibitor, AZD2014, in living cancer cells
JOURNAL OF PHOTOCHEMISTRY AND PHOTOBIOLOGY B: BIOLOGY, 213, 112055 (2020)

A Bhartiya, I Robinson, M Yusuf, SW Botchway
Combining Multicolor FISH with Fluorescence Lifetime Imaging for Chromosomal Identification and Chromosomal Sub Structure Investigation
FRONTIERS IN MOLECULAR BIOSCIENCES, 8, 631774 (2021)

SW Botchway, S Farooq, A Sajid, IK Robinson, M Yusuf
Contribution of advanced fluorescence nano microscopy towards revealing mitotic chromosome structure
CHROMOSOME RESEARCH, 29, 19-36 (2021)

Á dos Santos, AW Cook, RE Gough, M Schilling, N Olszok, I Brown, L Wang, J Aaron, ML Martin-Fernandez, F Rehfeldt, CP Toseland
DNA damage alters nuclear mechanics through chromatin reorganization
NUCLEIC ACIDS RESEARCH, 49, 340-353 (2021)

A Ahmed, J Schoberer, E Cooke, SW Botchway
Multicolor FRET-FLIM Microscopy to Analyze Multiprotein Interactions in Live Cells
METHODS IN MOLECULAR BIOLOGY, 2247, 287-301 (2020)

B Ambrose, JM Baxter, J Cully, M Willmott, EM Steele, BC Bateman, ML Martin-Fernandez, A Cadby, J Shewring, M Aaldering, TD Craggs
The smfBox is an open-source platform for single-molecule FRET
NATURE COMMUNICATIONS, 11, 5641 (2020)

N Omori, A Candeo, S Mosca, I Lezcano-Gonzalez, IK Robinson, L Li, AG Greenaway, P Collier, AM Beale
Multimodal Imaging of Autofluorescent Sites Reveals Varied Chemical Speciation in SSZ-13 Crystals
ANGEWANDTE CHEMIE INTERNATIONAL EDITION, 60, 5125-5131 (2021)

Y Zhu, D Sun, A Schertel, J Ning, X Fu, PP Gwo, AM Watson, LC Zanetti Domingues, ML Martin-Fernandez, Z Freyberg, P Zhang
Serial cryoFIB/SEM Reveals Cytoarchitectural Disruptions in Leigh Syndrome Patient Cells
STRUCTURE, 29, 82-87 (2021)

V Ciaffaglione, PA Waghorn, RM Exner, F Cortezon-Tamarit, SP Godfrey, S Sarpaki, H Quilter, R Dondi, H Ge, G Kociok-Kohn, SW Botchway, IM Eggleston, JR Dilworth, SI Pascu
Structural Investigations, Cellular Imaging, and Radiolabeling of Neutral, Polycationic, and Polyanionic Functional Metalloporphyrin Conjugates
BIOCONJUGATE CHEMISTRY, 32, 1374-1392 (2021)

NM Davidson, PJ Gallimore, B Bateman, AD Ward, SW Botchway, M Kalberer, MK Kuimova, FD Pope
Measurement of the fluorescence lifetime of GFP in high refractive index levitated droplets using FLIM
PHYSICAL CHEMISTRY CHEMICAL PHYSICS, 22, 14704-14711 (2020)

AV Nunn, GW Guy, SW Botchway, JD Bell
From sunscreens to medicines: Can a dissipation hypothesis explain the beneficial aspects of many plant compounds?
PHYTOTHERAPY RESEARCH, 34, 1868-1888 (2020)

M Bernabé-Rubio, M Bosch-Fortea, E García, J Bernardino de la Serna, MA Alonso
Adaptive Lipid Immiscibility and Membrane Remodeling Are Active Functional Determinants of Primary Ciliogenesis
SMALL METHODS, 5, 2000711 (2020)

INDIVIDUAL CONTRIBUTIONS AND COLLABORATIVE SCIENCE

P Hadjisolomou, H Ahmed, R Prasad, M Cerchez, S Brauckmann, B Aurand, AM Schroer, M Swantusch, O Willi, M Borghesi, S Kar
Dynamics of guided post-acceleration of protons in a laser-driven travelling-field accelerator
PLASMA PHYSICS AND CONTROLLED FUSION, 62, 115023 (2020)

D Kumar, S Singh, H Ahmed, R Dudžák, J Dostál, T Chodukowski, L Giuffrida, P Hadjisolomu, T Hodge, L Juha, E Krouský, M Krůs, Y Li, P Lutoslawski, M De Marco, M Pfeifer, Z Rusiniak, J Skála, J Ullschmeid, T Pisarczyk, M Borghesi, S Kar
Magnetic field generation using single-plate targets driven by kJ-ns class laser
PLASMA PHYSICS AND CONTROLLED FUSION, 62, 125024 (2020)

MM Michaelis, R Bingham, M Charlton, CA Isaac
A variety of levitrons: a review
EUROPEAN JOURNAL OF PHYSICS, 42, 15001 (2020)

K Beyer, G Marocco, R Bingham, G Gregori
Axion detection through resonant photon-photon collisions
PHYSICAL REVIEW D, 101, 95018 (2020)

G Aymar, T Becker, S Boogert, M Borghesi, R Bingham, C Brenner, PN Burrows, OC Ettlinger, T Dascalu, S Gibson, T Greenshaw, S Gruber, D Gujral, C Hardiman, J Hughes, WG Jones, K Kirkby, A Kurup, J Lagrange, K Long, W Luk, J Matheson, P McKenna, R McLauchlan, Z Najmudin, HT Lau, JL Parsons, J Pasternak, J Pozimski, K Prise, M Puchalska, P Ratoff, G Schettino, W Shields, S Smith, J Thomason, S Towe, P Weightman, C Whyte, R Xiao
LhARA: The Laser-hybrid Accelerator for Radiobiological Applications
FRONTIERS IN PHYSICS, 8, 567738 (2020)

PM Donaldson
Photon echoes and two dimensional spectra of the amide I band of proteins measured by femtosecond IR-Raman spectroscopy
CHEMICAL SCIENCE, 11, 8862-8874 (2020)

M Galletti, FG Bisesto, MP Anania, M Ferrario, R Pompili, A Poyé, V Tikhonchuk, A Zigler
Direct observation of ultrafast electrons generated by high-intensity laser-matter interaction
APPLIED PHYSICS LETTERS, 116, 64102 (2020)

F Bisesto, M Galletti, MP Anania, G Costa, M Ferrario, R Pompili, A Zigler, F Consoli, M Cipriani, M Salvadori, C Verona
Simultaneous observation of ultrafast electron and proton beams in TNSA
HIGH POWER LASER SCIENCE AND ENGINEERING, 8, e23 (2020)

V Hariton, CP João, H Pires, M Galletti, G Figueira
Thermal lens analysis in a diode-pumped 10 Hz 100 mJ Yb:YAG amplifier
HIGH POWER LASER SCIENCE AND ENGINEERING, 8, e13 (2020)

M Galletti, FG Bisesto, MP Anania, M Ferrario, R Pompili, A Poyé, A Zigler
Time-resolved characterization of ultrafast electrons in intense laser and metallic-dielectric target interaction
OPTICS LETTERS, 45, 4420-4423 (2020)

M Galletti, S Künzel, J Alves, V Hariton, H Pires, CP João, G Figueira, JM Dias
Direct refractive index retrieval from interferometry measurements
REVIEW OF SCIENTIFIC INSTRUMENTS, 91, 45111 (2020)

S Mosca, P Dey, M Salimi, B Gardner, F Palombo, N Stone, P Matousek
Estimating the Reduced Scattering Coefficient of Turbid Media Using Spatially Offset Raman Spectroscopy
ANALYTICAL CHEMISTRY, 93, 3386-3392 (2021)

B Gardner, P Matousek, N Stone
Self-absorption corrected non-invasive transmission Raman spectroscopy
ANALYST, 146, 1260-1267 (2021)

TA Tabish, P Dey, S Mosca, M Salimi, F Palombo, P Matousek, N Stone
Smart Gold Nanostructures for Light Mediated Cancer Theranostics: Combining Optical Diagnostics with Photothermal Therapy
ADVANCED SCIENCE, 7, 1903441 (2020)

S Mosca, P Dey, M Salimi, F Palombo, N Stone, P Matousek
Non-invasive depth determination of inclusion in biological tissues using spatially offset Raman spectroscopy with external calibration
ANALYST, 145, 7623-7629 (2020)

A Ghita, T Hubbard, P Matousek, N Stone
Non-invasive Detection of Differential Water Content inside Biological Samples using Deep Raman Spectroscopy
ANALYTICAL CHEMISTRY, 92, 9449-9453 (2020)

C Corden, P Matousek, C Conti, I Notingher
EXPRESS: Sub-Surface Molecular Aanalysis and Imaging in Turbid Media Using Time-Gated Raman Spectral Multiplexing
APPLIED SPECTROSCOPY, 75, 156-167 (2020)

L Ciaffoni, P Matousek, W Parker, EA McCormack, H Mortimer
Grating Spectrometry and Spatial Heterodyne Fourier Transform Spectrometry: Comparative Noise Analysis for Raman Measurements
APPLIED SPECTROSCOPY, 75, 241-249 (2020)

F Nicolson, MF Kircher, N Stone, P Matousek
Spatially offset Raman spectroscopy for biomedical applications
CHEMICAL SOCIETY REVIEWS, 50, 556-568 (2020)

A Botteon, C Colombo, M Realini, C Castiglioni, A Piccirillo, P Matousek, C Conti
Non-invasive andin situinvestigation of layers sequence in panel paintings by portable micro-spatially offset Raman spectroscopy
JOURNAL OF RAMAN SPECTROSCOPY, 51, 2016-2021 (2020)

A Botteon, J Yiming, S Prati, G Sciutto, M Realini, C Colombo, C Castiglioni, P Matousek, C Conti
Non-invasive characterisation of molecular diffusion of agent into turbid matrix using micro-SORS
TALANTA, 218, 121078 (2020)

S Mosca, C Conti, N Stone, P Matousek
Spatially offset Raman spectroscopy
NATURE REVIEWS METHODS PRIMERS, 1, 21 (2021)

V Istokskaia, V Stránský, L Giuffrida, R Versaci, F Grepl, M Tryus, A Velyhan, R Dudžák, J Krása, M Krupka, S Singh, D Neely, V Olšovcová, D Margarone
Experimental tests and signal unfolding of a scintillator calorimeter for laser-plasma characterization
JOURNAL OF INSTRUMENTATION, 16, T02006 (2021)

RA Simpson, GG Scott, D Mariscal, D Rusby, PM King, E Grace, A Aghedo, I Pagano, M Sinclair, C Armstrong, MJ Manuel, A Haid, K Flippo, L Winslow, M Gatu-Johnson, JA Frenje, D Neely, S Kerr, GJ Williams, S Andrews, R Cauble, K Charron, R Costa, B Fischer, S Maricle, B Stuart, F Albert, N Lemos, A Mackinnon, A MacPhee, A Pak, T Ma
Scaling of laser-driven electron and proton acceleration as a function of laser pulse duration, energy, and intensity in the multi-picosecond regime
PHYSICS OF PLASMAS, 28, 13108 (2021)

A Sagisaka, K Ogura, T Esirkepov, D Neely, T Pikuz, J Koga, Y Fukuda, H Kotaki, Y Hayashi, B Gonzalez-Izquierdo, K Huang, S Bulanov, H Kiriyama, K Kondo, T Kawachi, M Kando, A Pirozhkov
Observation of Burst Intensification by Singularity Emitting Radiation generated from relativistic plasma with a high-intensity laser
HIGH ENERGY DENSITY PHYSICS, 36, 100751 (2020)

SDR Williamson, RJ Gray, M King, R Wilson, RJ Dance, C Armstrong, DR Rusby, C Brabetz, F Wagner, B Zielbauer, V Bagnoud, D Neely, P McKenna
Energy absorption and coupling to electrons in the transition from surface- to volume-dominant intense laser-plasma interaction regimes
NEW JOURNAL OF PHYSICS, 22, 53044 (2020)

F Consoli, PL Andreoli, M Cipriani, G Cristofari, R De Angelis, G Di Giorgio, L Duvillaret, J Krása, D Neely, M Salvadori, M Scisciò, RA Smith, VT Tikhonchuk
Sources and space-time distribution of the electromagnetic pulses in experiments on inertial confinement fusion and laser-plasma acceleration
PHILOSOPHICAL TRANSACTIONS OF THE ROYAL SOCIETY A: MATHEMATICAL PHYSICAL AND ENGINEERING SCIENCES, 379, 20200022 (2020)

TZ Esirkepov, J Mu, Y Gu, TM Jeong, P Valenta, O Klimo, JK Koga, M Kando, D Neely, G Korn, SV Bulanov, AS Pirozhkov
Optical probing of relativistic plasma singularities
PHYSICS OF PLASMAS, 27, 52103 (2020)

MJ Manuel, H Tang, BK Russell, L Willingale, A Maksimchuk, JS Green, EL Alfonso, J Jaquez, L Carlson, D Neely, T Ma
Enhanced spatial resolution of Eljen-204 plastic scintillators for use in rep-rated proton diagnostics
REVIEW OF SCIENTIFIC INSTRUMENTS, 91, 103301 (2020)

SR Mirfayzi, A Yogo, Z Lan, T Ishimoto, A Iwamoto, M Nagata, M Nakai, Y Arikawa, Y Abe, D Golovin, Y Honoki, T Mori, K Okamoto, S Shokita, D Neely, S Fujioka, K Mima, H Nishimura, S Kar, R Kodama
Proof-of-principle experiment for laser-driven cold neutron source
SCIENTIFIC REPORTS, 10, 20157 (2020)

RW Assmann, MK Weikum, T Akhter, D Alesini, AS Alexandrova, MP Anania, NE Andreev, I Andriyash, M Artioli, A Aschikhin, T Audet, A Bacci, IF Barna, S Bartocci, A Bayramian, A Beaton, A Beck, M Bellaveglia, A Beluze, A Bernhard, A Biagioni, S Bielawski, FG Bisesto, A Bonatto, L Boulton, F Brandi, R Brinkmann, F Briquez, F Brottier, E Bründermann, M Büscher, B Buonomo, MH Bussmann, G Bussolino, P Campana, S Cantarella, K Cassou, A Chancé, M Chen, E Chiadroni, A Cianchi, F Cioeta, JA Clarke, JM Cole, G Costa, M- Couprie, J Cowley, M Croia, B Cros, PA Crump, R D'Arcy, G Dattoli, A Del Dotto, N Delerue, M Del Franco, P Delinikolas, S De Nicola, JM Dias, D Di Giovenale, M Diomede, E Di Pasquale, G Di Pirro, G Di Raddo, U Dorda, AC Erlandson, K Ertel, A Esposito, F Falcoz, A Falone, R Fedele, A Ferran Pousa, M Ferrario, F Filippi, J Fils, G Fiore, R Fiorito, RA Fonseca, G Franzini, M Galimberti , A Gallo, TC Galvin, A Ghaith, A Ghigo, D Giove, A Giribono, LA Gizzi, FJ Grüner, AF Habib, C Haefner, T Heinemann, A Helm, B Hidding, BJ Holzer, SM Hooker, T Hosokai, M Hübner, M Ibison, S Incremona, A Irman, F Iungo, FJ Jafarinia, O Jakobsson, DA Jaroszynski, S Jaster-Merz, C Joshi, M Kaluza, M Kando, OS Karger, S Karsch, E Khazanov, D Khikhlukha, M Kirchen, G Kirwan, C Kitégi, A Knetsch, D Kocon, P Koester, OS Kononenko, G Korn, I Kostyukov, KO Kruchinin, L Labate, C Le Blanc, C Lechner, P Lee, W Leemans, A Lehrach, X Li, Y Li, V Libov, A Lifschitz, CA Lindstrøm, V Litvinenko, W Lu, O Lundh, AR Maier, V Malka, GG Manahan, SPD Mangles, A Marcelli, B Marchetti, O Marcouillé, A Marocchino, F Marteau, A Martinez de la Ossa, JL Martins, PD Mason, F Massimo, F Mathieu, G Maynard, Z Mazzotta, S Mironov, AY Molodozhentsev, S Morante, A Mosnier, A Mostacci, A- Müller, CD Murphy, Z Najmudin, PAP Nghiem, F Nguyen, P Niknejadi, A Nutter, J Osterhoff, D Oumbarek Espinos, J- Paillard, DN Papadopoulos, B Patrizi, R Pattathil, L Pellegrino, A Petralia, V Petrillo, L Piersanti, MA Pocsai, K Poder, R Pompili, L Pribyl, D Pugacheva, BA Reagan, J Resta-Lopez , R Ricci, S Romeo, M Rossetti Conti, AR Rossi, R Rossmanith, U Rotundo, E Roussel, L Sabbatini, P Santangelo, G Sarri, L Schaper, P Scherkl , U Schramm, CB Schroeder, J Scifo, L Serafini, G Sharma, ZM Sheng, V Shpakov, CW Siders, LO Silva, T Silva, C Simon, C Simon-Boisson, U Sinha, E Sistrunk, A Specka, TM Spinka, A Stecchi, A Stella, F Stellato, MJV Streeter, A Sutherland , EN Svystun, D Symes, C Szwaj, GE Tauscher, D Terzani, G Toci, P Tomassini, R Torres, D Ullmann, C Vaccarezza, M Valléau, M Vannini, A Vannozzi, S Vescovi, JM Vieira, F Villa, C- Wahlström, R Walczak, PA Walker, K Wang, A Welsch, CP Welsch , SM Weng, SM Wiggins, J Wolfenden, G Xia, M Yabashi, H Zhang, Y Zhao, J Zhu, A Zigler

EuPRAXIA Conceptual Design Report

EUROPEAN PHYSICAL JOURNAL - SPECIAL TOPICS, 229, 3675-4284 (2020)

Z Xu, C Xiao, H Lu, R Hu, J Yu, Z Gong, Y Shou, J Liu, C Xie, S Chen, T Xu, R Li, N Hafz, S Li, Z Najmudin, P Rajeev, D Neely, X Yan

New injection and acceleration scheme of positrons in the laser-plasma bubble regime

PHYSICAL REVIEW ACCELERATORS AND BEAMS, 23, 91301 (2020)

NG Barnes, AW Parker, AA Ahmed Mal Ullah, PA Ragazzon, JA Hadfield

A 2-step synthesis of Combretastatin A-4 and derivatives as potent tubulin assembly inhibitors

BIOORGANIC & MEDICINAL CHEMISTRY, 28, 115684 (2020)

U Kamber, S Pakdel, R Stan, A Kamlapure, B Kiraly, F Arnold, A Eich, AS Ngankeu, M Bianchi, JA Miwa, CE Sanders, N Lanatà, P Hofmann, AA Khajetoorians

Moire-induced electronic structure modifications in monolayer V2S3 on Au(111)

PHYSICAL REVIEW B, 103, 115414 (2021)

D Curcio, AJ Jones, R Muzzio, K Volckaert, D Biswas, CE Sanders, P Dudin, C Cacho, S Singh, K Watanabe, T Taniguchi, JA Miwa, J Katoch, S Ulstrup, P Hofmann

Accessing the Spectral Function in a Current-Carrying Device

PHYSICAL REVIEW LETTERS, 125, 236403 (2020)

MD King, SH Jones, COM Lucas, KC Thompson, AR Rennie, AD Ward, AA Marks, FN Fisher, C Pfrang, AV Hughes, RA Campbell

The reaction of oleic acid monolayers with gas-phase ozone at the air water interface: the effect of sub-phase viscosity, and inert secondary components

PHYSICAL CHEMISTRY CHEMICAL PHYSICS, 22, 28032-28044 (2020)

J Tu, Y Zhao, X Zhang, Z Nie, Y Li, Y Zhang, ICE Turcu, L Poletto, F Frassetto, X Ruan, W Zhong, X Wang, W Liu, Y Zhang, R Zhang, Y Xu, L He

Impurity band assisted carrier relaxation in Cr doped topological insulator Bi_2Se_3

APPLIED PHYSICS LETTERS, 118, 81103 (2021)

AJ Tanner, B Wen, J Ontaneda, Y Zhang, R Grau-Crespo, HH Fielding, A Selloni, G Thornton

Polaron-Adsorbate Coupling at the TiO_2(110)-Carboxylate Interface

JOURNAL OF PHYSICAL CHEMISTRY LETTERS, 12, 3571-3576 (2021)

AJ Tanner, B Wen, Y Zhang, L Liu, HH Fielding, A Selloni, G Thornton

Photoexcitation of bulk polarons in rutile

PHYSICAL REVIEW B, 103, L121402 (2021)

Thesis

ARTEMIS

Warne, E.M.
Measuring Molecular Dynamics Using UV and XUV Photoelectron Spectroscopy
PhD Thesis, University of Southampton (2020)

Volckaert, K.
Ultrafast electronic and vibrational properties of Dirac materials
PhD Thesis, Aarhus University (2020)

Bobowski, K.
Magnetization Dynamics in the Lanthanide Metal Gadolinium
PhD Thesis, Technical University of Berlin (2020)

GEMINI

Hodge, T.
Radiographic applications and control of TNSA proton beams
PhD Thesis, Queen's University Belfast (2020)

Underwood, C.
Optimising Production of High Energy Radiation Using Laser Wakefield Acceleration
PhD Thesis, University of York (2021)

Gerstmayer, E.
Energetic Radiation from Wakefield Acceleration and its Applications
PhD Thesis, Imperial College London (2020)

VULCAN

Martin, P.
Schemes of ion acceleration employing high energy, petawatt laser pulses
PhD Thesis, Queen's University Belfast (2020)

McIlvenny, A.
Multispecies ion acceleration from intense laser interactions with thin foils
PhD Thesis, Queen's University Belfast (2021)

Aboushelbaya, R.
Orbital Angular Momentum In High-Intensity Laser Interactions
PhD Thesis, University of Oxford (2020)

Farley, D.
Resistive Guiding of Fast Electrons in High-Intensity Laser-Plasma Interactions
PhD Thesis, University of York (2020)

ULTRA

Cullen, A.
BODIPY copolymers as potential triplet photosensitisers for the photocatalytic generation of hydrogen and enhanced antimicrobial activity
PhD Thesis, Dublin City University (2020)

Omori, N.
Multimodal Spectroscopy and Imaging of Chabazite Zeolite
PhD Thesis, University College London (2020)

OCTOPUS

D'Abrantes, S.
Shedding Light on the Biological Effects of Ionising Radiation on DNA Using Advanced Optical Microscopy
PhD Thesis, Oxford Brookes University (2020)

McCulloch, A.
Gold nanoparticle cellular uptake and its implications for cancer therapy
PhD Thesis, Queen's University Belfast (2020)

Panel membership and CLF structure

Laser for Science Facility Access Panel 2020-2021

REVIEWERS

Professor P. Kukura (Chair)
Department of Chemistry
University of Oxford

Dr S. Ameer-Beg
School of Cancer and Pharmaceutical Sciences
King's College London

Professor A. Beale
Department of Chemistry
University College London

Dr J. Bernadino de la Serna
Faculty of Medicine
Imperial College London

Professor J. Bredenbeck
Johann Wolfgang Goethe-Universität

Dr A. Cowan
Department of Chemistry
University of Liverpool

Dr S. Cox
Faculty of Life Sciences and Medicine
King's College London

Dr I. Dobbie
Department of Biochemistry
University of Oxford

Dr M. Frogley
Diamond Light Source

Dr E. Gibson
School of Natural and Environmental Sciences
University of Newcastle

Dr M. Kuimova
Department of Chemistry
Imperial College London

Dr S. Leveque-Fort
Institut des Sciences Moléculaires d'Orsay

Professor G. McConnell
Centre for Biophotonics
University of Strathclyde

Professor J. Moger
University of Exeter

Professor S. Pascu
Department of Chemistry
University of Bath

Professor J. Weinstein
Department of Chemistry
University of Sheffield

RESEARCH COUNCIL REPRESENTATIVES

A. McGavigan
MRC

A. Chapman
EPSRC

J. Swarbrick
BBSRC

M. Simons
STFC

L. Garratt
NERC

SCIENCE & TECHNOLOGY FACILITIES COUNCIL REPRESENTATIVES

Dr D. T. Clarke (Head of Laser for Science Facility)
Central Laser Facility
Science & Technology Facilities Council

Prof J.L Collier (Director)
Central Laser Facility
Science & Technology Facilities Council

Professor M. Towrie (ULTRA Group Leader)
Central Laser Facility
Science & Technology Facilities Council

Dr M. Martin-Fernandez (OCTOPUS Group Leader)
Central Laser Facility
Science & Technology Facilities Council

Dr A. Kaye
ISIS & CLF User Office
Science & Technology Facilities Council

Professor D. Payne (Director)
Research Complex at Harwell

Professor L. Chapon (Physical Sciences Director)
Diamond Light Source

Dr E. Gozzard
Central Laser Facility
Science & Technology Facilities Council

Artemis Facility Access Panel 2020/21

REVIEWERS

Professor M. Vrakking (Panel Chairman)
Max Born Institute, Berlin

Professor H. Fielding
Department of Chemistry, Christopher Ingold Laboratories
University College London

Professor M. Aeschlimann
University of Kaiserslautern, Germany

Dr J. Stahler
Fritz Haber Institute, Germany

Professor J. Tisch
Department of Physics, Blackett Laboratory
Imperial College London

Professor L. Perfetti
Laboratoire des Solides Irradies, Ecole Polytechnique
Palaiseau Cedex

Professor A. Taleb-Ibrahimi
Synchrotron SOLEIL, L'Orme des Merisiers, France

Dr P. King
School of Physics and Astronomy
University of St. Andrews

SCIENCE & TECHNOLOGY FACILITIES COUNCIL REPRESENTATIVES

Professor J.L. Collier (Director)
Central Laser Facility
Science & Technology Facilities Council

Ms C. Hernandez-Gomez (Head, High Power Laser Programme)
Central Laser Facility
Science & Technology Facilities Council

Dr E. Springate (Artemis Group Leader)
Central Laser Facility
Science & Technology Facilities Council

Dr R.T. Chapman (Artemis, AMO and Imaging)
Central Laser Facility
Science & Technology Facilities Council

Dr D.T Clarke (Head of Laser for Science Facility)
Central Laser Facility
Science & Technology Facilities Council

Professor M. Towrie (Molecular and Structural Dynamics)
Central Laser Facility
Science & Technology Facilities Council

Vulcan, Gemini and Orion Facility Access Panel 2020/21

REVIEWERS

Professor N. Woolsey (Panel Chair)
York Plasma Institute
University of York

Professor B. Dromey
Department of Pure and Applied Physics
Queen's University of Belfast

Professor G. Gregori
Clarendon Laboratory
University of Oxford

Dr S. Mangles
Blackett Laboratory
Imperial College London

Dr J. Pasley
York Plasma Institute
University of York

Professor B. Hidding
Department of Physics
University of Strathclyde

Professor T. Arber
Department of Physics
University of Warwick

Dr R. Kingham
Blackett Laboratory
Imperial College London

Dr A. Klisnick
Institut des Sciences Moléculaires d'Orsay
Université Paris-Saclay

Dr B. Cros
Laboratory of Gas Physics and Plasmas
Université Paris-Sud

RESEARCH COUNCIL REPRESENTATIVES

Mr C. Danson
AWE

SCIENCE & TECHNOLOGY FACILITIES COUNCIL REPRESENTATIVES

Professor J.L. Collier (Director)
Central Laser Facility
Science & Technology Facilities Council

Ms C. Hernandez-Gomez (Head, High Power Laser Programme)
Central Laser Facility
Science & Technology Facilities Council

Dr I.O. Musgrave (Vulcan Group Leader)
Central Laser Facility
Science & Technology Facilities Council

Mr R.J. Clarke (Experimental Science Group Leader)
Central Laser Facility
Science & Technology Facilities Council

Dr R. Pattathil (Gemini Group Leader)
Central Laser Facility
Science & Technology Facilities Council

Dr D. Symes (Gemini Target Area Section Leader)
Central Laser Facility
Science & Technology Facilities Council

Dr D. Carroll (Panel Secretary)
Central Laser Facility
Science & Technology Facilities Council

Mr C. Spindloe (Target Fabrication)
Scitech Precision

Dr E. Gozzard (User Office Group Leader)
ISIS Neutron & Muon Source
Science & Technology Facilities Council

Central Laser Facility Structure

Director

Professor John Collier
john.collier@stfc.ac.uk

Research Complex Division

Dr Dave Clarke
dave.clarke@stfc.ac.uk

CALTA Division

Dr Chris Edwards
chris.edwards@stfc.ac.uk

High Power Lasers Division

Ms Cristina Hernandez-Gomez
cristina.hernandez-gomez@stfc.ac.uk

Engineering & Technology Division

Mr Steve Blake
steve.blake@stfc.ac.uk

Ultra

Prof Mike Towrie
mike.towrie@stfc.ac.uk

Octopus

Dr Marisa Martin-Fernandez
marisa.martin-fernandez@stfc.ac.uk

Gemini

Dr Rajeev Pattathil
rajeev.pattathil@stfc.ac.uk

Artemis

Dr Emma Springate
emma.springate@stfc.ac.uk

Experimental Science

Mr Rob Clarke
rob.clarke@stfc.ac.uk

Target Fabrication

Mr Martin Tolley
martin.tolley@stfc.ac.uk

Vulcan

Dr Ian Musgrave
ian.musgrave@stfc.ac.uk

Plasma Physics

Dr Alex Robinson
alex.robinson@stfc.ac.uk

Mechanical

Mr Steve Hook
steven.hook@stfc.ac.uk

Electrical

Vacancy
vacancy@stfc.ac.uk

Science and
Technology
Facilities Council

7852.12.22